TECHNICAL VOLUME 3

OF THE ENVIRONMENTAL ASSESSMENT APPLICATION

FOR THE

NAIKUN OFFSHORE WIND ENERGY PROJECT

MARINE PHYSICAL ENVIRONMENT



APRIL 2009

Prepared for: NaiKun Wind Development Inc.
Prepared by: RPS Energy

TABLE OF CONTENTS

3.0 Marine Physical Environment 1

3.1 Introduction to Marine Physical Environment 1

3.2 Marine Atmospheric Environment 1

3.2.1 General Setting 1

3.2.2 Meteorology 2

3.2.3 Oceanography 7

3.2.4 Summary 13

3.3 Marine Wind, Wave and Tidal Studies for Wind Farm Engineering 13

3.3.1 Data Sources 13

3.3.2 Winds 16

3.3.3 Waves 17

3.3.4 Tides 18

3.4 Regional Geology of the Dogfish Banks and Environs 22

3.4.1 Data Sources 22

3.4.2 Regional Environmental Conditions 23

3.4.3 Bathymetry and Current Regimes 23

3.4.4 Seabed Features and Bedforms 24

3.4.5 Pockmarks and Shallow Gas 26

3.4.6 Seabed Sediments 26

3.4.7 Quarternary and Solid Geology 27

3.4.8 Seismicity and Associated Events 37

3.5 Marine Geophysical Studies for Wind Farm Engineering 39

3.5.1 Geophysical Field Studies 40

3.5.2 Results of Geophysical Field Studies 40

3.5.3 Summary of Sea Bed and Sediment Conditions 44

3.6 Model Studies of Coastal Impacts of an Offshore Wind Farm - A Case Study of Codling Bank, Irish Sea 64

3.6.1 Hydraulic Computational Modelling 65

3.6.2 Cable Laying 71

3.6.3 Conclusions from Codling Bank Modelling 73

3.7 Studies of Impact of Offshore Wind Farms on Coastal Processes - A Case Study of Scroby Sands 73

3.8 HaidaLink 76

3.9 References and Sources 85

TABLE OF FIGURES

Figure 3.2-1 Sea-level pressure pattern of a Gulf of Alaska low with associated front 3
Figure 3.2-2 A summer storm track for a July mean sea-level pattern 4
Figure 3.2-3 A sea-level pressure pattern for a coastal low and frontal system with winds superimposed 5
Figure 3.2-4 Cold arctic air in the interior pushes cold front onto coast 6
Figure 3.2-5 Icing conditions for marine structures 7
Figure 3.2-6 Non-tidal currents for summer (solid arrows) and winter (broken arrows) 9
Figure 3.2-7 Wave heights (m) from Northwest gales onto west coast of the Queen Charlotte Islands 10
Figure 3.2-8 Tidal streams in Dixon Entrance and off Rose Spit 12
Figure 3.3-1 Annual Wind Rose, NOAA data Point 50.5ºN, 130.0ºW 14
Figure 3.3-2 Annual Wind Rose, South Hecate Strait Buoy 15
Figure 3.3-3 Annual Wind Rose for the Wind Farm Compiled from Hecate South and North Buoys 16
Figure 3.3-4 Wave Heights 1 in 50 years Waves Attenuated in Shallow Water 17
Figure 3.3-5 Significant Wave Height and Mean Direction, 1 in 50 year Storm from 165º 18
Figure 3.3-6 Typical Flood Spring Tidal Flows – Hecate Strait 20
Figure 3.3-7 Typical Ebb Spring Tidal Flows – Hecate Strait 21
Figure 3.4-1 Current Direction and Magnitude within Hecate Strait and Surrounding Area 24
Figure 3.4-2 Seabed features and Shallow Geohazards of Hecate Strait and Surrounding Area 25
Figure 3.4-3 Sea-Level reconstruction 12,000 years before the present if sea-level is lowered by 150m 28
Figure 3.4-4 General Ice Retreat Map 29
Figure 3.4-5 General Sea Level Curve for Juan Perez Sound 30
Figure 3.4-6 Tlell River Bridge Geotechnical Profile 32
Figure 3.4-7 Queen Charlotte Basin Showing Overview of Stratigraphic Systems and Exploratory Wells 33
Figure 3.4-8 Summary of Geological and Structural Terranes within Queen Charlotte Basin 34
Figure 3.4-9 Generalised Stratigraphy of Mesozioc (Triassic, Jurassic and Cretaceous) and Cenozioc (Tertiary) of Queen Charlotte Basin 35
Figure 3.4-10 Simplified Structural Cross Section for the Offshore Region of Hecate Strait 36
Figure 3.4-11 Seismicity map showing major earthquake epicentres in and near the study area between 1984 and 1996 38
Figure 3.4-12 Relationship between Earthquake Magnitude and Occurrences Per Year for the Northern Hecate Strait 39
Figure 3.5-1 Geological Areas 42
Figure 3.5-2 Site Bathymetry (South to North View) – 2 m Resolution 44
Figure 3.5-3 Shaded Relief Map NW Quadrant of Wind Farm 45
Figure 3.5-4 Shaded Relief Map NE Quadrant of Wind Farm 46
Figure 3.5-5 Shaded Relief Map SW Quadrant of Wind Farm 47
Figure 3.5-6 Shaded Relief Map SE Quadrant of Wind Farm 48
Figure 3.5-7 Detailed Sidescan Image of MET Station 49
Figure 3.5-8 Seafloor Geology NW Quadrant 51
Figure 3.5-9 Seafloor Geology NE Quadrant 52
Figure 3.5-10 Seafloor Geology SW Quadrant 53
Figure 3.5-11 Seafloor Geology SE Quadrant 54
Figure 3.5-12 Sediment Sample Locations with Boulder Contacts 55
Figure 3.5-13 2007 Single Beam and 2008 Multibeam Comparison Area 56

Figure 3.5-14 2007 Single Beam and 2008 Multibeam Comparison Area 57
Figure 3.5-15 2007 Single Beam and 2008 Multibeam Comparison Area 58
Figure 3.5-16 KP Junctions along Route 62
Figure 3.5-17 Profile along Centreline of Route 62
Figure 3.6-1 Extent and bathymetry of 135m – 45m – 15m nested models 66
Figure 3.6-2 Location of proposed extended turbine array at Codling Bank 67
Figure 3.6-3 Comparison of ebb tidal velocities with and without wind farm installed 68
Figure 3.6-4 Comparison of flood tidal velocities with and without wind farm installed 68
Figure 3.6-5 Net potential sediment transport rates for sand over full tidal cycle Spring tides – no waves 69
Figure 3.5-6 Rate of potential sediment transport of sand – Gale from 165^{o} 70
Figure 3.6-7 Percentage of time during cable installation when suspended sediment > 50 mg/l 72
Figure 3.7-1 Fledermaus image showing the scour protection around the base of a monopile 75
Figure 3.7-2 Fledermaus image showing results from the swathe bathymetry survey of Scroby Sands OWF 75
Figure 3.8.1 Regional Survey Lines relative to Haida Route Corridor along with regional bathymetry 79
Figure 3.8.2 Location of Grab Samples relative to Regional Survey Lines and Haida Route Corridor 80
Figure 3.8.3 Extract from Map 2 – PGC Grain Size and Cores of the 2006 RPS Energy Report. 81
Figure 3.8.4 Areas comprised of gravel with boulders and occasional patches of sand in a thin veneer of sand. 82
Figure 3.8.5 The area labeled as bedrock is most likely bouldery glacial till based on more recent data collected in the WFA in 2007 and 2008 83
Figure 3.8.6 Summary Bathymetry Profile showing the low relief along the Haida Link corridor 84

3.0 MARINE PHYSICAL ENVIRONMENT

3.1 INTRODUCTION TO MARINE PHYSICAL ENVIRONMENT

This volume of the NaiKun Wind Development Inc.'s (the Proponent) Environmental Assessment Application for the NaiKun Offshore Wind Energy Project addresses the marine atmospheric and physical environment of Hecate Strait. Section 3.2 provides an overview of the meteorology and oceanography of Hecate Strait based on a review of literature and other information specific to the Project area. The results of marine wind, wave and tidal studies conducted in the wind farm area are summarized in Section 3.3. Section 3.4 describes the results of the geophysical surveys completed for both the wind farm and the mainland cable route. A case study of the modelling undertaken to determine littoral and shoreline effects for a proposed wind farm in the Irish Sea is provided in Section 3.5.

In addition, the Terms of Reference also identified air quality as a component of the marine physical environment for assessment. This subject is discussed in Volume 11, Socio-economic Studies in context with public health as the principle concerns regarding this KIR focus on the effects of air-borne emissions on public health.

3.2 MARINE ATMOSPHERIC ENVIRONMENT

The discussion of the marine atmospheric environment was prepared by Dr. Noel Boston, for Hemmera Envirochem Inc.

3.2.1 *General Setting*

3.2.1.1 Meteorology

The general weather patterns over the Dixon Entrance-Hecate Strait region are prescribed by the large scale pressure systems over the North Pacific Ocean -- the North Pacific High of summer and the Aleutian Low of winter. Within these broad patterns significant variations can occur because of the mountainous terrain of the Queen Charlotte Islands and the mainland coast. Winds tend to blow parallel to the east coast of the islands and slow towards the mainland shore. Northern Hecate Strait has a high frequency and intensities of south-easterly winds.

The fair-weather months are June, July and August. According to Thomson (1981), the winds during this period range from 5.5 m/s in the seaward approaches to 4 m/s near the mainland. The prevailing winds are from the west in Dixon Entrance and from the northwest in northern Hecate Strait. The good weather may last into September but deteriorates rapidly in October heralding the winter storm season. The wind changes direction, coming from the southeast, and increases in speed to 9.5 m/s along the outer coast and 6 m/s closer to the mainland. The winter winds persist from November to February and into March and average 10 m/s over Dixon Entrance. The wind strength tapers over April and May before returning to the fair-weather season.

3.2.1.2 Oceanography

The Dixon Entrance – Northern Hecate Strait is sufficiently large and deep that deep sea processes occur but at the same time these regions are influenced by estuarine processes. Tides, winds and river discharges are important in determining currents and water structure.

Dixon Entrance is a 170 km east-west depression in the continental shelf, bounded by Dall and Prince of Wales islands on the north and Graham Island on the south. At the western entrance it is separated into two 400 m deep channels by Learmonth Bank that rises to within 35 m of the surface. East of the Bank the depression shoals to about 100 m.

The axis of Hecate Strait is a 220 m submarine valley. It runs close to the mainland shore from depths of 300 m in the south to 50 m in the north. The northwest side of the Strait is a broad expanse of glacial sands and gravels that lies adjacent to the flat coastal plain east of Graham Island.

Surface motions in Dixon Entrance and the Hecate Strait are dominated by semidiurnal tidal streams modified by the effects of wind, runoff, bathymetry and shoreline configuration. For example, river discharges create a persistent ebb bias in surface layers and a weaker flood bias at depth (Thomson, 1981). Counter-clockwise (cyclonic) gyres exist in Dixon Entrance in both summer and winter because of the combination of winds and river run-off. During the northwest winds of summer there is large river run-off but during the southeast winds of winter, run-off is low. Prevailing surface currents tend to flow south in northern Hecate Strait during the summer and north during the summer (Crean, 1967). The speed of surface currents in the open waters of Hecate Strait and Dixon Entrance is typically 3% of the wind speed, or 16.5 cm/s to 30 cm/s (~ 0.3 to 0.6 kts). Tidal currents will be higher and vary greatly depending on depth and channel features.

3.2.2 *Meteorology*

3.2.2.1 Systems

The Aleutian Low (also known as Gulf of Alaska Low) usually forms south of the Aleutian Island chain as a frontal wave between cold northern air and warmer air to the south. The wave may travel far eastward before it begins to take shape as a low pressure system. Once the low starts to develop, pressures fall rapidly. At the same time the low pressure system increases in size and wind speeds rise. The air flow is always cyclonic (counter-clockwise looking down) around the low (Figure 3.2-1).

The low may fall below 97 KPa as it moves northeast at 35 to 40 knots (56 to 74 km/h). It reaches its lowest central pressure over the Gulf of Alaska. The front that extends southward from the low centre moves over coastal waters bringing south-easterly gale-to-storm-force winds, rain and heavy seas. Intense lows can briefly rise to hurricane-force strength (64 knots and higher) at the southern entrance to Hecate Strait (Queen Charlotte Sound) but weaken further northward.

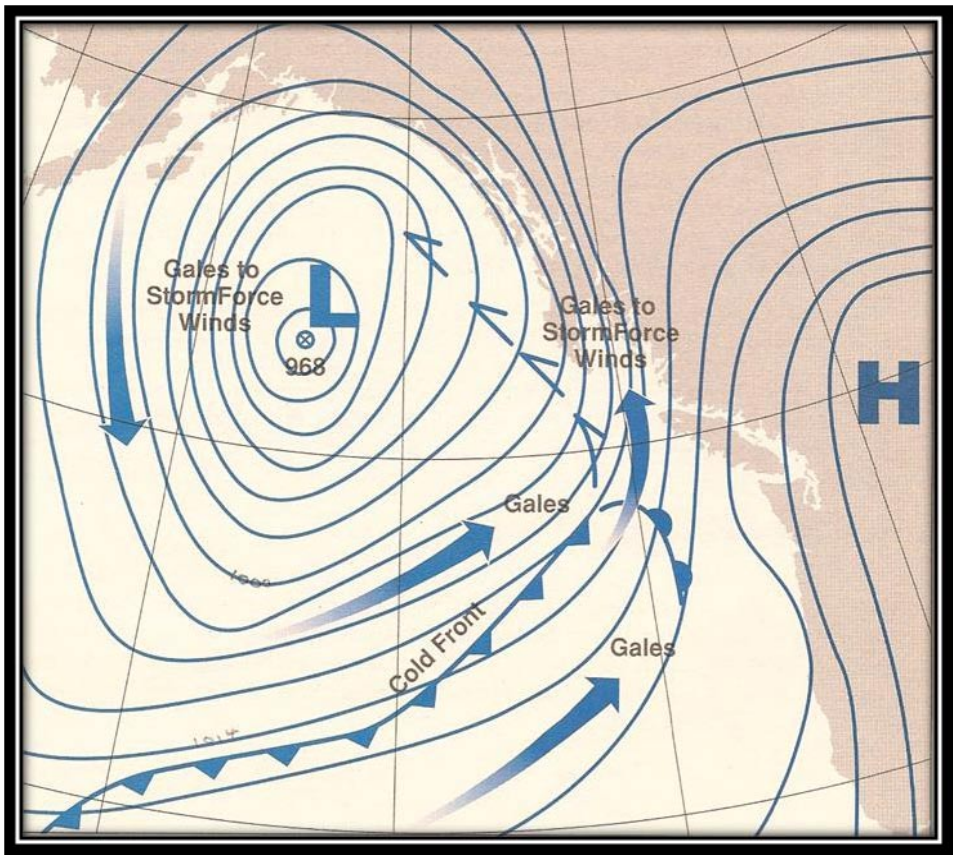


Figure 3.2-1 Sea-level pressure pattern of a Gulf of Alaska low with associated front.
Adapted from *Marine Weather Hazards Manual*. Pressure at low in millibars.

The North Pacific High forms during the summer months of May to September as a semi-permanent high-pressure area off California. It strengthens as it moves to the north. In so doing it deflects summer storm tracks into the northern Gulf of Alaska (Figure 3.2-2).

Summer storms are not as intense as winter storms because the contrast between warm and cold air is not as strong during the summer. The frontal systems which approach the Queen Charlotte Islands are much weaker. A ridge of high pressure develops near the coast and controls the direction and strength of the coastal winds which occasionally reach gale-force strength. The prevailing winds are from the northwest.

In spring and early summer strong winds may develop since the fronts still retain some of the strengths of winter storms.

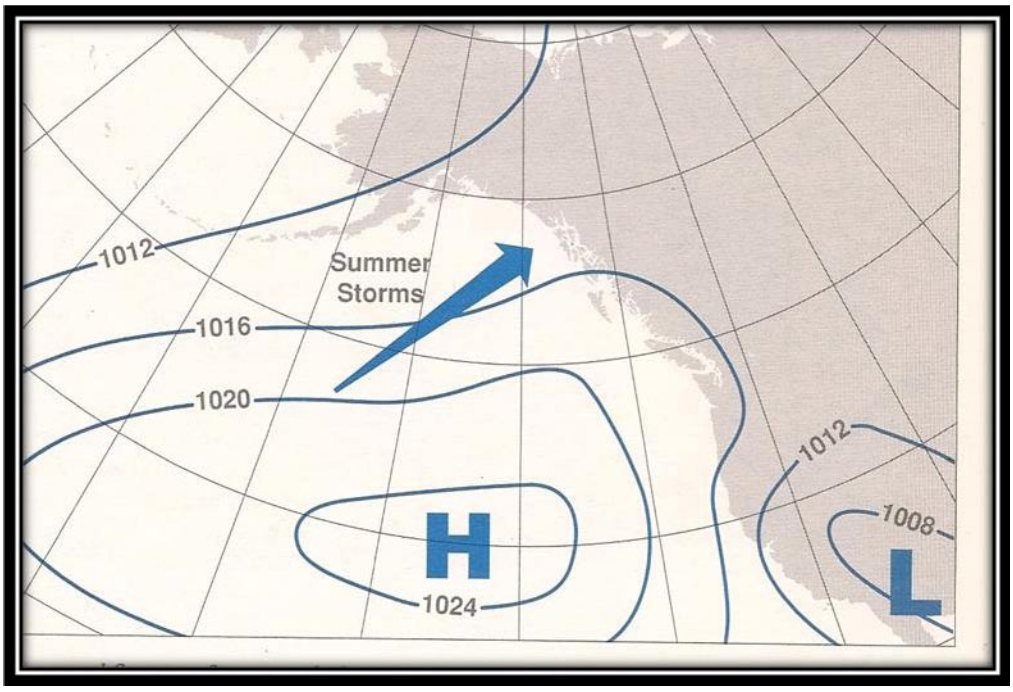


Figure 3.2-2 A summer storm track for a July mean sea-level pattern.
Adapted from Marine Weather Hazards Manual. Pressure in millibars.

3.2.2.2 Weather Features

Winter storms occur over the northeast Pacific Ocean from approximately early October to April. About 10 to 15 storms affect the west coast each month. The winds generally rise to gale force and often to storm force. Hurricane force winds usually occur several times during the winter at some exposed locations.

The transition from the quiet days of summer to the severe weather can be dramatic rather than gradual. Storms that occur near the time of the autumn equinox often mark this transition. The *Marine Weather Hazards Manual* (1992) sites a 28 September 1990 storm that occurred at the west Dixon Entrance during which winds rose from light to 54 knots (with accompanying seas building from 2.5 m to 11.4 m) in 10 hours.

Most winter storms are associated with Gulf of Alaska lows that remain well offshore and track northward into the Gulf of Alaska. However frontal systems will move away from the low and pass south-eastward over the coast. The strongest winds and the heaviest seas generally occur just ahead of the front. The front usually weakens as it crosses the southern coastal waters. After the front passes over the coast the winds usually decrease, the visibility improves and the seas diminish. Heavy swell, typically from 4 to 6 m arrive at the coast up to 12 hours after the front has passed. These waves were formed with the strong west or northwest wind on the western edge of the low.

Coastal lows create another type of winter storm. They form rapidly near the coast and move directly over B.C.'s inland seas (Figure 3.2-3). They can change from a very weak system into a severe storm in just 9 hours. Atmospheric pressure may fall 300 to 400 Pa (3 to 4 mb) every hour just ahead of the storm

as it moves toward the coast. Winds vary considerably around the low with the strongest winds and highest seas usually occurring south of the low. Coastal lows which develop in a rapid and explosive manner are referred to as 'bombs' by forecasters.

The strongest winds are usually to the east or southeast of the low ahead of the front and may reach south-easterly winds of 70 knots (~ 130 km/h). Gusts up to 100 knots (185 km/h) occasionally occur in very severe storms.

Summer storms develop in the spring and early summer. The storms may be severe as the fronts can retain energy from winter storms. Summer fronts may have little cloud warning. Winds in advance of the front may decrease or remain light north-westerly with steady barometric pressure. Behind the front, pressures rise rapidly with sudden increases in wind speed. Winds may become gusty and reach gale force form the northwest. Heavy seas may build and visibility decrease.

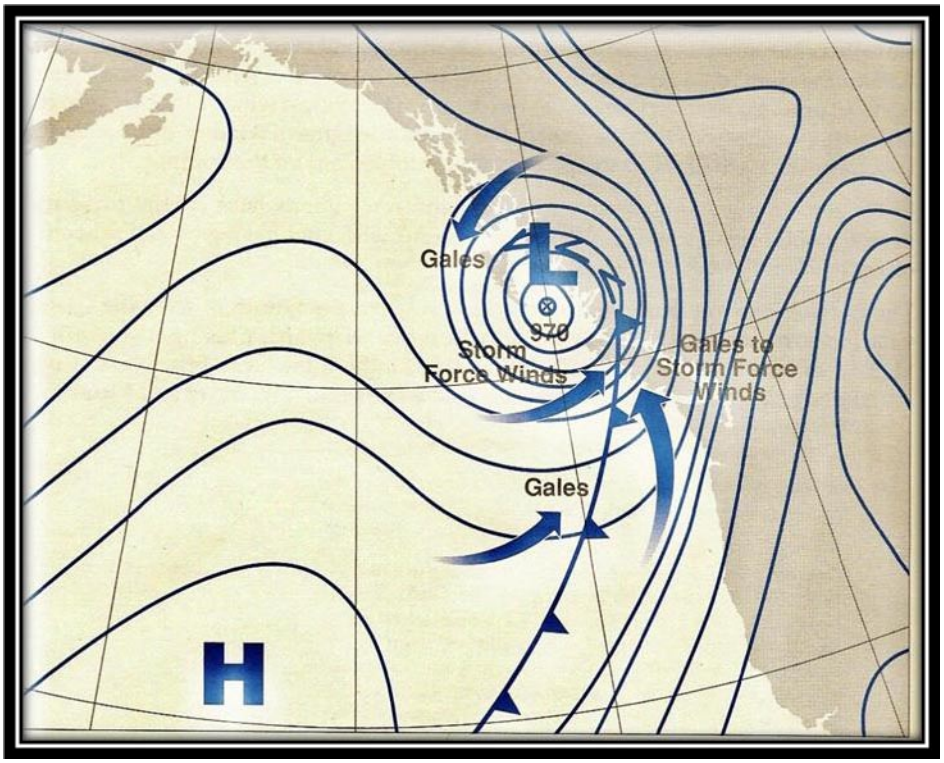


Figure 3.2-3 A sea-level pressure pattern for a coastal low and frontal system with winds superimposed. Adapted from *Marine Weather Hazards Manual*. Pressure at centre of low in millibars

3.2.2.3 Arctic Outbreaks

During the winter very cold air forms an area of high pressure over Alaska and Arctic Canada. The cold arctic air spreads in a layer over northern British Columbia. When the layer thickens, cold air can flow down mountain passes producing very strong winds. In particular, these winds can create treacherous weather in coastal inlets over a period of several days. These outflow winds of 60 knots (110 km/h) or

more, though strongest at the mouths of inlets, may persist into Dixon Entrance and northern Hecate Strait (Figure 3.2-4).

An Arctic front is at the leading edge of cold air and is the first indication of deteriorating weather conditions. Weather preceding the front gives little warning of impending change as the barometer may remain steady and the weather settled. The arrival is usually accompanied by snow or sleet. As the front passes temperatures drop, barometric pressure rises rapidly and strong northerly outflow winds begin. The snow moves westward with the front, drier air moves in and the sky clears. The cold dry air flowing over Hecate Strait picks up moisture and brings snow to the east coast of the Queen Charlotte Islands.

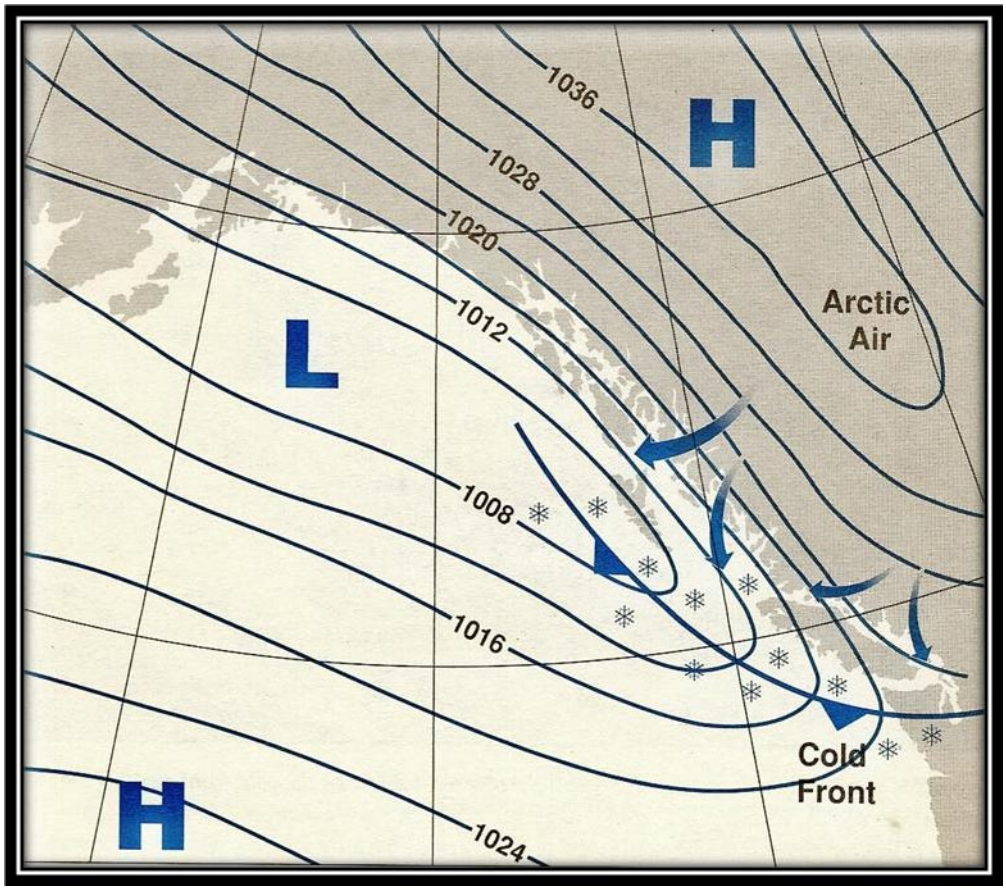


Figure 3.2-4 Cold arctic air in the interior pushes cold front onto coast.
Out flow winds may exceed 60 knots through the mouths of inlets.
Adapted from *Marine Weather Hazards Manual*. Pressure in millibars

The strong winds carrying arctic air out of the mouths of inlets may continue for some distance over open water but weaken when they are no longer constrained by the inlet. Strong, gusty winds can whip spray off the tops of waves. The smallest particles freeze in the air and reduce visibility and the larger particles of freezing spray may cause icing on structures.

3.2.2.4 Consequences and Concerns

The description of the wind fields associate with the two dominant pressure systems, Gulf of Alaska low and the Aleutian high, clearly match the wind roses presented in the RPS Metocean Report (2008).

Approximately four times as much wind energy is available in winter as in summer. Further the prevailing winds come from almost opposite directions. Hurricane force winds can occur accompanied by heavy seas. These should be used as design parameters in the engineering of the turbines.
Although the winds associated with the North Pacific high are moderate, attention is drawn to spring/early summer when quite strong winds can occur with little warning. The transition from serene to severe may occur within hours with wave build-up from 3 m to 11 m in less than 12 hours. Structures must be able to withstand such waves frequently.

The "bombs" of Coastal lows may contain winds of 130 km/h and gusts of 185 km/h. The potential hazards associated with arctic outbreaks consist of gale to storm force winds, severe icing conditions and poor visibility. Possible icing of turbine structures, including blades, is a concern. Icing conditions can extend as far as 40 km from the heads of inlets (Sailing Directions – North Portion of BC Coast, 1991). Icing on structures can occur when air temperatures are -2C or less and winds moderate to strong (Figure 3.2-5). The *BC Sailing Directions* (1991) report that such conditions occur less than 5% of the time. A side concern is that freezing rain and snow significantly reduce radar efficiency.

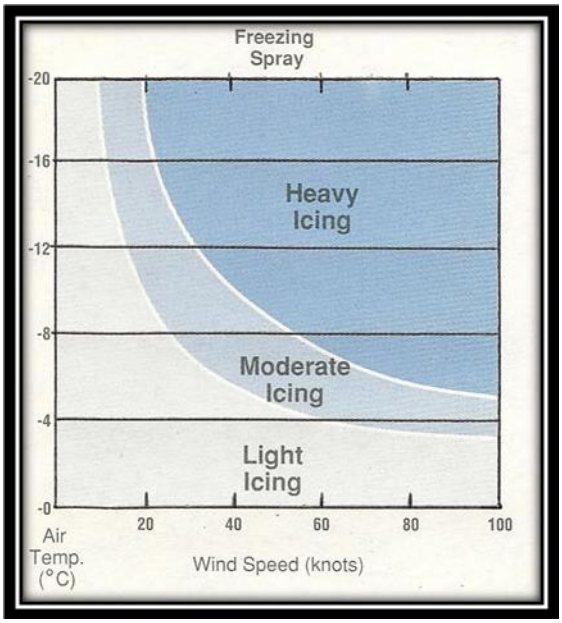


Figure 3.2-5 Icing conditions for marine structures.
Light – less than 0.7cm/h; moderate – 0.7 to 2cm/h; heavy – more than 2cm/h.
Adapted from *Marine Weather Hazards Manual*.

3.2.3 *Oceanography*

3.2.3.1 Circulation

Open ocean surface circulation is primarily wind driven and exhibits large scale features that persist for weeks to years. Near the coast, the non-tidally generated circulation is subject to rapid spatial and temporal variations due to transient variations in wind and run-off. They may be considered to be a geophysical random process which can be described statistically by means and averages which

practically translates into looking at prevailing seasonal conditions. The situation in Hecate Strait-Dixon Entrance has been aptly described by Thomson (1981)[1].

> *During November through February, the low fresh-water drainage from the land has but a minor influence on currents in the seaway. The reverse is true of the winds, which commonly blow with considerable vigor from the southeast over the entire north coast. To appreciate fully the importance of these winds to the long-term, non-tidal component of the flow within the seaway, the study should begin along the outer coast. In this region, southeast winds initially generate a downwind surface drift which is then deflected to the right by the earth's rotation[2]. This, in turn, leads to a net onshore Ekman transport[3] within the top 100 m or so of the water column. Where this transport is blocked by the coast there is an onshore accumulation of surface waters and a depression of the isopycnals[4], with only a partially compensating offshore transport at depth. Resulting pressure gradients are then balanced by the establishment of northward coastal currents in the upper layer. If the winds die, the piled-up surface waters collapse seaward and the current disappears. If the winds reverse to the northwest, the antithesis occurs; the surface Ekman transport is offshore, isopycnals are raised (upwelling), and the ensuing coastal current is southward.*

Surface currents that enter Queen Charlotte Sound encouraged by the persistent southeast winds will be directed northward into Hecate Strait. If the winds are weak to moderately strong, the flow will bear northward across the eastern portion of Dixon Entrance. However, if the winds are strong over the coast the northward transport will create a concentrated seaward flow along the north side of Dixon Entrance. During March to May the strength of the southeast winds lessen with a reduction in the onshore convergence of oceanic surface water and a weakening of the northward wind-generated current through Hecate Strait. During June to August winds are minimal and there is negligible wind-induced flow within the coastal seaway. The annual pattern re-establishes during September and October.

The effect of run-off is to superimpose a highly variable estuarine circulation on the tide and wind-generated circulations. A well defined estuarine circulation occurs in the eastern section of Dixon Entrance due to discharges from the Skeena and Nass rivers. Run-off has only a small influence on the surface currents of Hecate Strait.

A cyclonic gyre persists in the portion of Dixon Entrance between Prince of Wales Island and the northwest coast of Graham Island in both summer and winter. This is because in summer there are northwest winds and large run-off whereas in winter there are southeast winds and low run-off (Figure 3.2-6).

---

[1] Oceanography of the British Columbia Coast, Page 243.
[2] The Coriolis force
[3] The current drift associated with the Ekman spiral, first described by Ekman (1905). With increasing depth, the wind-induced current turns more and more to the right of the current above but with decreased speed.
[4] Lines of equal density

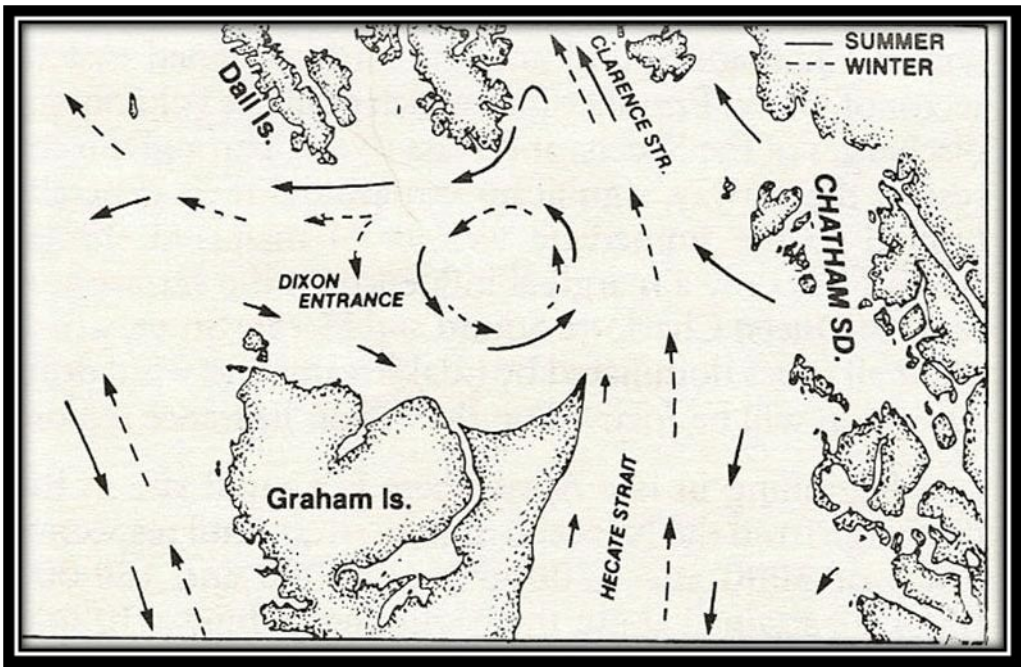


Figure 3.2-6 Non-tidal currents for summer (solid arrows) and winter (broken arrows).
Adapted by Thomson (1981) from Crean (1967).

3.2.3.2 Waves

Wind Waves

Because of the limited extent and partially sheltered nature of the Dixon Entrance-northern Hecate Strait seaways, wave conditions are typically less severe than in the open ocean to the west. There is a gradation within the seaway with average wave heights in Dixon Entrance lower than those in Queen Charlotte Sound to the south but higher than in Hecate Strait (Figure 3.2-7).

Dixon Entrance is protected from ocean waves that arrive from the southern quadrant of the compass. Swell entering Dixon Entrance from the west may travel a considerable distance before heights are reduced by refraction and breaking in gradually shoaling waters. Over Learmonth Bank in Dixon Entrance swell may be amplified by the focussing effect of the bottom contours. This bank is noted for the sizable rips formed when such amplified waves move against ebb currents over the bank.

In Hecate Strait and Dixon Entrance measurements of wave heights were taken at three locations between 1982 and 1984 (Table 3.2-1). Compared with data from other parts of the world, the statistics indicate that the wave fields are less severe than Hibernia on the Grand Banks of Newfoundland and comparable with the central North Sea. However, greater background energy, associated with swell, is present in Dixon Entrance. Hecate Strait is less exposed to swell but more severe in terms of the occurrence of large winter waves.



Figure 3.2-7 Wave heights (m) from Northwest gales onto west coast of the Queen Charlotte Islands. Hecate Strait is sheltered from high waves due to limited fetch.
Adapted from *Marine Weather Hazards Manual*.

Location	Time of Year	Significant Wave Heights (m)	
		Mean	Maximum
Hecate Strait	Mar – May	1.2	5.6
(53°21.2'N, 130°46.7'W)	Sep – Nov	1.6	8.2
	Dec – Feb	1.7	6.8
	Maximum wave height – not available		
Dixon Entrance			
West of Learmonth Bank	Mar – May	2.5	7.9
(54°26.9'N, 133°19.4'W)	Jun – Aug	1.6	4.3
	Sep – Nov	2.6	9.0
	Dec – Feb	3.2	8.8
	Maximum wave height	15.2 m	
East of Learmonth Bank	Mar – May	2.1	6.9
(54°26.2'N, 132°48.3'W)	Jun – Aug	1.2	3.5
	Sep – Nov	2.2	6.7
	Dec – Feb	2.9	7.3
	Maximum wave height	13.6 m	

Table 3.2-1. Selected Wave Data (BC Sailing Directions, Vol. 2, 1991)

Tsunamis

Tsunamis are waves of long period and wave length caused by strong earthquakes (magnitude 7 or larger on the Richter scale), volcanic eruptions, submarine landslides or avalanches into coastal waters. A tsunami event consists of a group of waves which spread rapidly from their source, moving at speeds

close to 500 knots (more than 900 km/h) in the deep ocean. The interval between successive crests ranges from 10 minutes to 40 minutes. The open sea height is only a fraction of a metre. As they approach shore, the speed decreases, the wavelength shortens and the wave height builds to the point they become very destructive. About 80% of all tsunamis occur in the Pacific and have reached the B.C. coast from as far away as Chile, Kamchatka, Kuril Islands, northern Japan and from as near as Alaska and the Aleutian Islands. Earthquakes local to the west coast have not produced major tsunamis. The largest tsunami on the west coast originated near Anchorage, Alaska in 1964 and was felt severest along the west coast of Vancouver Island.

3.2.3.3 Tides

Tidal Range[5]

Tides within Hecate Strait are mixed but in the northern Hecate Strait – Dixon Entrance region they are strongly semidiurnal (period of 12 h, 25 min). Shoaling causes the tidal range to increase from southern to the northern part of the strait and from west to east in Dixon Entrance. The range across the opening to Queen Charlotte Sound is about 3.0 m and increases to 4.8 m midway to 5.0 m at Prince Rupert. The range at the entrance to Dixon Entrance is 3.5 m and increases towards Prince Rupert as above.
The north-going flood through Queen Charlotte Sound meets the south-going flood from Dixon Entrance over an ill-defined region which is further north in winter than in summer (about 50 km further). There appears to be a partial reflection of the two floods that suggests standing wave behaviour. Current observations in the seaway support the standing wave idea.

Tidal Currents

The speed of tidal currents in the northern Hecate Strait-Dixon Entrance region, like the heights, is repeated every 12 hours and 25 minutes (half of a lunar day). In the open ocean tidal currents rarely exceed 0.1 knots but over the continental shelf and shoaling coastal waters the speeds are often significant.

Tidal currents in northern Hecate Strait off Rose Spit tend to be rectilinear (back and forth) due to restrictions of coastline and bathymetry. Floods move north and ebbs move south at maximum rates of approximately 50 cm/s (~1 knot). Ebb rates are approximately one-half this value (1/2/ knot). There is considerable distortion of the tidal currents near the broken shorelines of the mainland and off Graham Island. Details are found in the *Pacific Coast Tide and Current Tables* (published annually by the Canadian Hydrographic Service). The tables give not only tide predictions for major ports and tidal differences (in height and time of occurrence) for most other locations of interest, but also the times and speeds for slack water and maximum currents speeds for the more important passes and narrows.

The tidal streams within the central portion of Dixon Entrance vary. The flood streams are stronger on the southern side and ebb streams stronger on the northern side. A net cyclonic vortex is established over a tidal cycle with centre half way between Cap Chacon and Rose Spit (Figure 3.2-8). The strongest currents within the vortex (50 cm/s to 100 cm/s) occur around the outer circumference midway between high and low water. Toward the mouth of Dixon Entrance tidal streams tend to run east-west (flood – ebb).

[5] Difference in height between low tide and high tide.

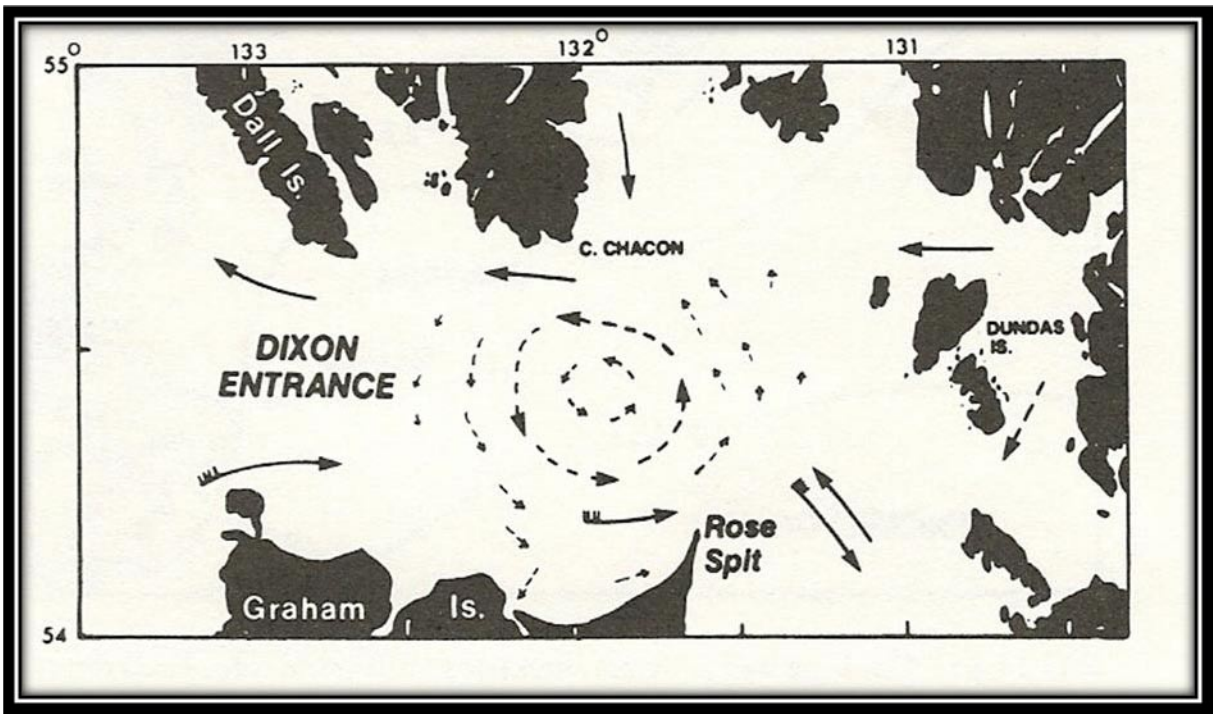


Figure 3.2-8 Tidal streams in Dixon Entrance and off Rose Spit.
Broken arrows show resultant cyclonic circulation created by asymmetric tidal current pattern.
Adapted by Thomson (1981) from Crean (1967).

3.2.3.4 Consequences and Concerns

In the area of the turbines, the non-tidal currents are of no concern with the exception that there is a net motion parallel to the east shore of Graham Island to the north. This will lead to a gradual erosion of the shoreline (depending on the composition of the beach) and an accretion of shoreline on the north coast. The tidal currents to the east of Graham Island and northern Hecate Strait are rectilinear in a north-south orientation so will move sediment during monopile foundation installation to the north and south of the site. The volumes indicated in the RPS (February 2009) report would be easily dispersed and offer no environmental impact.

The waves present engineering rather than environmental concerns. The wave periods suggest wave lengths that would pass almost unheeded through the monopod field (since wave length much greater than diameter of monopod). No alteration of the wave field would occur.

The Marine Weather Hazards Manual offers this warning: *Southeast gales and heavy seas in Hecate Strait affect shallow area from Cape Ball to Rose Spit ("The Hook"). Waves steepen and break on shallow bars and on tidal currents. With erratic patterns of rocks and sifting sandbars along the east coast of Graham Island, it is often safest to remain about five miles off the coast.*

The tidal range is large, and this has been well documented in the RPS (2008) report. The large tidal range could potentially present operational problems for servicing of turbines, though no problems are

expected for structural design. The tidal currents should not present operational problems but are not negligible (0.5 to 1.0 knots).

3.2.4 *Summary*

The Dixon Entrance – Hecate Strait region is well documented. The region has been of interest to the Fisheries Research Board of Canada (one of the precursors of Fisheries and Oceans) and was even the subject of a large hydraulic model investigation in the early 1960s (Boston, 1963).

The consequences of the physical setting (meteorology and oceanography) present primarily engineering and operational concerns for the project but no environmental concerns. The engineering and operational concerns are associated with extreme weather events (major storms), the generation of extreme seas (structural), the icing of structures and turbine blades, small but persistent coastal erosion (naturally occurring), possible scour around monopods, and the integrity of the poser line from the generating field to Ridley Island from geophysical disturbances (earthquakes, locally generated tsunamis).

3.3 MARINE WIND, WAVE AND TIDAL STUDIES FOR WIND FARM ENGINEERING

NaiKun Wind Development Inc commissioned studies by RPS Energy to support engineering design of the wind farm and submarine cable corridors. The studies undertook an assessment of wind, wave and water level conditions expected at the vicinity of the wind farm on the Dogfish Banks, on the east side of Haida Gwaii in the northern Hecate Strait.

This section was extracted from a report prepared by RPS Energy (2008).

3.3.1 *Data Sources*

Data from a number of sources were used to model the patterns and magnitudes of wind, wave and tidal behavior in the vicinity of the wind farm. The principle data sets included bathymetry, wind, waves and tides.

3.3.1.1 Bathymetry

Hydrographic survey data around the wind farm in the northern Hecate Strait was gathered by NaiKun Wind Developments Inc. Other more general bathymetric information of the Hecate Strait and adjoining sea areas was obtained from digital navigation charts supplied by C-MAP.

3.3.1.2 Wind, Wave and Tidal Data Sources

Wind data was obtained from both the National Oceanic Atmospheric Administration of the United States (NOAA) Alaskan Wave model for an offshore point at 50.5ºN, 130.0ºW, and two Canadian moored (C46183 and C46185) buoys located in the Hecate Strait. The buoys are located at 53.62ºN, 131.10ºW and 52.42ºN, 129.80ºW and record wind speed (both gust and mean hourly) and direction at hourly intervals. The NOAA model data on the other hand provided only mean hourly wind speeds and directions on a three hourly basis. Annual wind roses for the NOAA data point and the south Hecate Strait Buoy (C46185) are shown in Figure 3.3-1 and Figure 3.3-2 respectively.

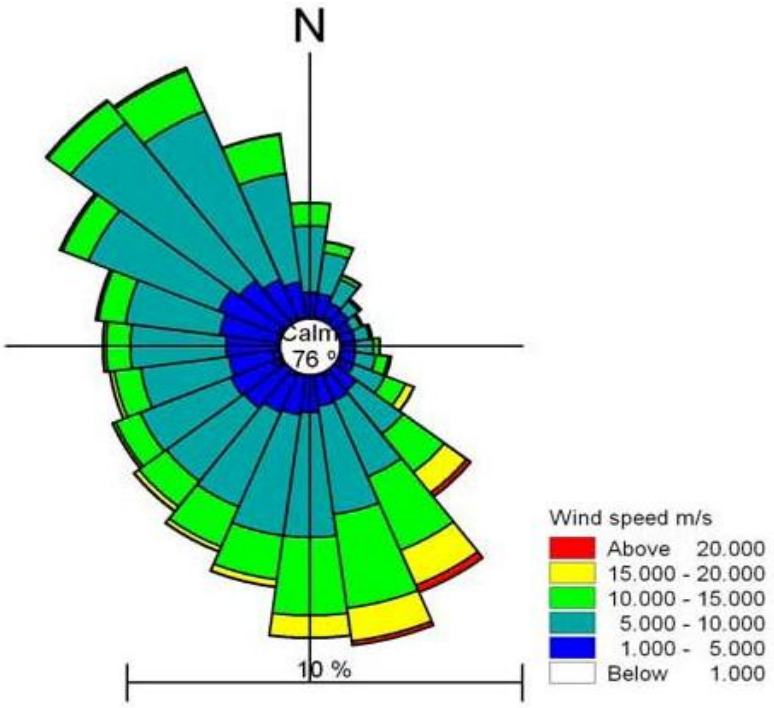


Figure 3.3-1 Annual Wind Rose, NOAA data Point 50.5ºN, 130.0ºW

NaiKun Wind Development Inc. Metocean Study North Hecate Strait, BC

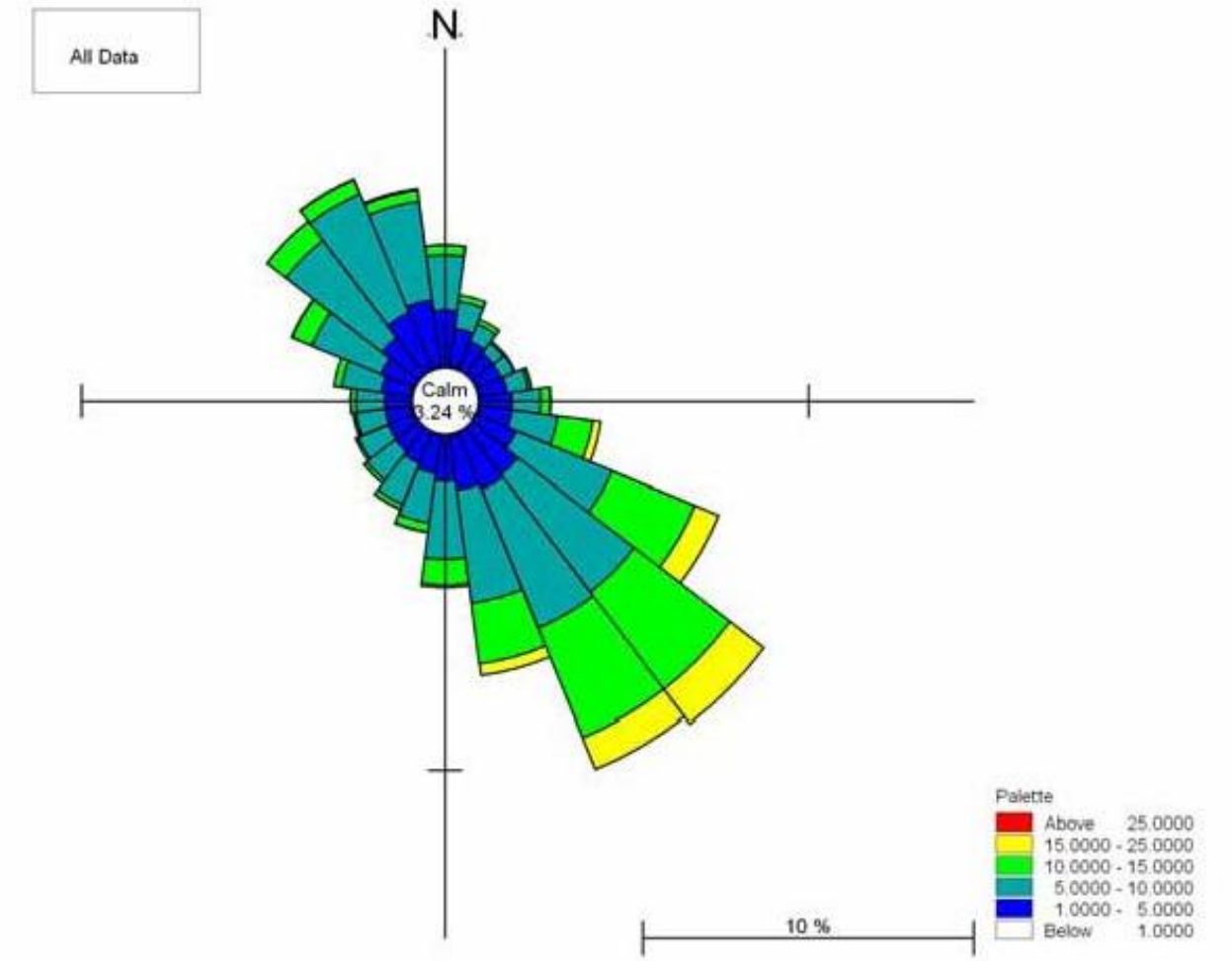


Figure 3.3-2 Annual Wind Rose, South Hecate Strait Buoy
NaiKun Wind Development Inc. Metocean Study North Hecate Strait, BC

Comparison of the two wind roses in Figures 3.3-1 and 3.3-2 indicate that Hecate Strait is exposed to waves which approach from the SE and NNW, but is relatively sheltered from the easterly and westerly sectors by the mainland and Haida Gwaii respectively. In terms of the offshore wind farm the most significant fetch is from the southerly sector and thus it is expected that the major storm waves will approach the wind farm from the SSE.

Offshore wave data was also obtained from the NOAA Alaskan Wave model for the offshore point indicated above. The dataset used consists of Significant Wave Heights, Mean Wave Periods, and Mean Wave Directions every three hours for the period July 1999 to November 2007 inclusive. The dataset also includes Mean Hourly Wind Speed and Mean Wind Directions recorded on a three hourly basis. Non-directional wave data for the period May 1991 to June 2008 was also obtained from the two Canadian moored buoys located in the Hecate Strait.

The AWAC measurement taken by Axys (2007) at the NaiKun Hecate Strait test platform in autumn 2007 indicated that the tidal amplitude at the proposed site was similar to that recorded at the Prince Rupert tide gauge. The tidal measurements made at Prince Rupert from 1991 to 2007 inclusive were therefore obtained to form the basis of the extreme water level and surge analysis for the proposed site.

3.3.1.3 Analysis of Datasets

The various datasets for wind, waves and water levels were analyzed to obtain extreme values using the MikeZero EVA tool and the Mike21 model. These tools are designed to fit a range of theoretical probability distributions to observed or predicted series of data values.

3.3.2 *Winds*

NOAA data compiled and modelled for the wind farm was analyzed to produce the wind rose shown in Figure 3.3-3, showing dominant winds from the SE.

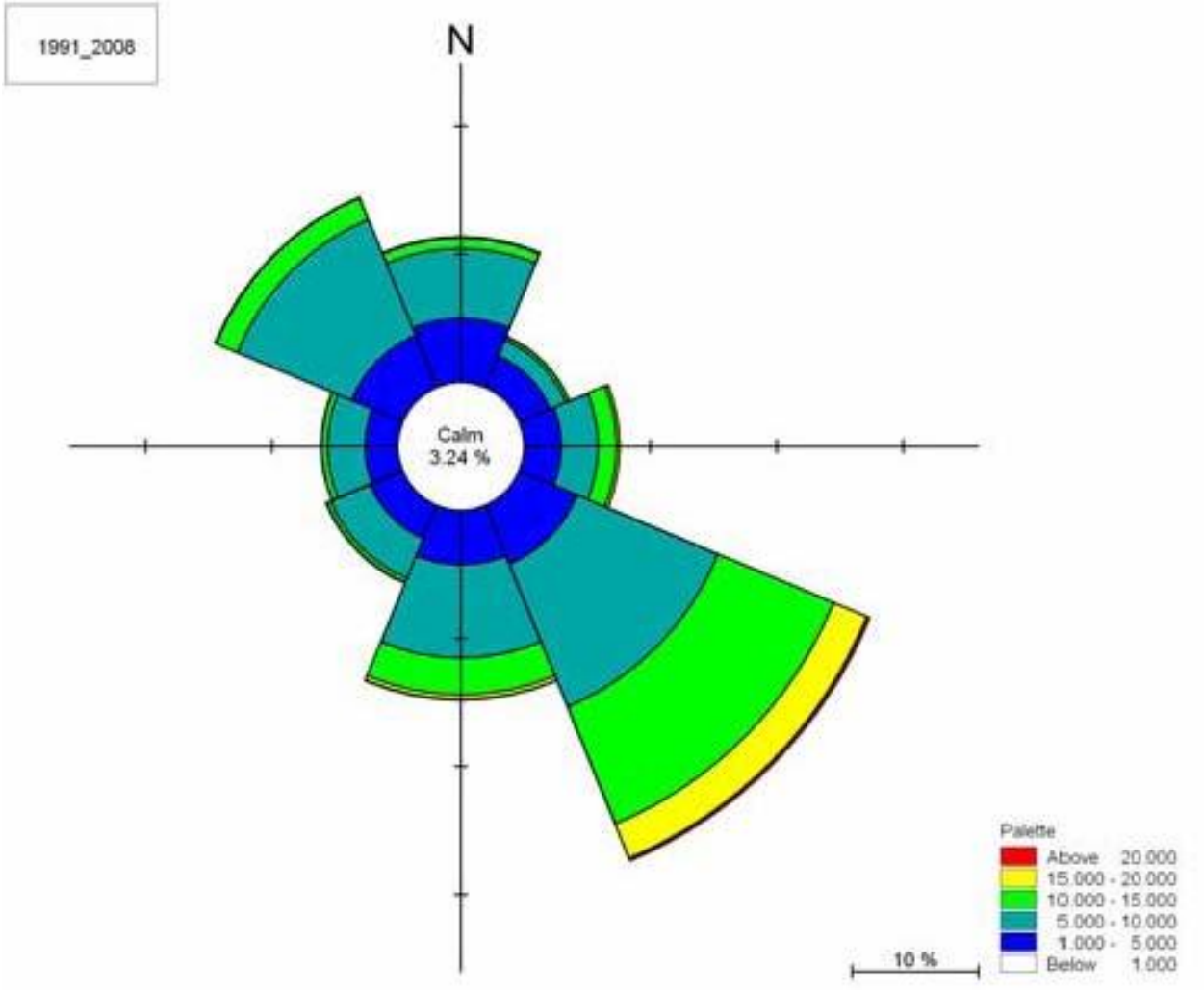


Figure 3.3-3 Annual Wind Rose for the Wind Farm Compiled from Hecate South and North Buoys

3.3.3 *Waves*

Wave and tidal conditions were modelled using available information and data collected in the wind farm in 2007 (Axys, 2007; ASL, 2007).

The wave transformation analysis used to characterize the inshore wave climate was undertaken using the MIKE21NSW wave model. This model, developed by the Danish Hydraulic Institute, is a stationary, directionally decoupled parametric wind-wave model, which describes the propagation, growth and decay of short-period and short-crested waves in near shore areas. The model takes into account the effects of refraction, shoaling due to varying depth, wave current interaction, local wind generation and energy dissipation due to bottom friction and wave breaking. The inputs to the model include directional distribution of wave energy at the offshore boundary plus the wind field within the model area. In the case of directions where the waves are generated in front of a land boundary (e.g. northerly and easterly waves) the waves are generated by the wind field alone.

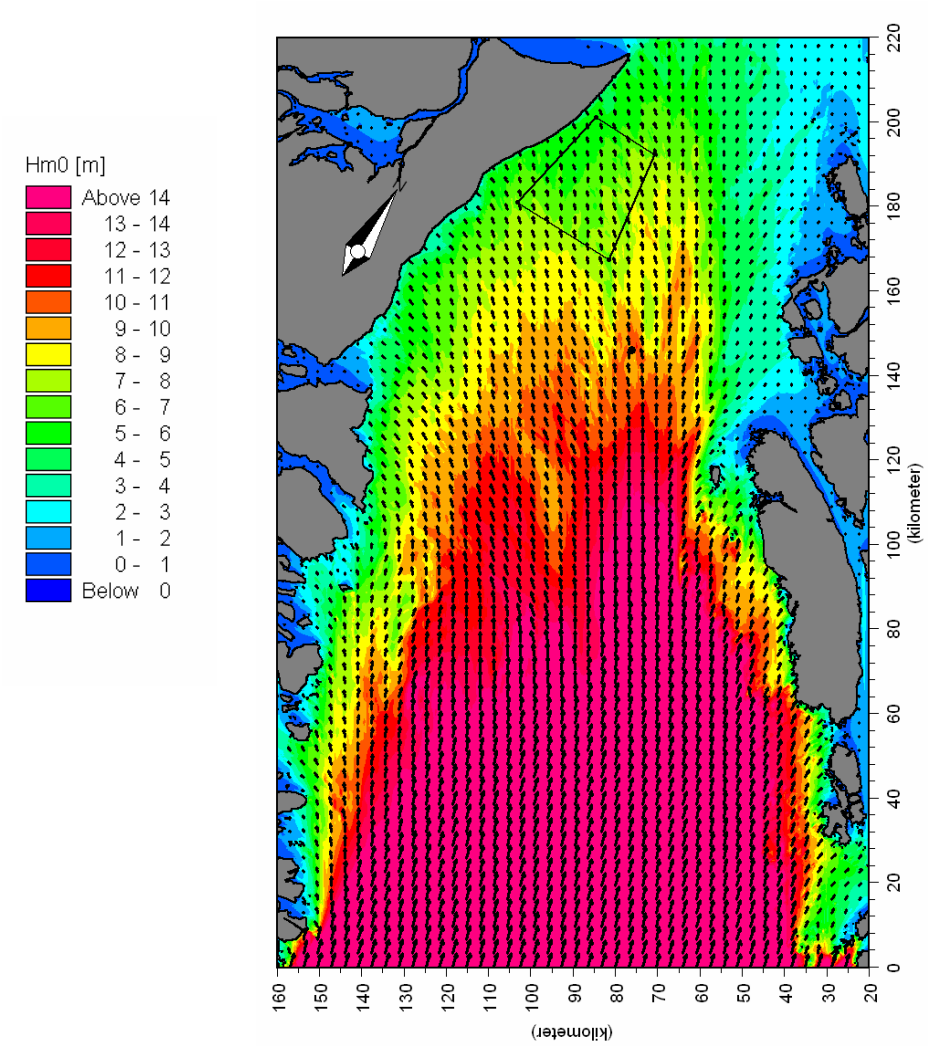


Figure 3.3-4 **Wave Heights 1 in 50 years Waves Attenuated in Shallow Water**
Source: RPS, 2008

The models were used to produce maps showing wave heights projected for different frequencies of events ranging from 1 in 5 years to 1 in 100 years. Figure 3.3-4 shows the way 1 in 50 year wave heights are distributed in the Hecate Strait and around the wind farm. Wave height in the wind farm is attenuated by the shallower waters.

Figure 3.3-5 shows the same wave height distribution in more detail in the vicinity of the wind farm.

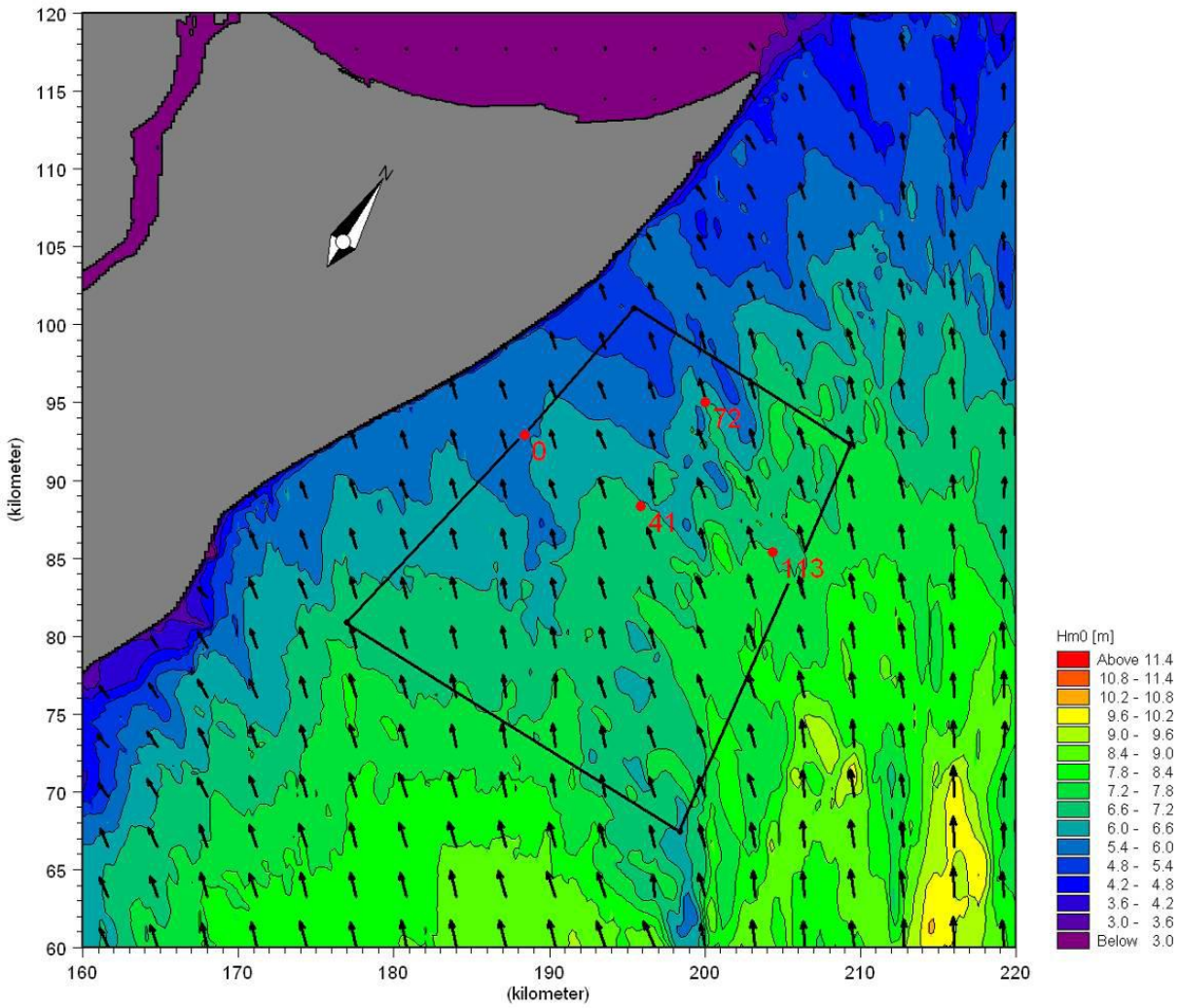


Figure 3.3-5 Significant Wave Height and Mean Direction, 1 in 50 year Storm from 165°

3.3.4 *Tides*

The tidal flow characteristics of the area were determined using a suite of two-dimensional depth integrated hydrodynamic models, Mike21 HD developed at DHI, Denmark. The HD Module is a 2-dimensional, depth averaged hydrodynamic model which simulates the water level variations and flows in response to a variety of forcing functions in lakes, estuaries and coastal areas. Using inputs for bathymetry, bed resistance coefficient, wind field, hydrographic boundary conditions, etc., the model generates water levels and flows on a rectangular grid covering the area of interest.

The results of the tidal modeling for typical spring tide flood and ebb flow patterns in the Hecate Strait are shown in Figure 3.3-6 and Figure 3.3-7 respectively. Both of these figures indicate that tidal current speeds within the Hecate Strait are generally low and therefore wave-current interaction will not have a significant impact on wave climate at the proposed wind power development site.

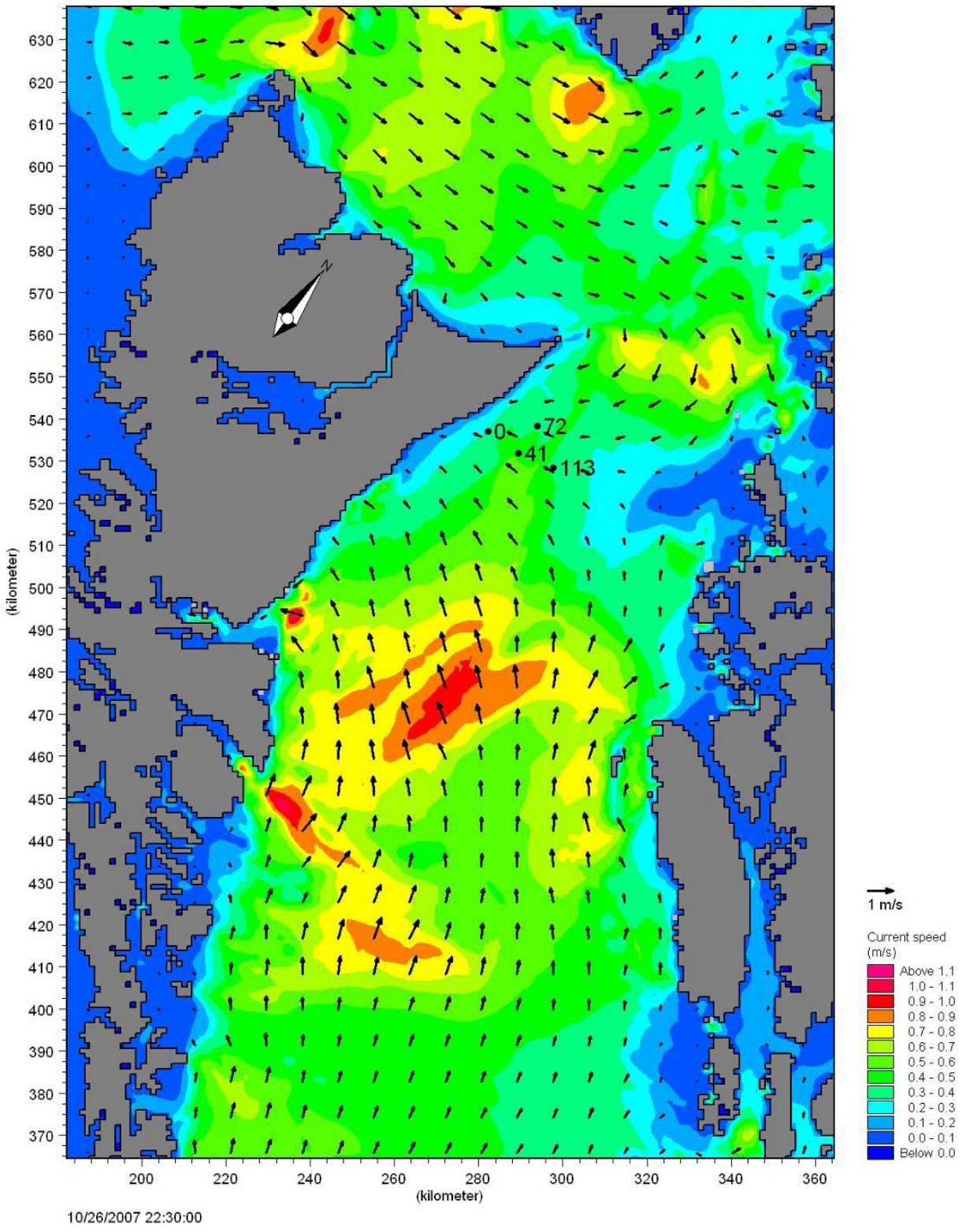


Figure 3.3-6 Typical Flood Spring Tidal Flows – Hecate Strait

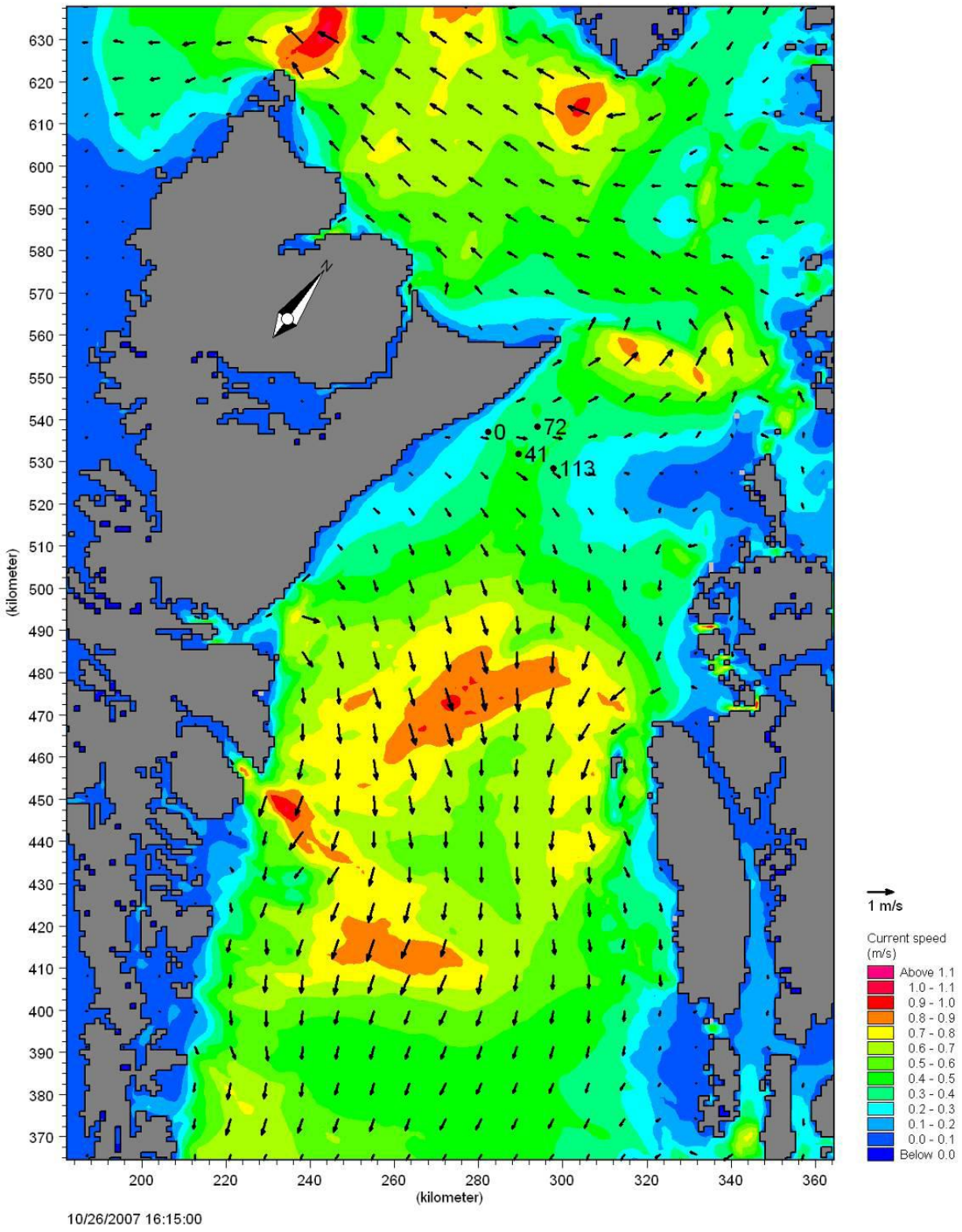


Figure 3.3-7 Typical Ebb Spring Tidal Flows – Hecate Strait

3.4 REGIONAL GEOLOGY OF THE DOGFISH BANKS AND ENVIRONS

This section is extracted from the RPS report entitled, Regional Engineering Geological Assessment of Hecate Strait, Offshore British Columbia, for Proposed NaiKun Windfarm Development March, 2007), prepared for NaiKun Wind Development Inc.

3.4.1 Data Sources

The Hecate Strait area has not been studied intensively but a regional seismic reflection survey with sea bed sample acquisition has been performed by the Geological Survey of Canada (GSC), the Pacific Geosciences Centre (PGC) and Natural Resources Canada (NRC). The seismic data from two cruises (PGC 91006 and PGS 94007) were examined. They comprise:

Geophysical data sources:

- Sidescan sonar (100 kHz to 120 kHz);
- Seistec surface towed boomer;
- Huntec Deep Towed subsurface boomer;
- Airgun (5 cubic inch).

Sea bed sampling sources:

- Van Veen and Shipek bottom grab samplers;
- Large volume IKU grab sampler;
- Gravity and vibrocoring systems to obtain subsurface samples.

The location of all existing data (seismic and sidescan sonar data) along with the location of grab samples and offshore cores are shown in Section 3.5 on Figures 3.5-8 to 3.5-11.

Seismic line separation is in the order of 10 km and the regional grid and the seismic data were calibrated by a limited number of piston and vibrocore samples.

Other data presented are based on available data in published texts.

It should be noted that the thickness values of any units interpreted from the geophysical data are based on an assumed velocity of sound in the soils of 1600 m/s and a velocity of sound in seawater of 1480 m/s. The values used are uncalibrated estimations as no temperature/salinity profile data is available. Therefore the thickness data should only be used as an approximate value.

It should also be noted that navigational accuracy of the seismic profiles is variable but may be in error by up to 200 m (V. Barrie, Pers Comm. nd RPS Energy).

3.4.2 Regional Environmental Conditions

3.4.2.1 General

The regional environmental conditions summarized in the following sections are based on the analysis of the datasets defined in Section 3.4.1 of this report. This data set is regional and therefore only a broad overview can be presented of the conditions presented in each of the following sections. The study area is from 130^0 W to 130^0 W and 54^0 N to 54^0 40' N.

3.4.3 Bathymetry and Current Regimes

Water depths range from less than 10 m Lowest Astronomical Tide (LAT) within the north-west corner of the study area to in excess of 30 m in the south-east corner of the study area. To the east of the proposed development area water depths in Hecate Strait attain in excess of 50 m, mainly associated with a north-south oriented channel.

Strong semi-diurnal tidal currents combined with intense storms from the south-east, create a very energetic wave regime within these relatively shallow waters of Dogfish Banks

The bathymetry map exhibits two prominent areas of raised sea bed where the sea bed is generally sloping to the east. The area first extends south-south-east from the main shallow platform area to the south-east corner of the study area. The second area occurs as an isolated ridge to the east of the main shallow shelf area. In both areas the sea bed falls away from approximately 10m LAT to 20m LAT. The possible origins of these bathymetric features are discussed in later sections. The limited available data does not allow us to provide detailed information of the range of current velocities affecting the area. A summary of the maximum current directions and magnitudes is presented below in Figure 3.4-1. The size of the arrows in Figure 3.4-1 is proportional to the magnitude of the current, the largest being 320 cm/s (6kn) and the smallest 20cm/s, (0.4kn) with an average of approximately 50cm/sec, (1kn) in the centre of Hecate Strait. Near bottom tidal currents are generally in the region of 15 to 25cm/sec, (0.3 to 0.5kn).

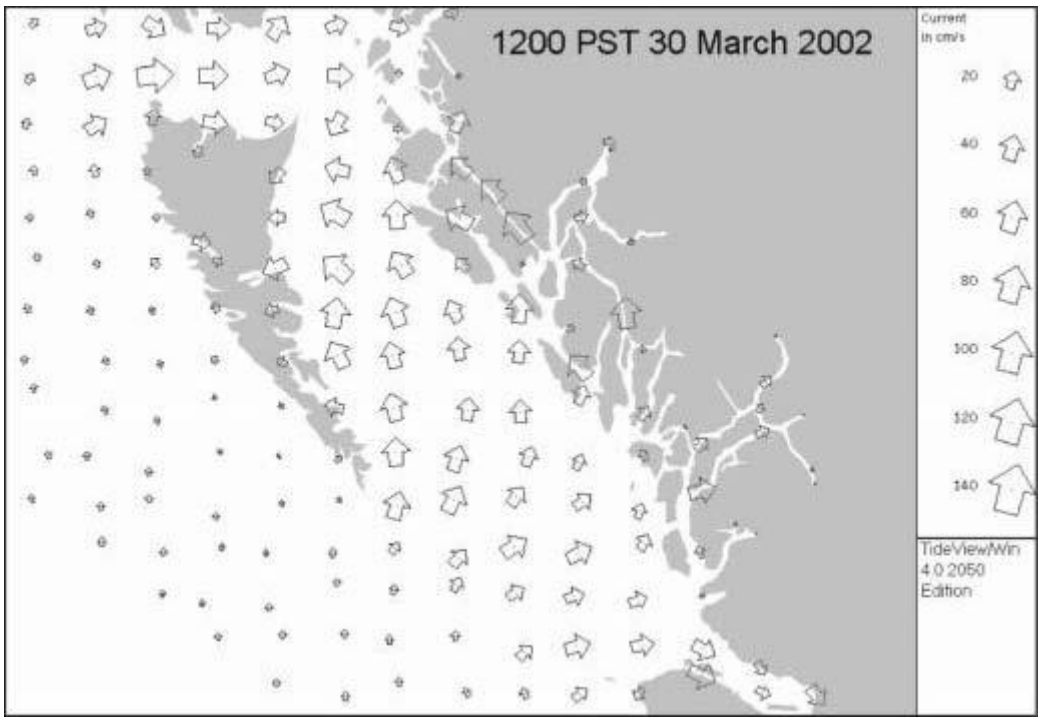


Figure 3.4-1 Current Direction and Magnitude within Hecate Strait and Surrounding Area
(Thomson, 1981)

Storm wave heights of up to 12 m and tidal ranges from 5 m to greater than 8 m also contribute to the highly active environmental conditions within the area. The tidal range increases from south to north along the eastern coast of the Queen Charlotte Islands. A series of current mooring stations are located in and around Dogfish Banks, the data from which should be accessed in order to provide a basic assessment of the current dynamics. It should however be noted that the system of weather buoys located in and around Queen Charlotte Sound indicate that the Dogfish Banks area is the most sheltered in the region, with an annual significant wave height of approximately 1.3 to 1.6 m.

3.4.4 Seabed Features and Bedforms

3.4.4.1 General

The shallow water of the study area, combined with the hard nature of the sandy and gravelly seafloor and interpreted high sediment mobility, makes the Dogfish Banks a very active environment for foundation design and construction. The site investigation tools employed in the regional geophysical survey have, however, allowed a preliminary assessment of likely sea bed feature distribution and thickness.

Throughout the study area, sand ridges and sand lenses with a thickness of 10 cm to 30 m occur above the lag surface. The lag surface is interpreted to equate to an unconformity marking 2500 years of exposure prior to the most recent phase of a rise in sea level. The surface of the unconformity is covered by gravel, cobble and boulder armour.

An overview of the seabed features mapped across the Hecate Strait is presented in Figure 3.4-2.

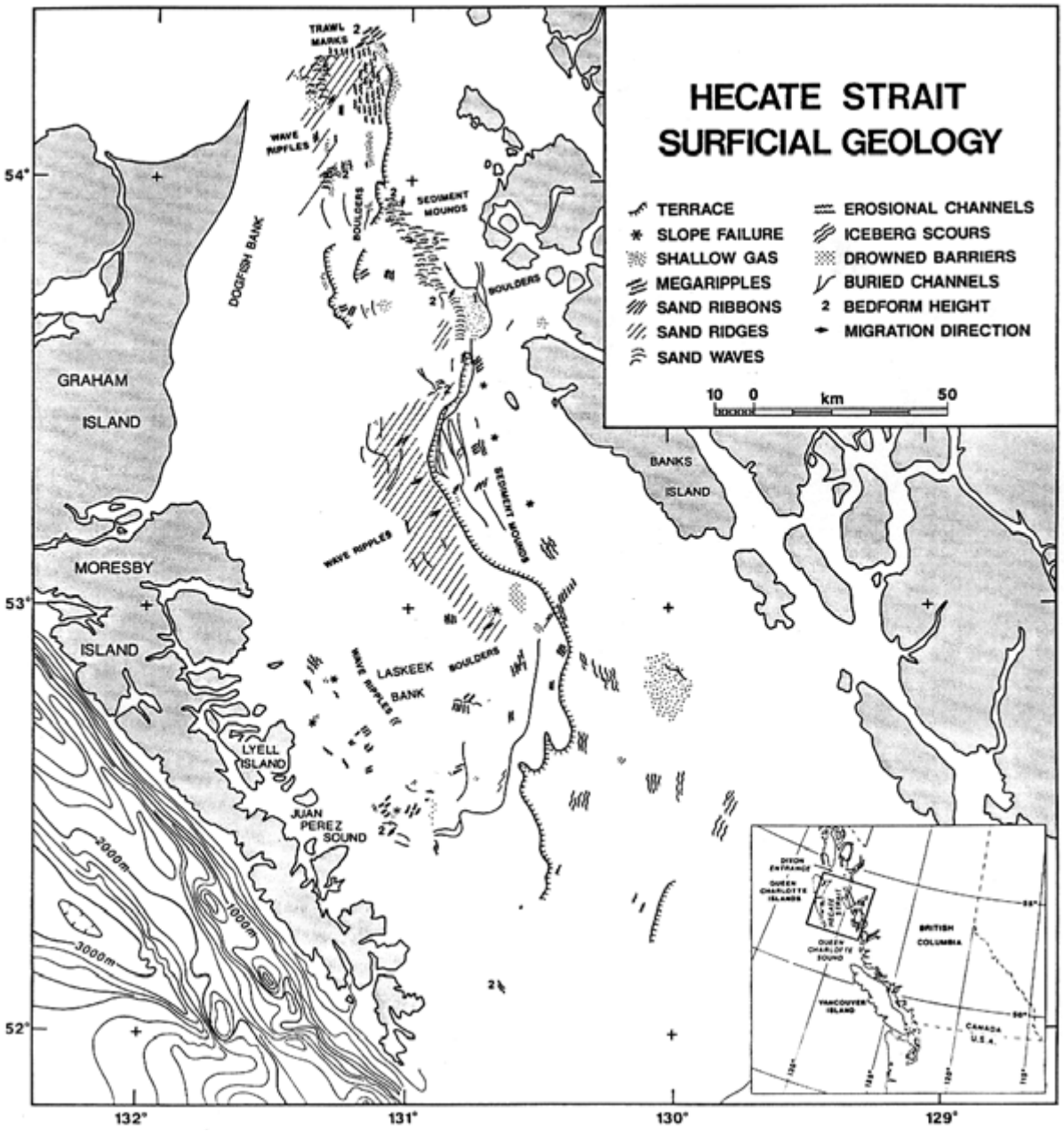


Figure 3.4-2 Seabed features and Shallow Geohazards of Hecate Strait and Surrounding Area
Barrie (1988)

3.4.4.2 Small to Medium Scale Surface Bedforms

Interpretation of the sidescan sonar records reveal a wide variety of bedforms in the Dogfish Banks area which include: sand ripples along with small and large sand waves, gravel waves, gravel ribbons, sand ribbons, sand ridges and obstacle marks (Stride 1982 - Appendix B, Figures B-1 and B-2). The type of bedform produced on the seafloor is dependant on current strength, sediment supply and sediment grain size. The shape of the bedform is also determined by current strength and oscillatory versus unidirectional water motion.

Sediment transport direction is determined by the cumulative effect of all current forces. Barchan (horseshoe-like sand features), sand ribbons, gravel waves and obstacle marks are observed throughout the region and indicate current velocities in the region of 150 cm/sec. At present however, the level of survey detail is insufficient to accurately determine the density, localized velocity variations and migratory trends.

3.4.4.3 Sand Ridges and Sand Banks

Sand ridges and sand banks are the largest active features interpreted to be present on Dogfish Banks. Both of these features are formed above the basal lag deposit surface: Sand ridges are the most widely sampled unit in the study area. These bedforms are highly variable and indicative of active seafloor mobility. Large sand ridges of different origins and ages, with ridge crests oriented northeast to southwest, dominate the general area.

The depth of current reworking and volume of sediment mobility on Dogfish Banks is not accurately known from the available data. All the cores referenced for the purposes of the study, have sampled the surface unit which ranges in thickness from less than 10 cm to a thickness interpreted to be greater than 30 m from interpretation of the seismic data. In places these sand bodies contain active surface bedforms indicative of sediment mobility.

Active bedforms are interpreted to be more common across the eastern part of Dogfish Banks, probably associated with the more exposed offshore area. The lateral and extent and depth of sediment mobility requires further detailed investigation with an appropriately designed survey. The surface morphology of some 8 m high sand ridges in the eastern part of the study area show a clear stoss (steep) sides and lee sides (shallow sloping). Sidescan sonar records reveal smaller active bedforms on surfaces of the sand ridges. It is not known at present if these sand ridges are actively migrating across the sea bed

3.4.5 Pockmarks and Shallow Gas

It should be noted that regional petroleum surveys have identified numerous gas seeps in the general Queen Charlotte Basin area, interpreted to be due partly to the evolution of biogenic gas from Holocene sediments. The seepages appear as a series of shallow craters in the sea bed where gas escapes. Available data indicate that these pock marks are confined to the eastern part of Hecate Strait and to the south of Dogfish Banks. Sediments containing gas are generally near the contact of glacial till with an underlying sand or gravel unit. These shallow gas seeps are also present over the western side of Hecate Strait where a thin sequence of sands are interpreted to lie directly on Tertiary bedrock but these may be confined to areas to the south of Dogfish Banks.

3.4.6 Seabed Sediments

Based on the available geotechnical spot data reviewed, sand and gravel are interpreted to cover most of the seafloor and to be the dominant material in most if not all of the active bed forms. Gravel lag deposits are interpreted to locally crop out at the seafloor between the sand ridges, as observed on the limited sidescan and seismic data.

Based on the limited available geophysical sub-bottom (seismic and sidescan) data and the bathymetric data, a gravel lag (coarse sea bed deposits left behind after removal of finer material) is interpreted to be exposed over approximately 30 to 50 percent of Dogfish Banks. Some of these gravels are interpreted to contain material up to boulder size. Based on available data, gravel lag is interpreted to be present at the seabed over large parts of the south-west corner of the Banks.

These analyses were provided by the PGS and are based on analysis of a variety of bottom grab samples including material obtained from Van Veen, Shipek and large volume IKU sampler. Subsurface geotechnical cores were obtained by gravity and vibrocoring systems.

Sand ridges are interpreted to be composed of dense and possibly very dense sand, densified due to wave action. Similar features are encountered in other offshore areas. Based on the bedform characteristics observed from the data reviewed, sand waves appear to be most active in the eastern regions of the study area.

Interpretation of the reviewed data suggests that there is significant variability in thickness of the surficial sands These records suggest that sand thickness ranges from less than 0.5m to 12 m over a horizontal distance of as little as 300 m, although a more complete data set may reveal a greater range of sea bed sediment thickness variation.

Measured sediment transport rates from previous surveys conducted within the area are in the order of 0.0005 kg/m2/s but can be as high as 0.05 kg/m2/s during storm events. These transport events produce regions of net erosion and deposition within the Dogfish Banks area.

3.4.7 Quarternary and Solid Geology

3.4.7.1 General

About 14,000 years ago glaciers up to 2500 m thick blanketed and loaded the mainland coastal mountains, (Clague 1983). A smaller glacier, approximately 500 m thick covered most of Graham Island. As this smaller glacier receded, it deposited several tens of meters of well sorted outwash sands and gravels on north eastern Graham Island, (the largest island within the Queen Charlotte group, Figure 3.4-4), (Argonaught Plain) and on Dogfish Banks, along with areas of lodgement till (material deposited under the ice sheets).

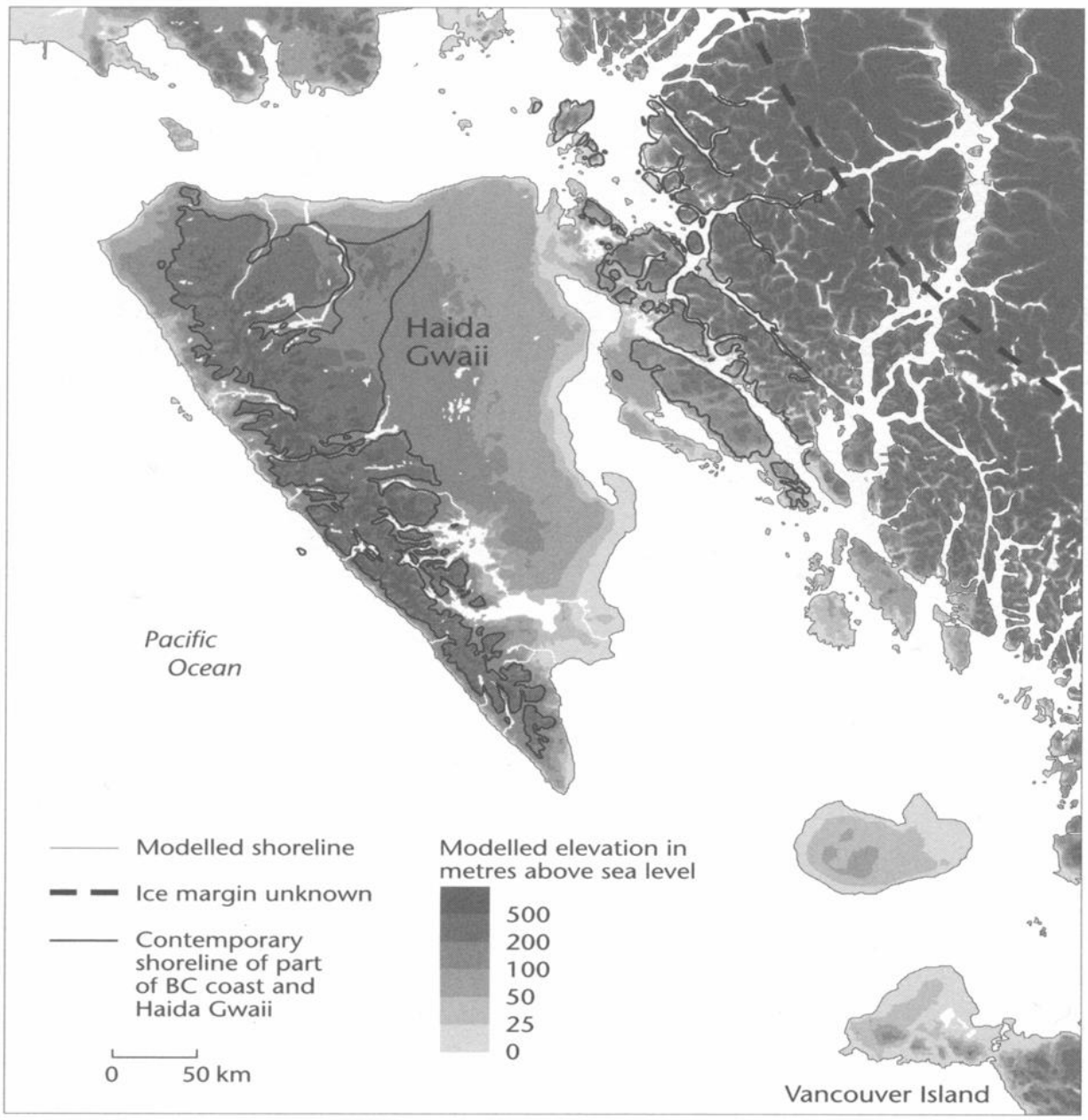


Figure 3.4-3 Sea-Level reconstruction 12,000 years before the present if sea-level is lowered by 150m

(Fedge and Mathewes 2005)

An interpretation of the Quaternary (glacial) and solid geology is presented in the following sections and is based on a very limited amount of physical data, most of which originates from outside the immediate study area. Interpretations of the presence and distribution of glacial soils are primarily based on the very limited amount of geophysical and geotechnical data available from within the general Dogfish Banks area.

The glacial units were deposited during periods when sea levels were significantly lower than today (Figure 3.4-3). A generalized map showing the interpreted direction of ice retreat is presented in Figure 3.4-4.

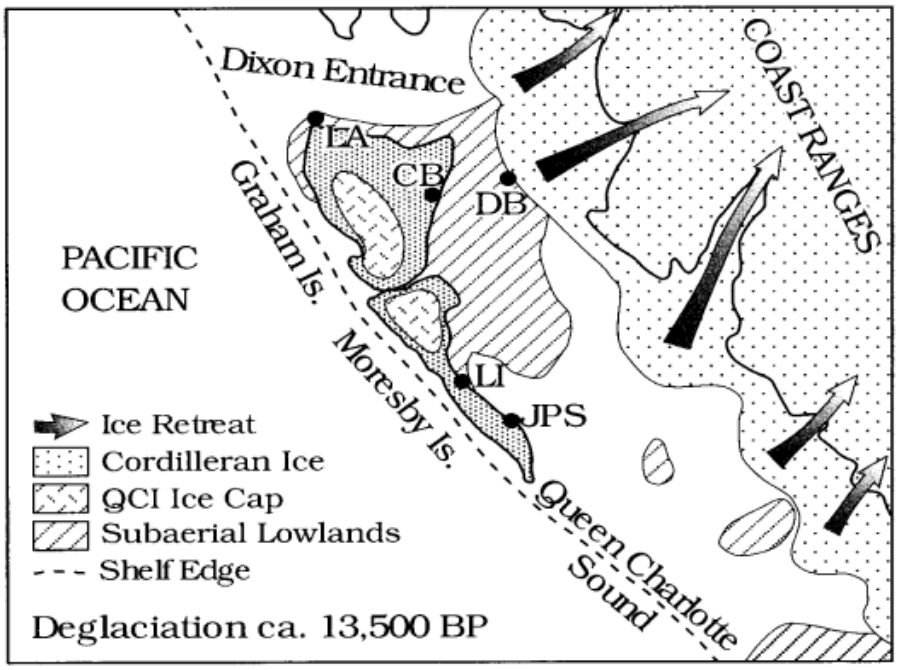


Figure 3.4-4 General Ice Retreat Map (Fedge and Mathewes 2005)

It should be noted that the linear north-south oriented sea bed features may represent glacial moraines deposited at the front margins of ice sheets. If this is so, then based on analyses of similar "terminal" moraines elsewhere, a range of material sizes from clay to boulders may be present.

3.4.7.2 Summary of Sea Level Rise

Subsequent to glacial retreat, sea levels along the western Canadian coast are interpreted to have risen to the same elevations as the present coast by about 9400 years before the present (BP), reaching a maximum of approximately 16 m above present sea level by approximately 8900 years BP, and retreating to the present levels by approximately 2000 years BP. The Dogfish Banks study area was subjected to similar sea-level changes and was dry land for about 2500 years.

Erosion along rapidly migrating shorelines produced an erosional unconformity across all the Quaternary strata, and where exposed, solid geological units. This unconformity is most clearly seen at the top of the glaciomarine sediments where truncated beds are clearly recognized. A residual gravel and boulder lag surface marks this erosional episode. The lag horizon is interpreted to occur across the entire study area and is interpreted to crop out at the seafloor over approximately 50 percent of the area. In other offshore areas of Canada, desiccation of seabed sediments by sub-aerial exposure has produced a "Hard Pan" layer of iron cemented sands. This may exist in the study area but has not been documented from the available data.

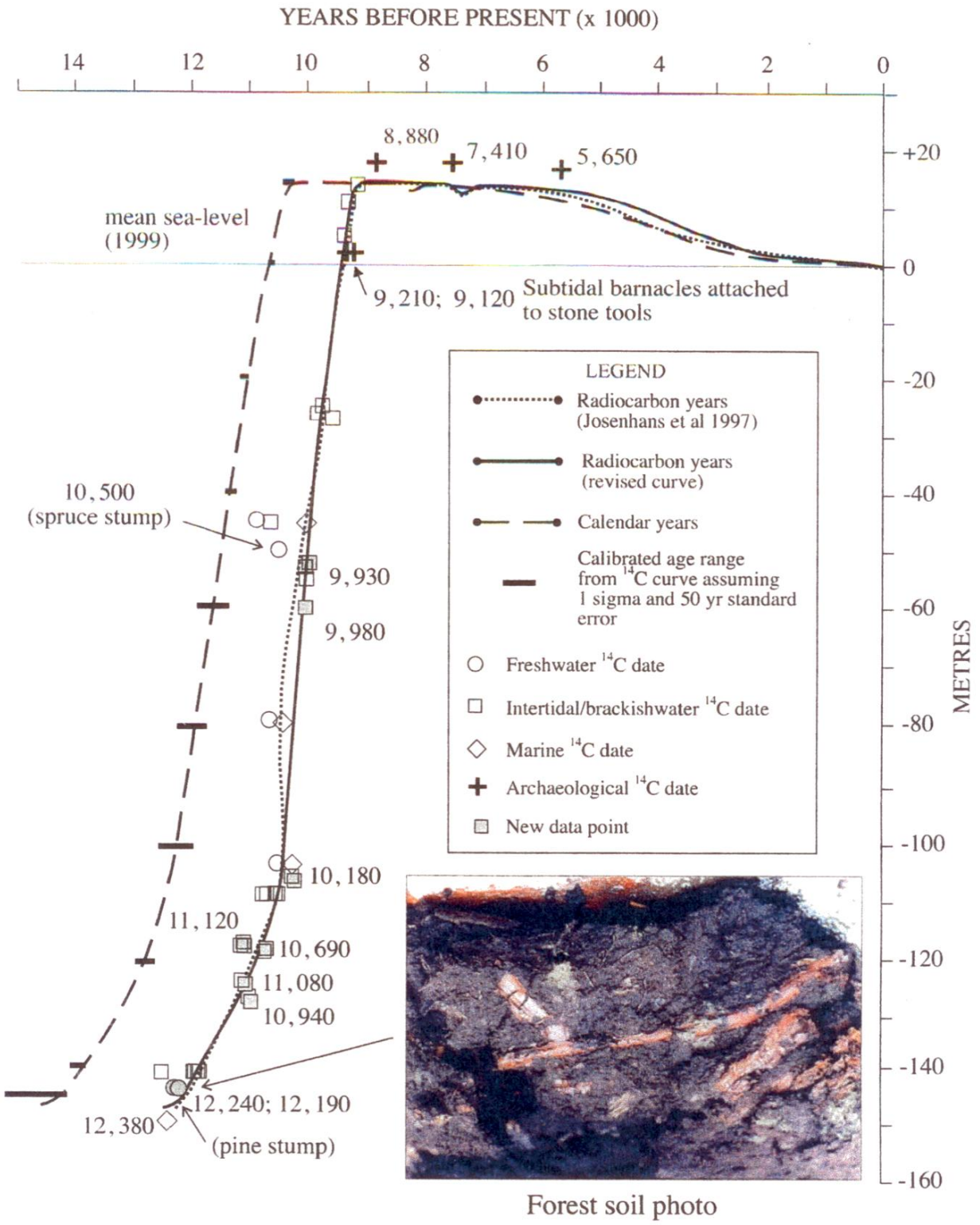


Figure 3.4-5 General Sea Level Curve for Juan Perez Sound (Southern Queen Charlotte Islands)

It should be noted that the remains of organic material, predominantly tree stumps, have been recorded at various elevations within the sea level curve. Given the nature of the low relief across the Dogfish Banks area, it may thus be possible that other units of organic origin are present beneath more recent deposits across the study area.

3.4.7.3 Summary of Glacial Units

A summary of the interpretation of glacial soils is presented in the following sections and is described from youngest to oldest.

Glaciomarine Sediments

The glaciomarine sediments are interpreted to have a similar origin and age to those outcropping on Graham Island at Cape Ball as described by Clague et al, 1982b. The silts and clays were deposited in a marine environment fed from glacial outwash rivers.

These sandy clays were deposited in the distal regions of the glacial outwash margins up to 40m thick. The units were deposited within local bedrock depressions and in paleoriver valleys that once flowed across Dogfish Banks.

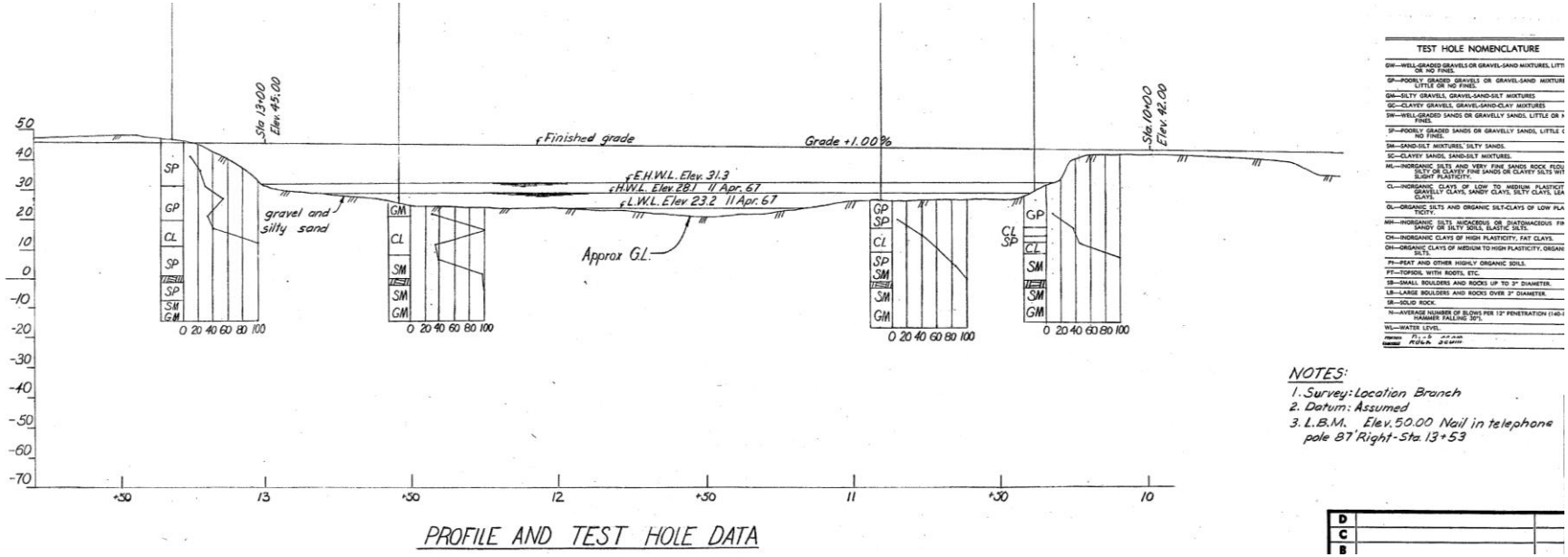
Stratified glaciomarine sediments occur within paleo-channels and infilling bedrock. These sediments were sampled by Core VEC94A-21 where the core penetrates the surface sand/gravel. Although there is no evidence of significant exposure of soft clay within the study area, soft clay was encountered in the upper section of Core TUL91C-33. This core was in a localized bathymetric low and is indicative of what may occur below the surficial sands.

Ice Marginal Glacial

Outwash sands and gravels (material deposited from glacial melt water) are generally confined to the western part of the study area. According to the seismic data these sediments are poorly defined and weakly stratified. Within the study area these sediments were not penetrated in vibrocores collected in research surveys.

Profile and borehole data for Tlell River Bridge located about 25 km southwest of the study area are shown in Figure 3.4-6. They illustrate the rapid variation in soil types both laterally and vertically. The profiles presented below may be a lateral equivalent of the outwash gravels and sands which underlay the boulder and cobble lag layer across the study area. The numeric values tabulated next to the profiles are N values obtained from in-situ Standard Penetration Test, (SPT).

Figure 3.4-6 Tlell River Bridge Geotechnical Profile



Glacial Till

A unit interpreted as a boulder clay (and which may form a lodgement till), lies above the bedrock surface and is interpreted to occur particularly across the deeper areas, in the vicinity of the eastern margin of the Dogfish Banks. Material interpreted to comprise fine grained and well stratified glaciomarine sediments were clearly defined, though restricted in distribution. Based on available data, they are interpreted to be generally confined to localized depressions on the bedrock surface or within subsurface paleo-channels. Shear strengths of this cohesive material are interpreted to range from stiff to hard, (75 kPa to 300 kPa)

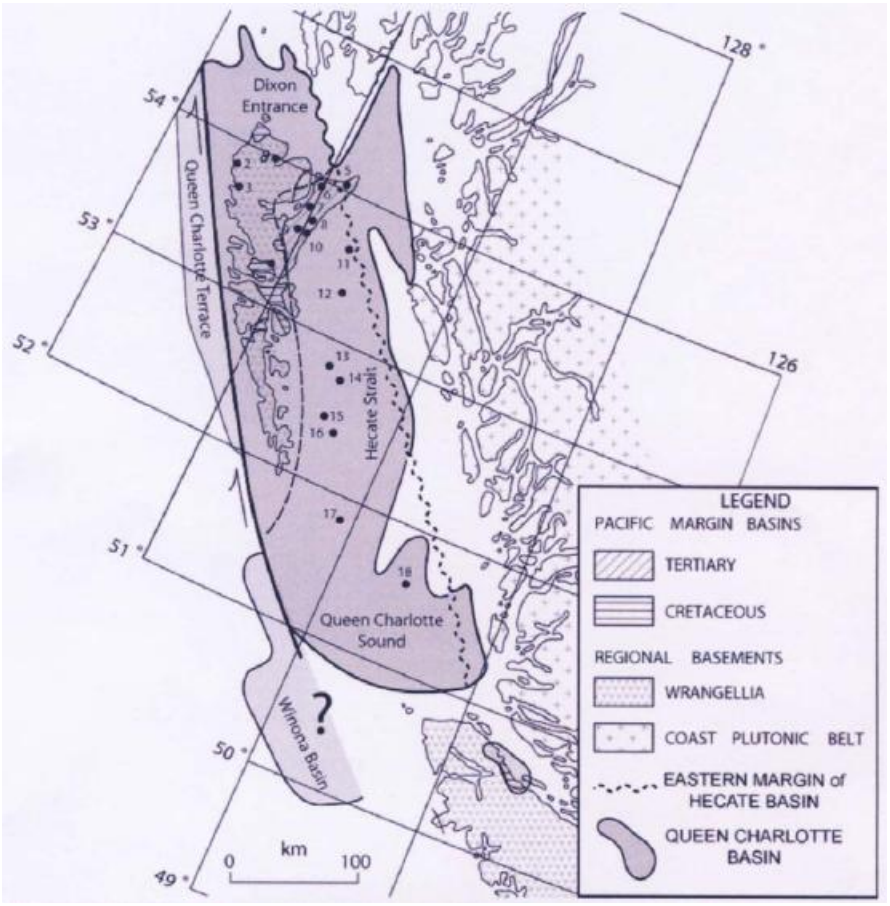


Figure 3.4-7 Queen Charlotte Basin Showing Overview of Stratigraphic Systems and Exploratory Wells, (after Hannigan et al, 2001)

3.4.7.4 Solid Geology

General

The solid geology of the Queen Charlotte Basin area is complex and is dominated by the structural north-south orientated faults that have controlled deposition. The solid units identified within the area are summarized in Figure 3.4-8 and presented as a simplified map in Figure 3.4-7. It should be noted that the locations listed 1 through 18 are previously drilled exploration wells.

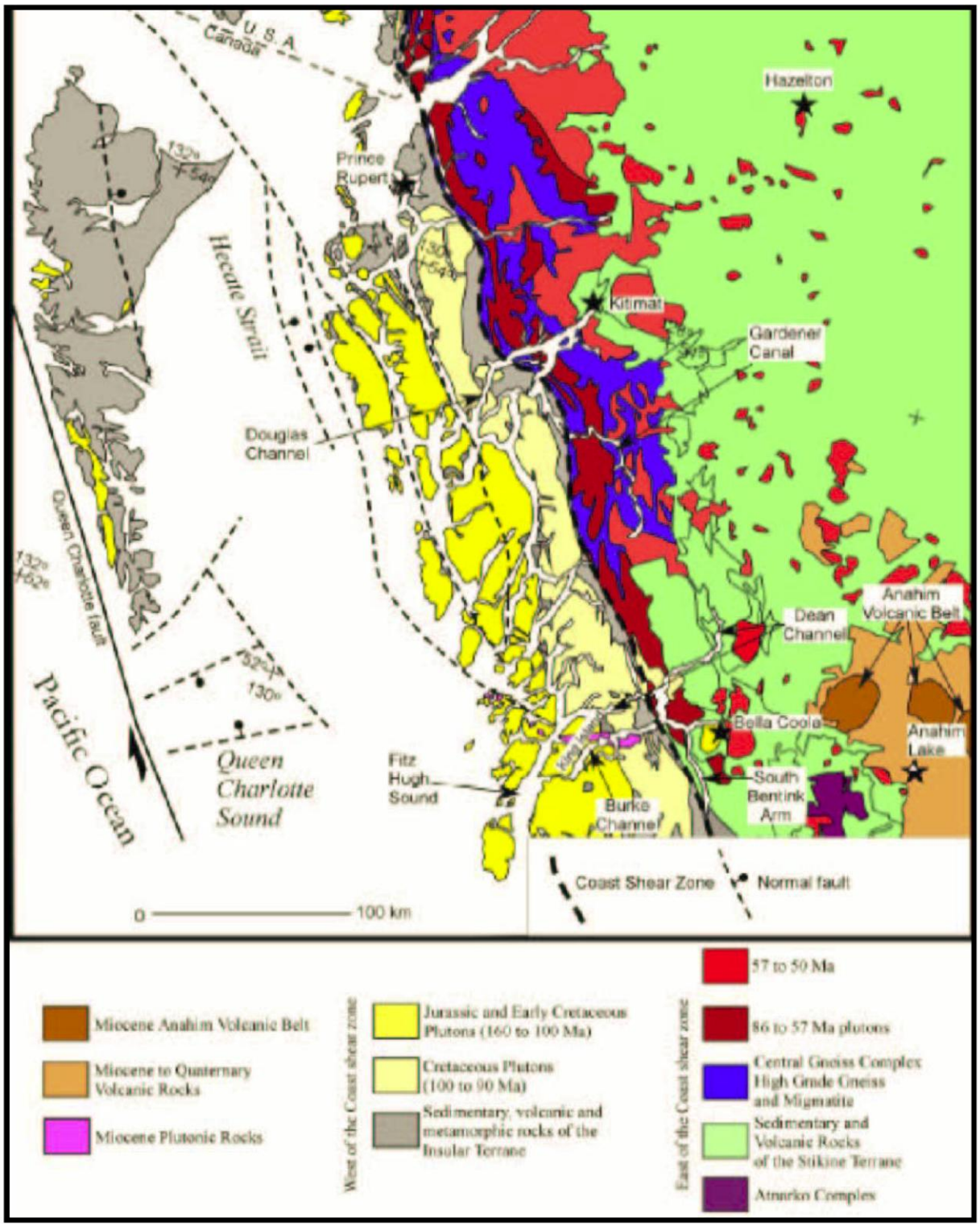


Figure 3.4-8 Summary of Geological and Structural Terranes within Queen Charlotte Basin, (extract from E A and Outreach, (2006))

Figure 3.4-8 presents the geological terranes and associated lithological units present within the Queen Charlotte Basin. The main fault and shear zones are identified in Figure 3.4-9.

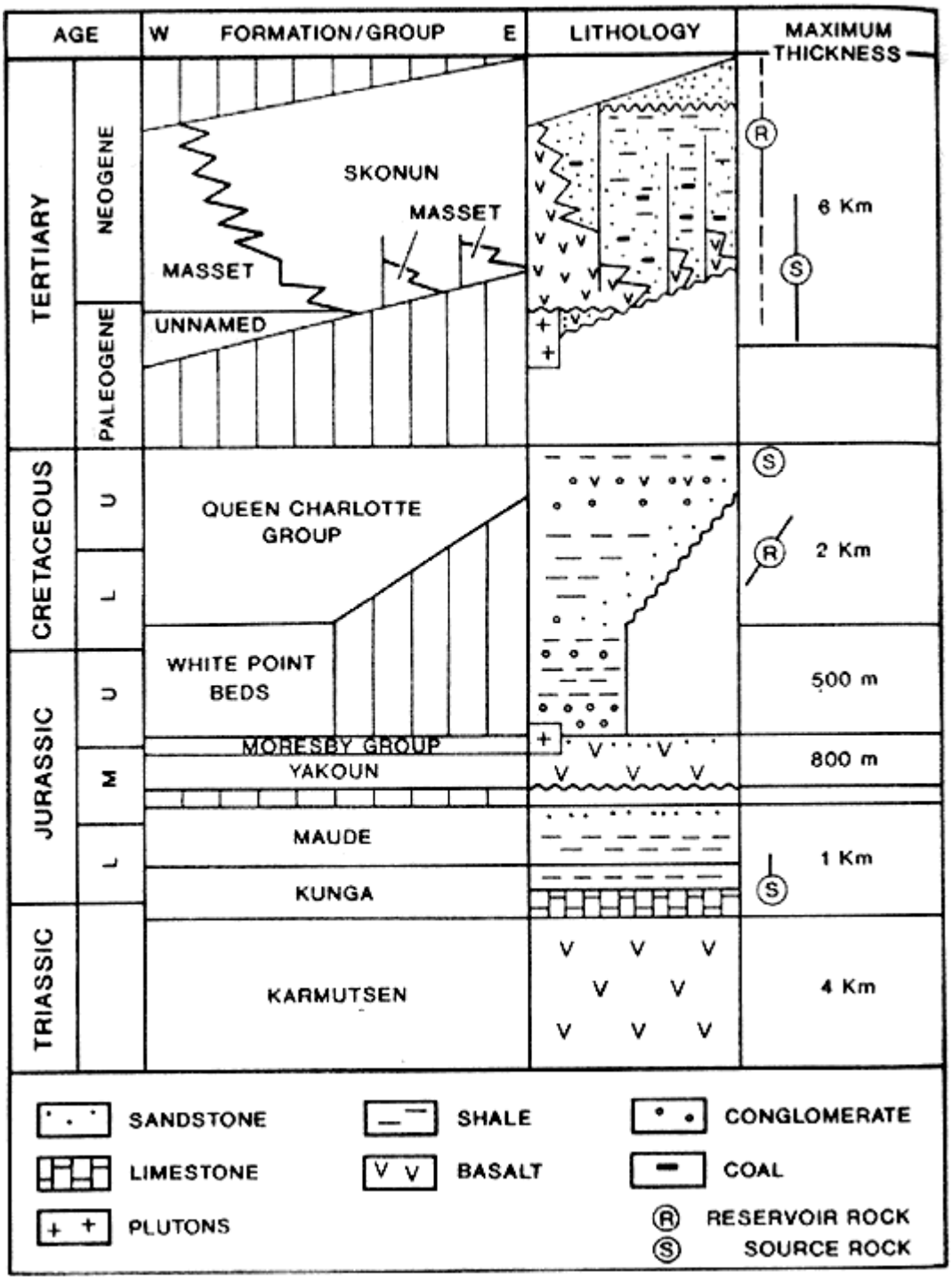


Figure 3.4-9 Generalised Stratigraphy of Mesozioc (Triassic, Jurassic and Cretaceous) and Cenozioc (Tertiary) of Queen Charlotte Basin, (after Dietrich,1995).

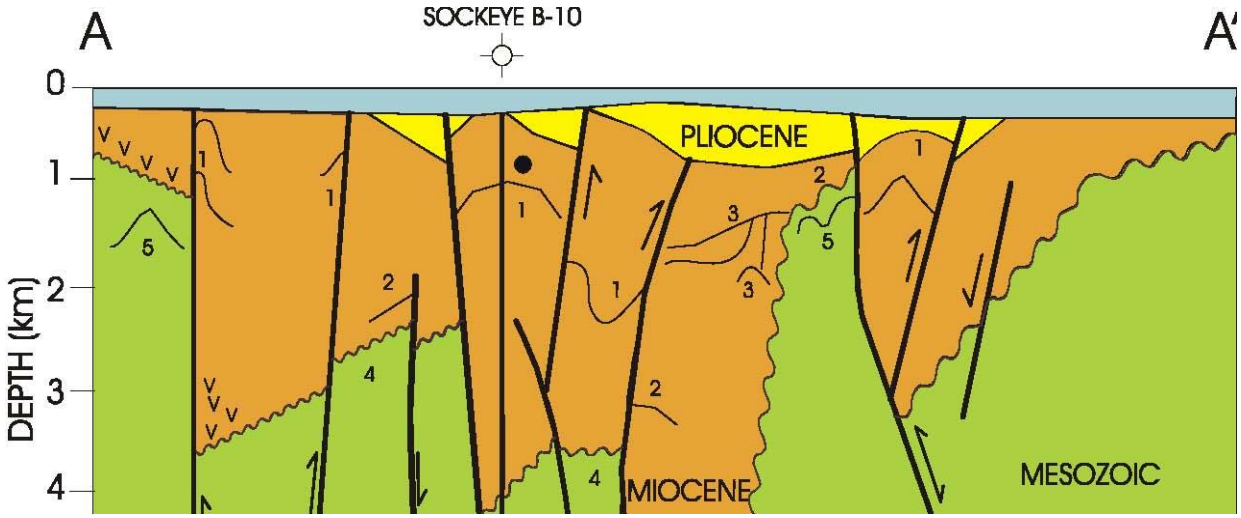


Figure 3.4-10 Simplified Structural Cross Section for the Offshore Region of Hecate Strait, (from Hannigan et al. 1998), modified after Dietrich (1995).

The generalied sequence of rocks interpreted to be present within the Dogfish Banks area of the Queen Charlotte Basin, and possibly within foundation depth, are detailed below, starting with the youngest. The general sequence is also summarized in Figure 3.4-9 and on Table 3.4-1 below:

Unit / Formation	Age	Rock Type	Environment
Skonun Formation	Late Tertiary: Neogene 1.6 to 23.7Ma	sandstone shale conglomerate, lignite	marine and terrestrial depositional environment
Masset Formation		basalt, rhyolite flows and pyroclastics	Extrusive igneous environment
Unnamed volcanic flows and sedimentary rocks	Early Tertiary: Palaeogene 23.7 to 66.4Ma	basalts, andesites, conglomerates, black shale and sandstones	Intrusive volcanic and Subaerial and marine depositional environment
Queen Charlotte Group: Haida, Skidgate, Honna and Unnamed Formations	Mid to late Cretaceous: Albian through Maastrichian: 68 to 98 Ma	sandstone, siltstone, mudstone, conglomerates and volcanics	Marine and extrusive volcanic depositional environments
Longarm Formation	Early Cretaceous: Barlasian through Aptian: 98 to 114Ma	weak to strong sandstones, shale and conglomerate	Shelf shallow marine depositional environment
Yakoun and Moresby Group	Mid to Late Jurassic: Alenian through Tithonian: 144 to 185Ma	shallow volcanics, conglomerates, sandstone and siltstones	Shelf shallow marine and intrusive volcanic environments

Table 3.4-1 Summary of Solid Statigraphic Units within Hecate Strait

Based on available data it is possible that strata of the Early and Late Tertiary dominate the bedrock types present within the survey area, however it is possible that older Cretaceous strata subcrop to the western boundary of the area. This will, however, have to be confirmed from the appropriate detailed surveys. A schematic section illustrating the vertical relationship is presented in Figure 3.4-9.

3.4.8 *Seismicity and Associated Events*

3.4.8.1 REGIONAL SEISMICITY

The Dogfish Banks area is subject to earthquakes (Figure 3.4-11) and storm-related sediment transport. Strong semi-diurnal tides combined with southeast winter winds generate bottom currents strong enough to erode and transport seafloor sediments to the north.

The Queen Charlotte Fault is a major horizontal slip fault, which lies to the west of the Queen Charlotte Islands. It is Canada's most active fault in terms of earthquakes and magnitudes of between 7 and 8 are not uncommon.

Other earthquake foci lie on linear belts in the northern part of the Queen Charlotte Basin close to known faults such as Rennel Sound Fault and the Sandspit Fault. The trends of these faults are similar to that of the Queen Charlotte Fault. Data also suggests that many earthquakes on the northern part of the Queen Charlotte Basin are not associated with known faults but are rather associated with a diffuse set of minor faults.

Four large earthquakes have impacted the area in the last century, with the largest (magnitude 8.1) (Barrie et al Chapter 2 (Fedge and Mathewes 2005)) occurring just west of Graham Island in 1949. Tsunamis resulting from earthquakes were observed in Tasu Sound at the time of the 1949 quake. The most recent (magnitude 6.1) occurred in 2001. Liquefaction and dewatering of sand deposits caused by earthquake motion have been observed within the sandy sediments of the Fraser River delta in southern coastal BC (Clague et al). The liquefaction potential of the sand ridges observed on Dogfish Banks is not known at this time.

One additional source of earthquake potential is related to the strain build up along the Cascadia Fault Zone located in the coastal zone of the Canadian hinterland. Potential seismic events along this rupture are caused by the movement of the Pacific Plate relative to the North American Plate.

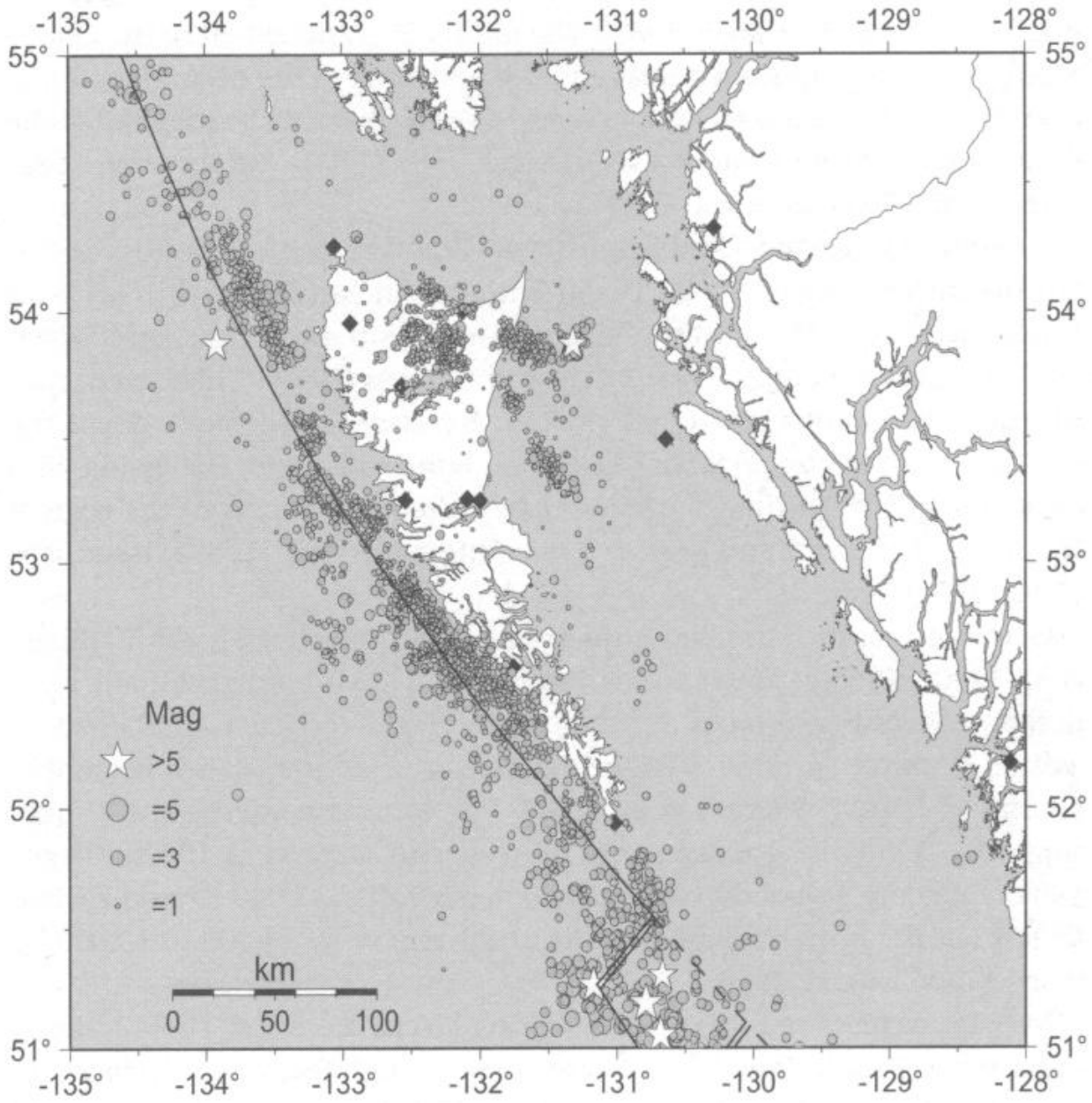


Figure 3.4-11 Seismicity map showing major earthquake epicentres in and near the study area between 1984 and 1996 (after Fedge and Mathewes 2005)

Illustrations of ground motion for 'firm ground' show that the floor of the Queen Charlotte Basin is less susceptible to ground motions than much of the Queen Charlotte Islands, but that accelerations for an annual reoccurrence probability of $4x10^{-4}$ are still quite significant, being in the range of 0.25 to 0.4g and the possibility of large local ground motions close to active faults within the north Hecate Strait area cannot be discounted.

Based on available data, return periods for magnitude 3, 4, 5 and 6 events in the Hecate Strait area are 1.1, 0.3, 0.04 and 0.006 years respectively. These relationships are summarized graphically in Figure 3.4-12.

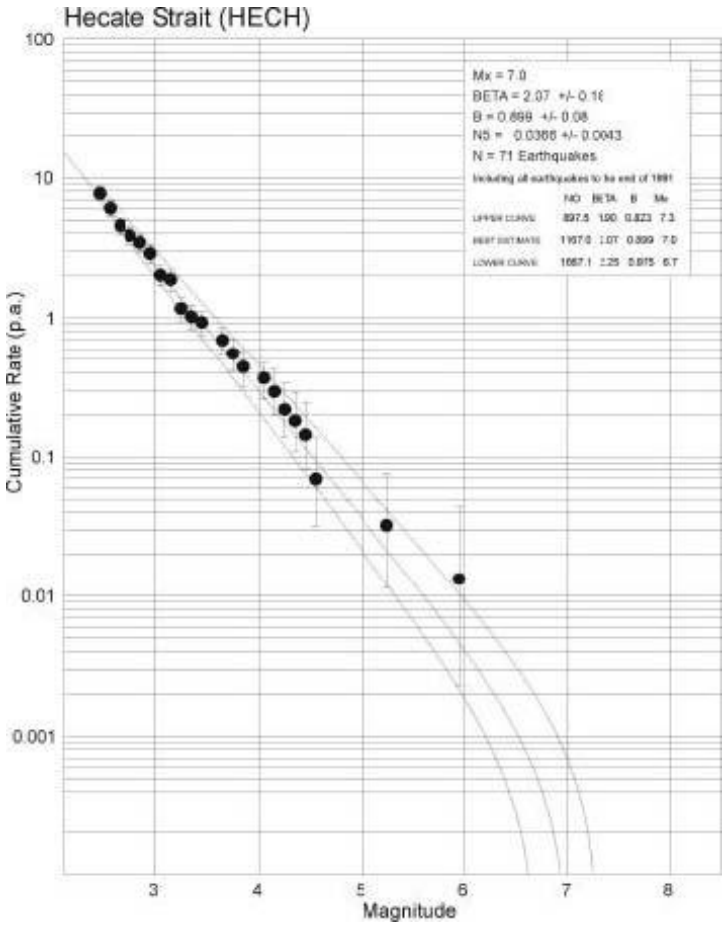


Figure 3.4-12 Relationship between Earthquake Magnitude and Occurrences Per Year for the Northern Hecate Strait (Adams and Halchuk, 2003)

3.4.8.2 Tsunamis

Tsunami threats to the Queen Charlotte Basin originate from both distal and proximal sources. The main distal sources are interpreted to be from the Aleutian Islands, Kamchatka Peninsula and Chile. However, proximally produced tsunamis from the Cascadia Subduction zone and Queen Charlotte Fault are of more concern as a tsunami produced from a large earthquake close to the Queen Charlotte Basin would be severe with very little warning time.

3.5 MARINE GEOPHYSICAL STUDIES FOR WIND FARM ENGINEERING

NaiKun commissioned studies by RPS Energy (RPS Energy 2009a) to assess bathymetry and seabed sediments in the wind farm in the northern part of the IUP. This section describes the studies and findings of the 2007 and 2008 geophysical surveys and data interpretation completed for both the wind farm and the mainland cable route.

3.5.1 *Geophysical Field Studies*

The work on the 2008 geophysical surveys follows the analysis of data from two geophysical surveys completed in 2007 in the Dogfish Banks area: one in June 2007 by NaiKun, and the other in October 2007 by Pacific Geoscience Centre (PGC). In addition, a borehole was drilled by NaiKun on September 6th, 2007.

The NaiKun 2007 and PGC 2007 surveys concurrently employed a variety of geophysical tools consisting of: airgun, Huntec DTS, Seistec surface-towed boomer, Uniboom surface-towed boomer, echosounder, sidescan sonar, and magnetometer. Analysis of the data indicated that the Uniboom system obtained the best results for sub-bottom penetration. The Uniboom seismic data collected in the survey area were of excellent quality and allowed the shallow subsurface geology to be routinely seen to a depth of 25 metres and locally up to 40 metres below seafloor.

The 2007 and 2008 NaiKun surveys employed a variety of geophysical tools, with the common tools between each year being a Uniboom surface-towed boomer, single beam echosounder, and sidescan sonar. The 2007 survey collected airgun data, and the 2008 survey collected multibeam data. The 2008 data were also of high quality, but were susceptible to the weather conditions, and overall, the 2008 data were not as high a quality as 2007.

The survey work on the Northern NaiKun Trapezoid (Investigative Use Permit area) was completed between May 16th and June 12th, 2008 and the mainland submarine Cable Route Survey was completed between September 6th and 20th, 2008.

The NaiKun 2008 survey was conducted to infill the coarse 2007 survey grid of lines which ran East-West and North-South with a 2 km spacing. The 2008 data provided geophysical data on a grid with 180 metre spacing, which allowed a more detailed interpretation of the surficial conditions and sub-surface geology throughout the surveyed area.

The survey systems used in the Reconnaissance Cable Routing Survey included a Uniboom surface-towed sub-bottom profiling system, sidescan sonar, single beam echosounder, and multibeam bathymetry system.

After the data collection phase of the Reconnaissance Cable Route Survey, the vessel conducted a vibrocoring program in the Northern NaiKun Trapezoid, and those results were related to the shallow seismic data. Due to the nature of the sediments at the site, the vibrocoring had very limited penetration and only sampled the uppermost unit, and very locally, the underlying material.

3.5.2 *Results of Geophysical Field Studies*

The multibeam data provides details of the seafloor topography (i.e. water depths and seafloor morphology), whereas the sidescan provides details about the sediment types present on the seafloor (i.e. areas of sand, areas of gravel, areas of clay with boulders). The spatial sampling of the sidescan

allows individual boulders to be recognized on the data, and these areas of boulders have been verified from the underwater video and sediment samples.

The final multibeam images presented in this report were gridded to 1 metre and 2 metres, and have a vertical resolution in the order of 0.1 metres. The sidescan image has a spatial resolution of 0.2 metres, and objects with heights of less than 0.2 metres are detected on the seafloor.

The sub bottom data collected in this study showed variable penetration with the geological conditions. Geological units have been mapped in many places from 25 – 30 metres and in one instance a local penetration of 50 metres was observed. The data collected provides a basis to characterize the geology in the upper 30 metres and because of the dip of the strata the deeper geology may also inferred.

The mapping completed in this work provides a baseline for monitoring future effects and also for the engineering design work. What has emerged is a comprehensive understanding of the seafloor and the relationship of this seafloor geology to the subsurface conditions.

The study area, which is slightly larger than the proposed wind farm, is very large (over 180 square kilometres) and the subsurface control is extremely sparse. Despite this limitation, it is possible to infer some important characteristics of the subsurface conditions for turbine placement.

Seafloor scour is variable geographically within the site. There are large areas of the site with little change (i.e. less than 0.5 metres year-over-year) and areas where vertical changes in seafloor elevation of up to 3.5 metres have occurred between successive year surveys – both erosion and accretion. These areas of greatest change are related to specific bedforms located east of the central sand in the study area (wind farm).

Borehole data are required to refine this interpretation and the mapping work, and to better qualify sediment physical properties at depth. The latter can only be inferred at present, from the seismic data and limited ground-truthing available. Despite the lack of borehole control to ground-truth the seismic, the need remained to provide some guidance to the range of geological conditions for initial design purposes.

3.5.2.1 Surficial and Shallow Sub-Bottom Sediments Regions

To relate the geological conditions to the turbines the following maps show the 110 turbine layout with the geological results in plan and profile view. The wind farm is divided into three (3) areas based on the geological information. These areas, referred to as Areas 1 (eastern region), 2 (central region), and 3 (western region) are shown in Figure 3.5-1.

From regional studies discussed in Section 3.4, there are four primary sediments units identified that are useful when considering sediments in the wind farm:

- Unit A: Uppermost sands.
- Unit B: Channel fill deposits (sands and gravels) and lagoonal silts and clays.
- Unit C: Prograding deposits comprising sands and gravels and clays.

- Unit D: Glacial outwash deposits and ice contact deposits comprising sands and gravel and bouldery muds respectively.

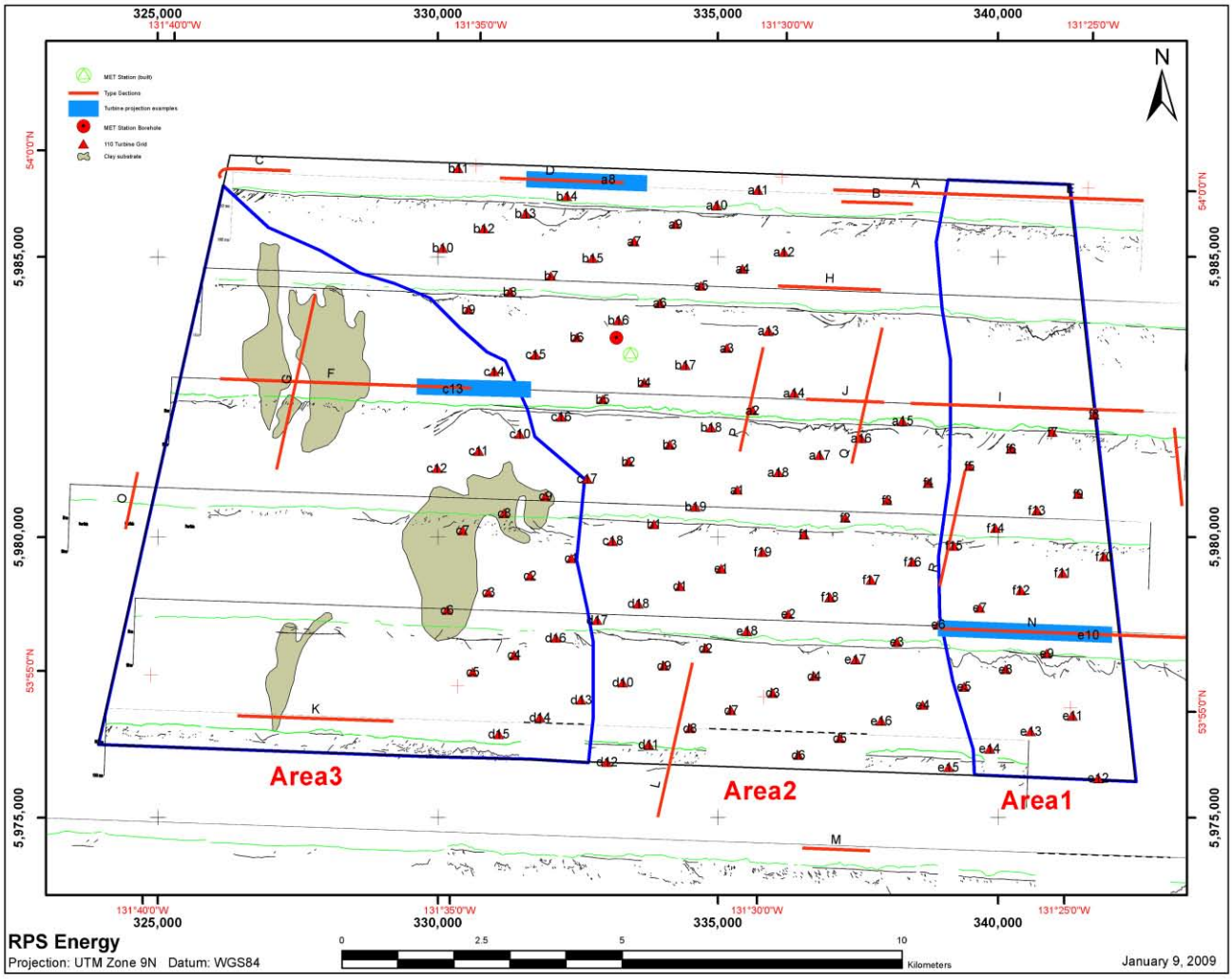


Figure 3.5-1 Geological Areas

Area 1 Summary

The preliminary project design shows 20 of the 110 turbines are located in Area 1. The water depth for the turbines in this area range from 16.8 m to 24 m, with an average water depth of 20.5m.

This area comprises the deeper water portions of the wind farm and is characterized by very little (i.e. less than 1 m) surficial sand (Unit A). Acoustic data indicates that underneath these sands are finer sediments such as interbedded clay, silt, and sand deposits in this area, which are up to 30 metres thick locally.

The sidescan sonar over this area indicates sand and gravel at the seabed, however this surficial unit is expected to be very thin based on the sub-bottom data and regional mapping. There is very little change in seafloor elevation between 2007 and 2008 in this area.

In the north these sand and gravel deposits appear to form a large wedge of sediment prograding from east to west. In the south these deposits infill depressions in what appears to be a hummocky buried surface, likely marking the top of over-consolidated bouldery muds below.

There are small, localized concentrations of boulders at the seafloor in this area, and these are thought to correspond to areas of outcropping of bouldery muds.

Mapping in this area shows that the relationship between the bathymetry, seabed geology, and the sub-bottom geology provides useful information to assist final turbine site selection, because lateral changes in conditions evident in the mapping can guide final placements.

Area 2 Summary

This central area of the wind farm is characterized by north-south oriented sand ridges. The preliminary project design shows 72 of the turbines would be located in this area. The water depth in this area ranges from 9.3 m to 19.3 m at the turbine sites with an average water depth of 13.4 m. There are also several large gravel bodies mapped on the seafloor in this area, one of which is located immediately west of the MET station mast that was installed by NaiKun for this Project (Figure 3.5-1). There are also many large sand waves in this area which are often superimposed on the sand ridges. These sand waves are important from the standpoint of local sediment transport and the areas of seabed mobility. There are local concentrations of boulders at the seafloor in this area.

In Area 2 the thickness of surficial sand varies from less than 1 m to 14 m (Unit A).

Area 2 is the most dynamic part of the wind farm in terms of year-over-year changes in seafloor elevation.

Area 3 Summary

The preliminary project design shows 18 of the 110 turbines in this area of the wind farm. The water depth at the turbines in this area ranges from 11.9 m to 17 m with the average water depth of 14.3 m.

This western area of the site is complex but is distinguished by large areas of bouldery mud outcropping at the seafloor, a proliferation of boulder contacts on the sidescan images in this area and the thin Unit A sediments. These areas of boulder contacts are interpreted to be surface outcropping of glacial outwash sands and gravels, or boulder muds (Unit D), based on the presence of hard clay in vibrocores in this area, and are therefore significant from the standpoint of foundation conditions.

There are two (2) large areas of sand on the seafloor in this area, located southwest of the areas of bouldery mud. These areas are thought to be the result of the winnowing of sediments from this area. This sediment layer is thin (less than 1 m). There is very little change in seafloor elevation between the 2007 and 2008 surveys in this area, perhaps indicating an absence of large sand waves. Where the area of bouldery mud and sand are not present, the remaining seafloor is a mixture of sand and gravel. There

are no large areas of gravel mapped in this area, however there are occasional shallow channels infilled with softer sediment.

3.5.3 *Summary of Sea Bed and Sediment Conditions*

3.5.3.1 Wind Farm

Multibeam Bathymetry, Water Depth, and Seafloor Morphology

The multibeam imagery is particularly effective at communicating the shape of the seafloor, as shown in Figure 3.5-2, looking from south to north across the wind farm. Note the ridge on the east side of the site which generally separates the shallow water areas (red being shallowest) from the deeper water areas (blue being deepest). The water depth on this image ranges from 7.3 to 26.5 metres.

Note the vertical data for all bathymetric values presented in this report are relative to Chart Datum corrected using tide gauge from Prince Rupert No. 9354.

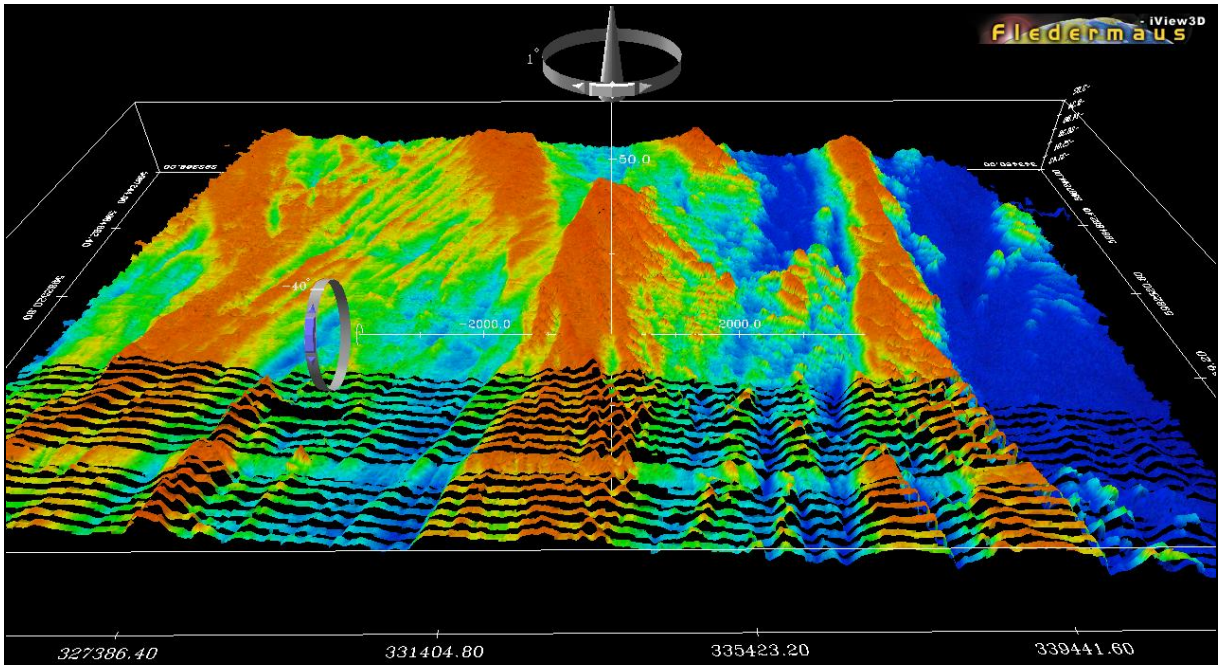


Figure 3.5-2 Site Bathymetry (South to North View) – 2 m Resolution

The data shown represent water depth readings every 2 metres. The gaps in the lines on the south end of the site are due to the increased line spacing of the multibeam lines during the survey in that area. Despite this limitation valuable information was acquired to the southern limit of the site and the main morphological features can be traced through this area.

Detailed Multibeam Bathymetry Maps

Detailed colour shaded relief maps, and contour maps, have been created using the multibeam bathymetry data collected within the wind farm. The contour interval is as low as 2 metres.

Figure 3.5-3 Shaded Relief Map NW Quadrant of Wind Farm

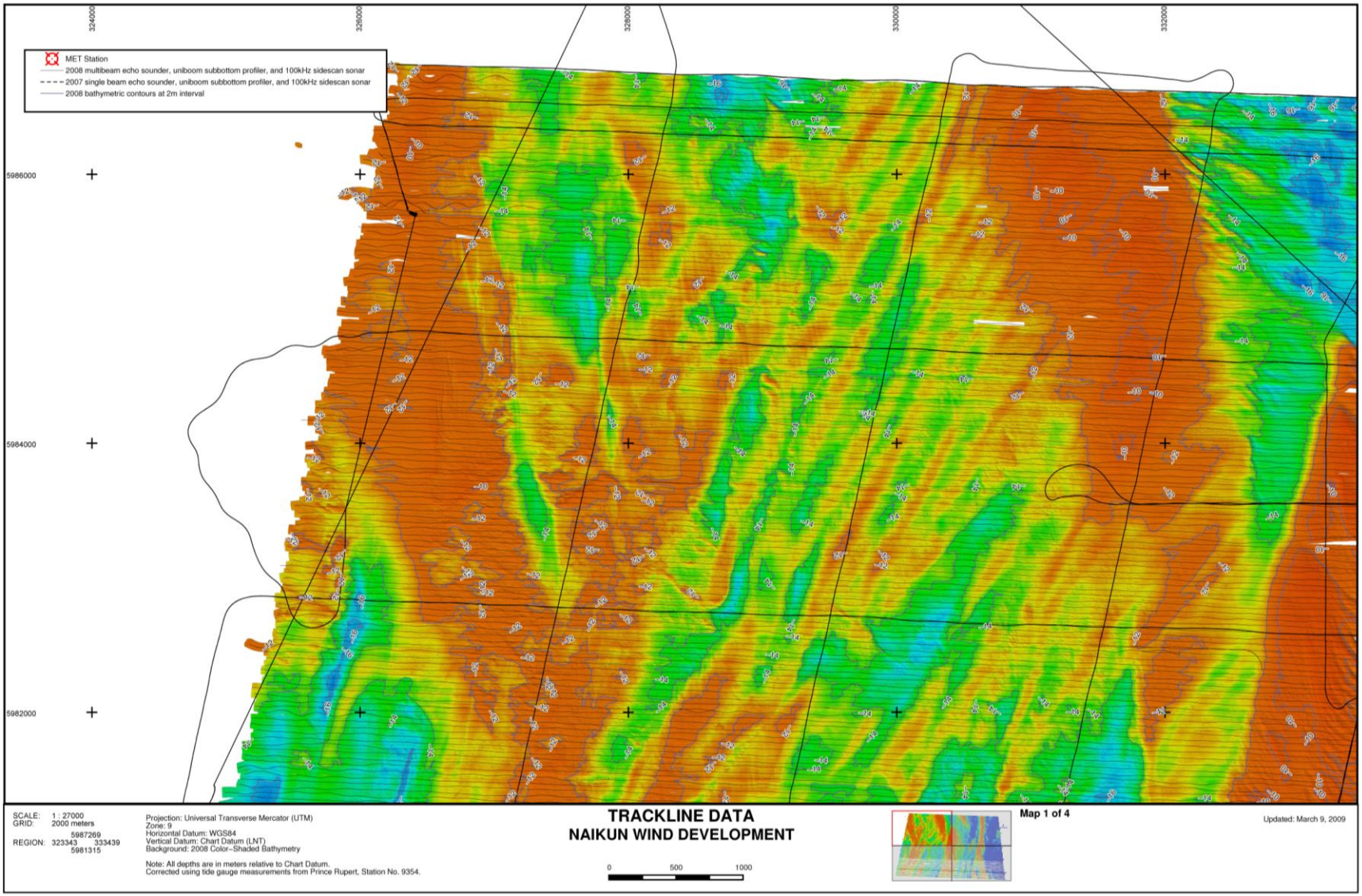


Figure 3.5-4 Shaded Relief Map NE Quadrant of Wind Farm

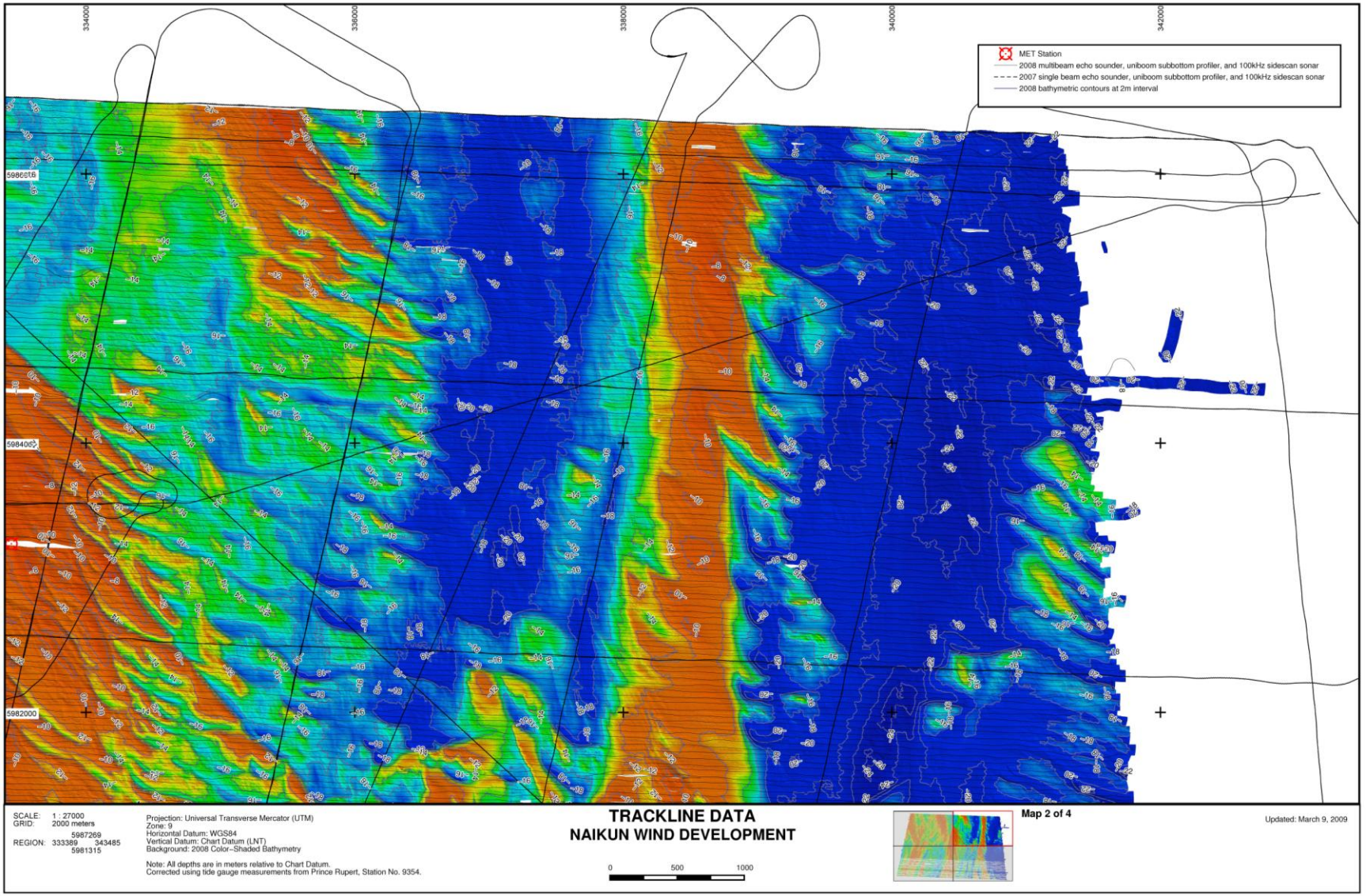


Figure 3.5-5 Shaded Relief Map SW Quadrant of Wind Farm

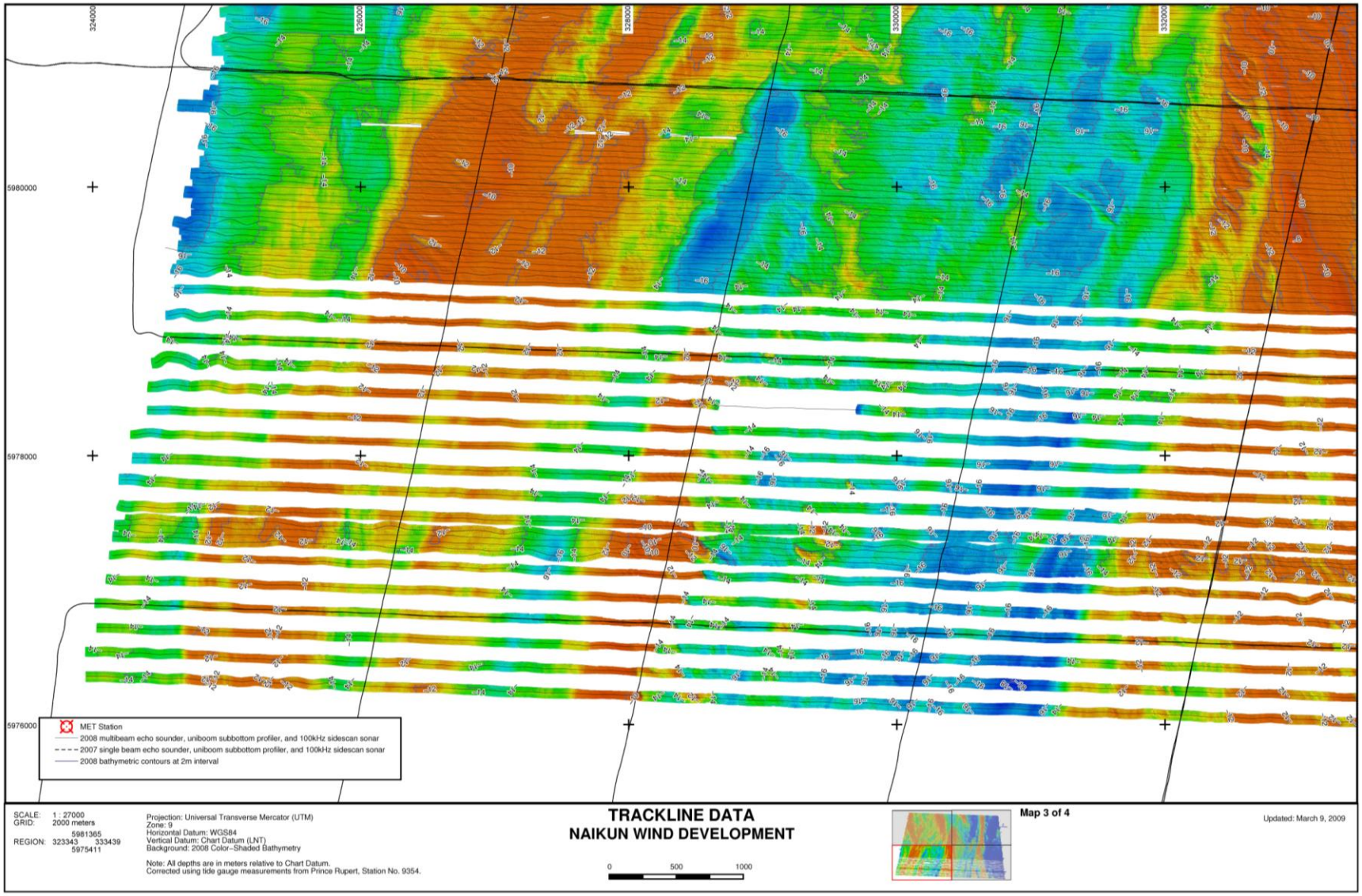
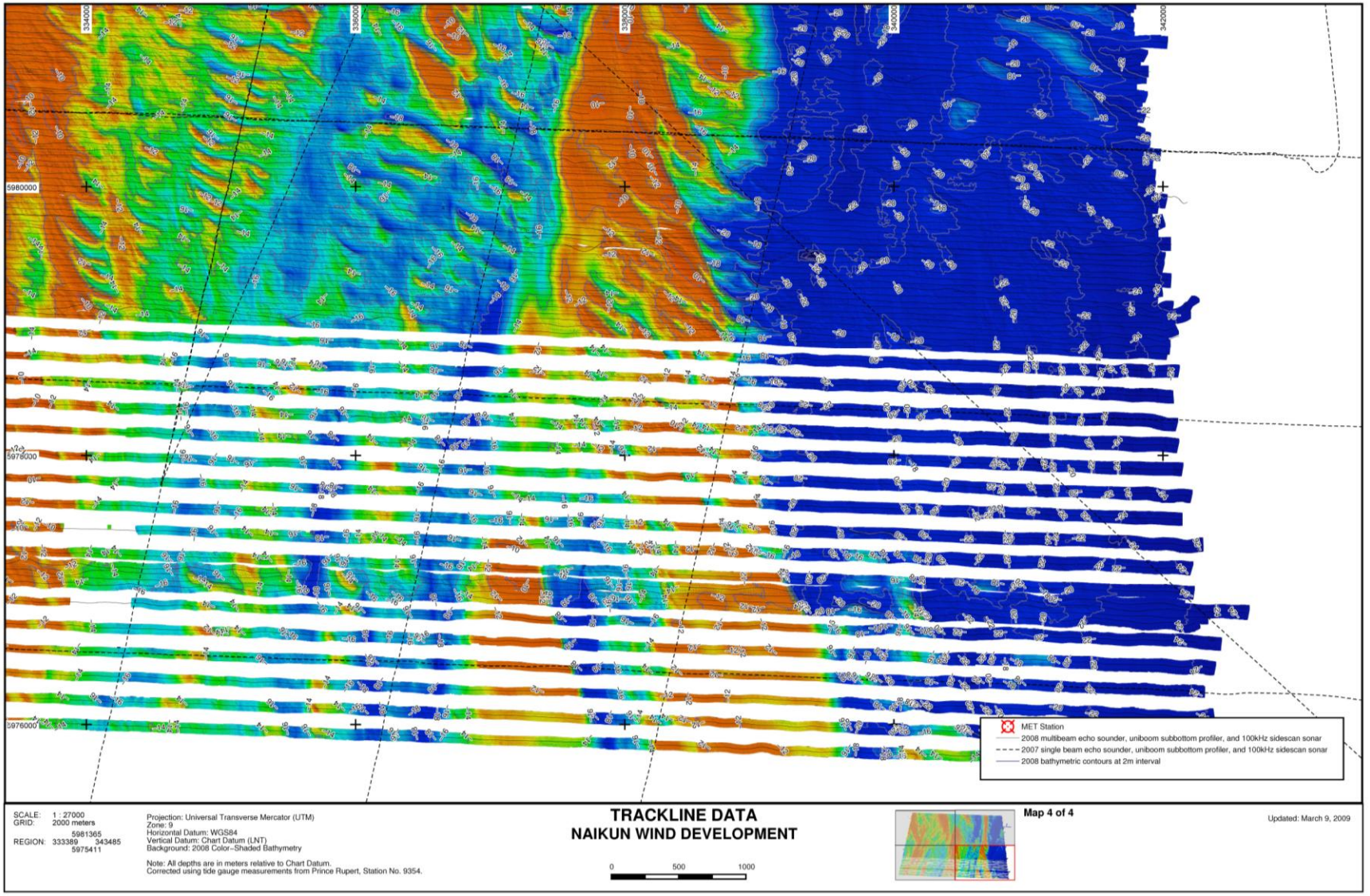


Figure 3.5-6 Shaded Relief Map SE Quadrant of Wind Farm



Detailed Sidescan Data Maps

Detailed maps of the sidescan data collected within the wind farm can be generated to provide detailed information on the seafloor sediments. For example, the sidescan data in Figure 3.5-7 shows areas of gravel ripples (also referred to in the geological literature as coarse-grained megaripples) with wavelengths of 1.5 to 3 metres.

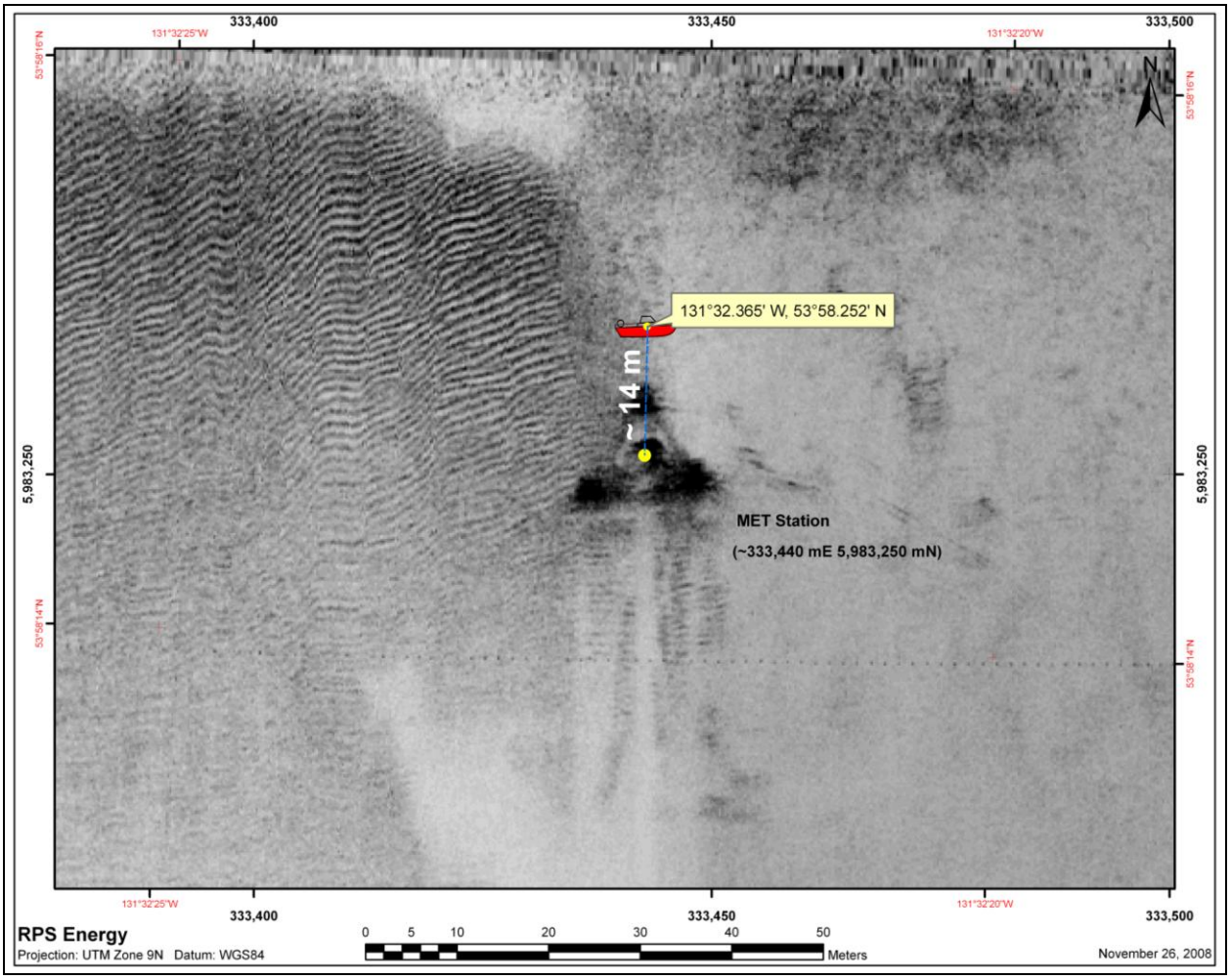


Figure 3.5-7 Detailed Sidescan Image of MET Station

Surficial Geology

Mapping of the surficial geology was completed based on interpreting the changes in reflectivity from the sidescan data and ground-truthing these with seafloor sediment sampling information.

Four (4) primary seabed types were classified:

1) **Primarily gravel – covers an area of 5.7 square kilometres**
These areas have gravel ripples (also known as coarse-grained megaripples) with crest-to-crest wavelengths of 1.5 to 2 metres; heights in the order of 25 to 40 centimetres are typical. This area is characterized on the sidescan by high reflectivity.

2) **Primarily sand – covers an area of 44.5 square kilometres**.
These areas are characterized on the sidescan as ubiquitous planar sand bed conditions and by their low reflectivity.

3) **Mixed sand / gravel – covers an area of 121.2 square kilometres**
This is the most common surficial geology area and is characterized by intermingled sand and gravel deposits on the seafloor. The sand is common on sand waves, and gravel in the troughs of these waves. In some instances the sand and gravel are present in patches and ribbons. This area is characterized on the sidescan by alternating low and high reflectivity areas which relate to sand and gravel sediments, respectively.

4) **Clay substrate with boulders – covers an area of 8.6 square kilometres**
There is a concentration of boulder contacts in these areas. The location of the boulders was based on careful interpretation of the sidescan and done independently of the mapping of the surficial reflectivity contacts. It is also clear that boulders are very common on the site and that further surficial sediment zones will need to be defined at the micro siting phase.

It is evident that there are areas of boulders occurring in areas of clay substrate, and in those areas there is a patchy veneer of sand and gravel. The boulders mapped are 0.25m to 1.0m diameter. It should be noted that these boulders are present where the surficial sediment layer is thinnest.

The interpretative surficial mapping for the Wind Farm is presented in Figures 3.5-8 to 3.5-11. Each map covers a quadrant of the wind farm. The level of information provided by the sidescan data is large. The resolution will allow more detailed mapping at individual turbine locations to assist with the final siting of each turbine.

The study mapped the most significant sediment boundaries to calculate the percentage of each sediment type within the entire mapped area (180 square kilometres).

Within the available data there is no indication of bedrock at the seafloor or below the seafloor in the upper 25 metres, and based on the seismic information no bedrock is expected to occur in the upper 40 metres.

Figure 3.5-8 Seafloor Geology NW Quadrant

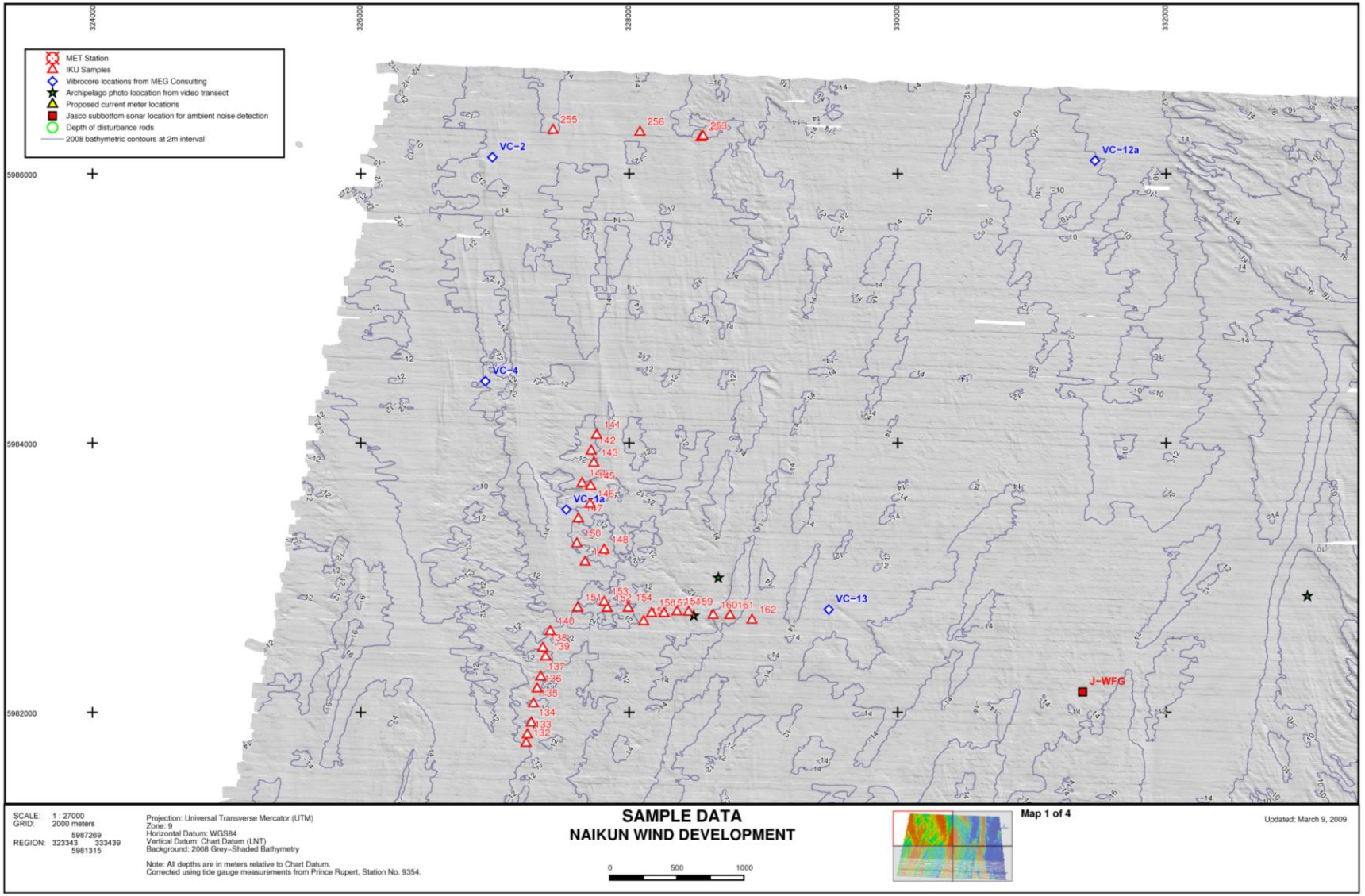


Figure 3.5-9 Seafloor Geology NE Quadrant

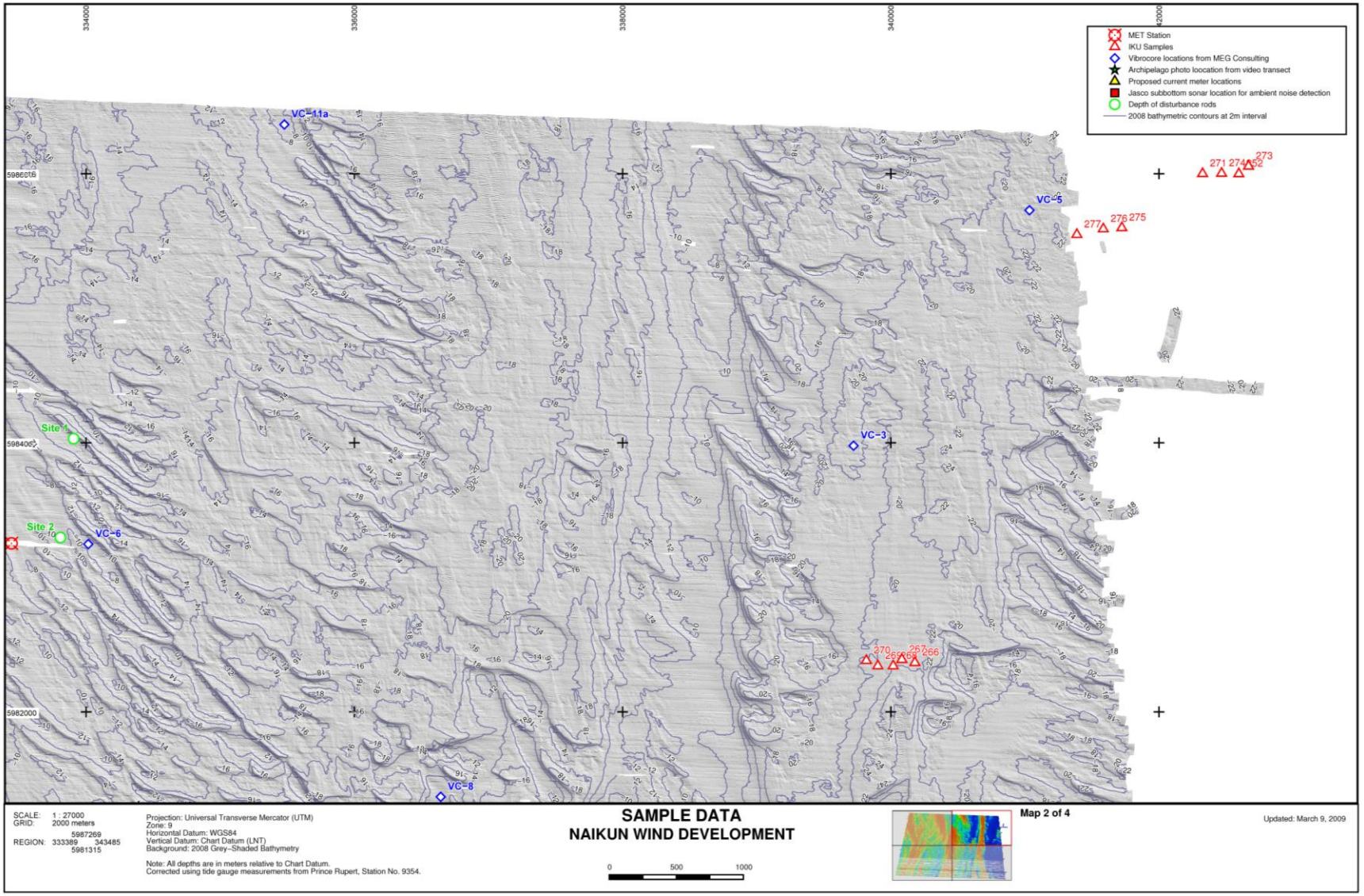


Figure 3.5-10 Seafloor Geology SW Quadrant

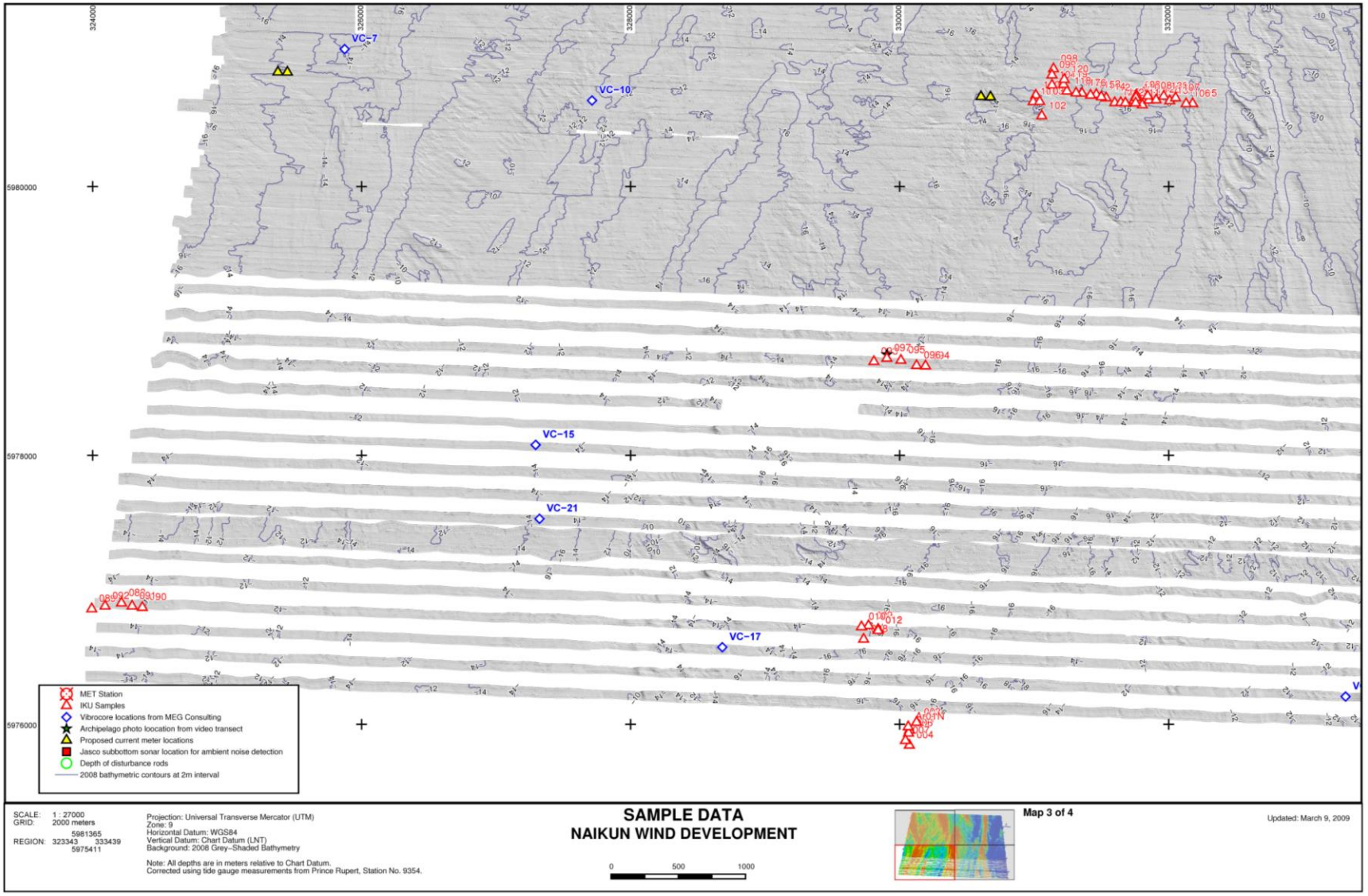
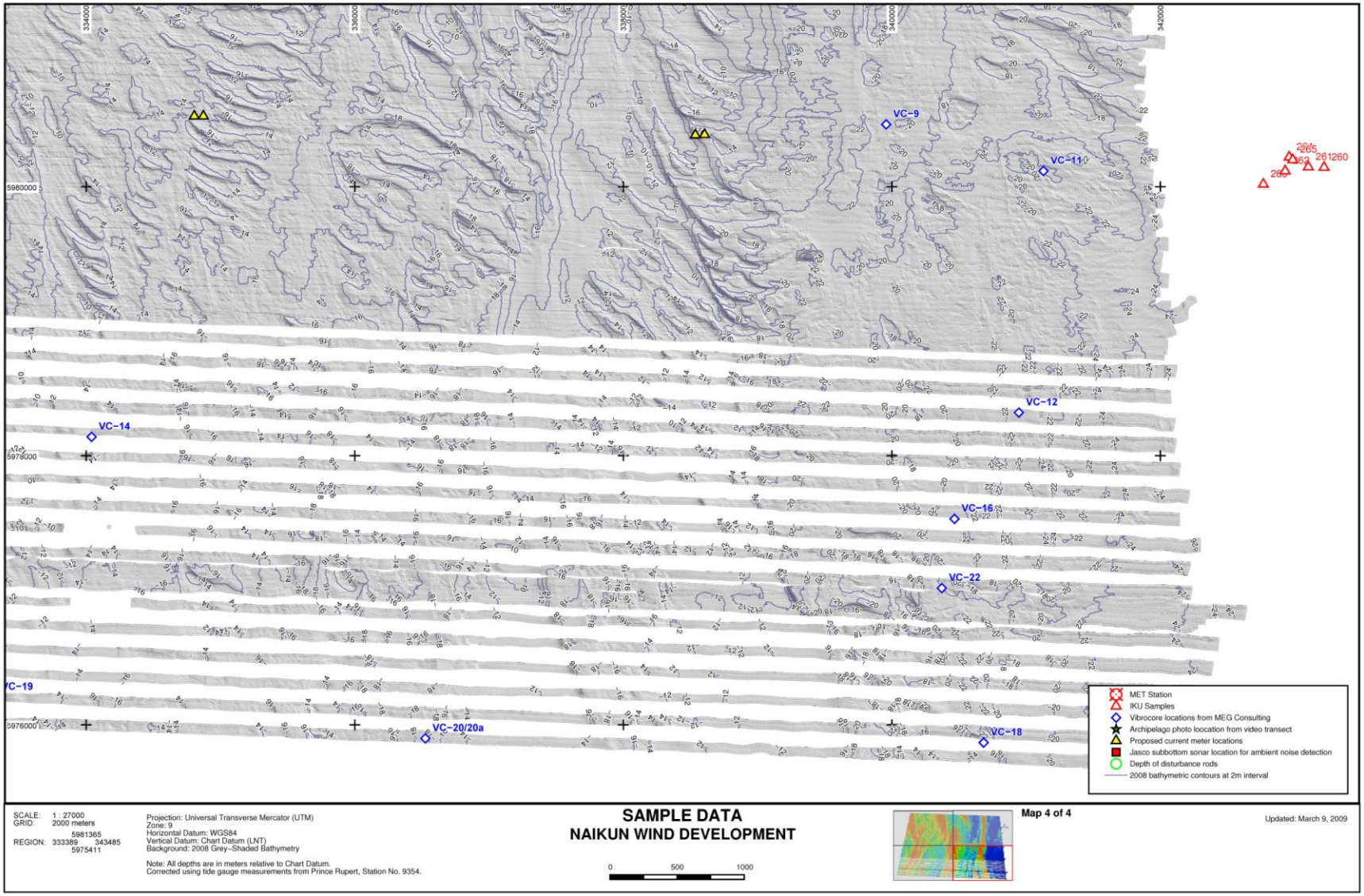


Figure 3.5-11 Seafloor Geology SE Quadrant



The seafloor sediment samples used to ground-truth the sidescan include existing PGC grab samples, samples collected using the IKU sampler as part of the environmental work, and vibrocores collected as part of the 2008 geotechnical light program (Figure 3.5-12).

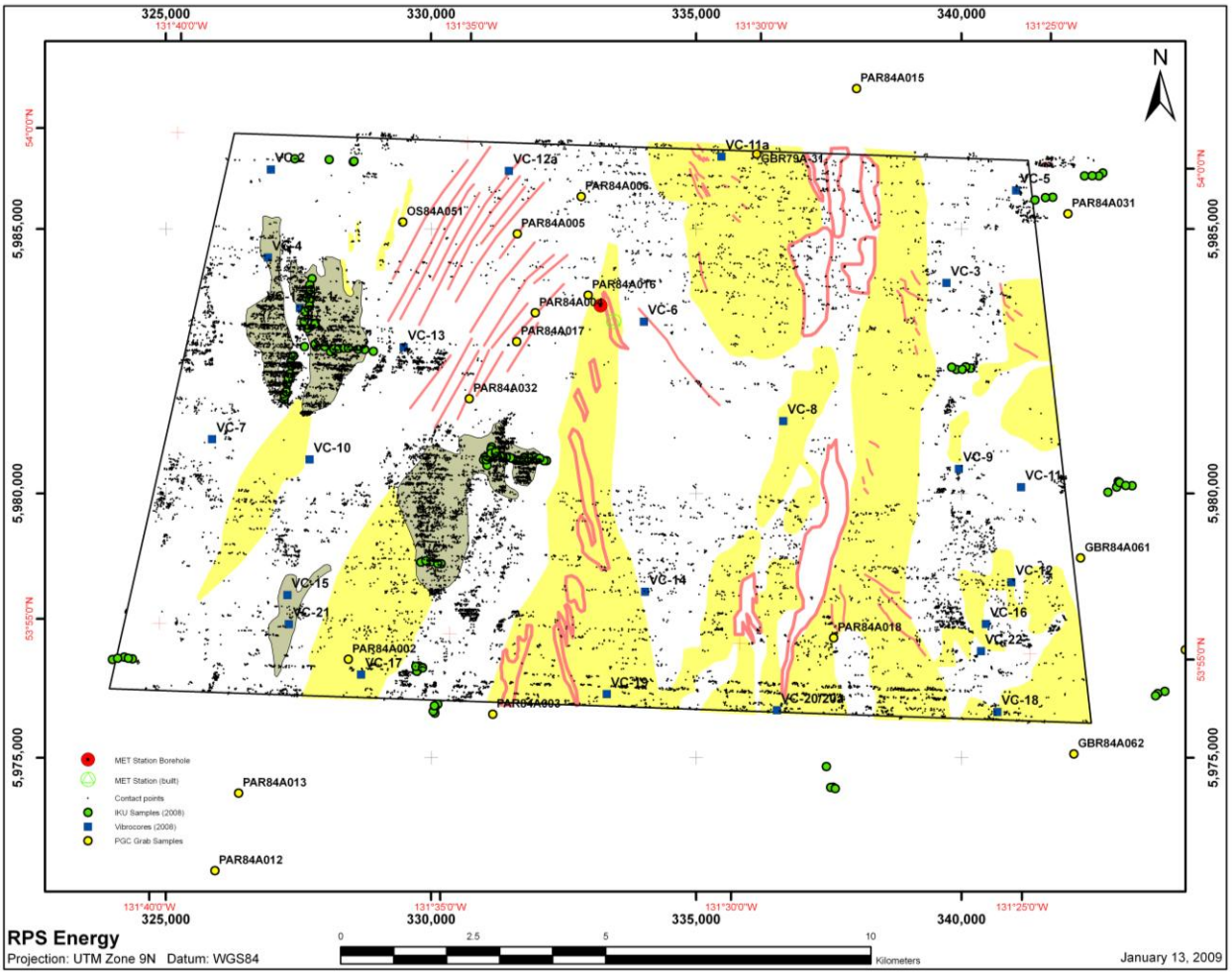


Figure 3.5-12 Sediment Sample Locations with Boulder Contacts

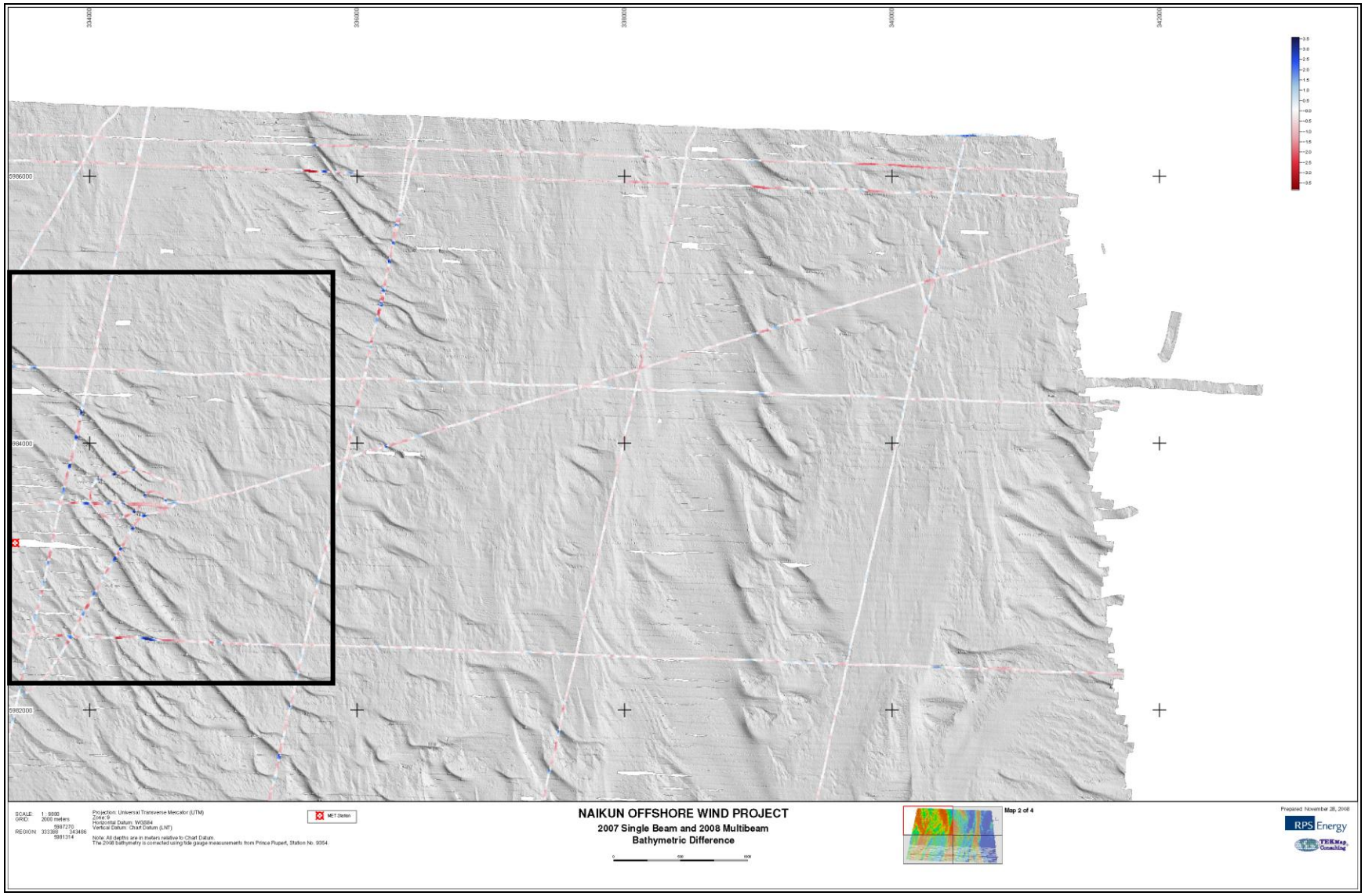
Sediment Mobility

A comparison between the June 2007 single beam and May-June 2008 multibeam data over the entire wind farm was conducted to assess sediment mobility.

The area of greatest bathymetric change between 2007 and 2008 occurs over a 2 kilometre wide band on the east side of the central sand ridge. The scale of the profiles makes visualization of the differences year-over-year somewhat difficult, so plan view maps were produced. An example of the changes that occurred in the NE quadrant of the wind farm, east of the central sand ridge is shown in Figures 3.5-13, 3.5-14 and in a cross-sectional profile in Figure 3.5-15.

At the northeast tip of the central ridge there are three (3) large scale sand waves identified in Figure 3.5-14 as A, B, and C. The cross-section of the ridges is shown on profiles NS4 and NS5, and have wavelengths (crest to crest) of approximately 2 kilometres and heights (trough-to-crest) of 7m, 8m, and up to 12 metres (C, B, and A respectively).

Figure 3.5-13 2007 Single Beam and 2008 Multibeam Comparison Area
Black box represents area detail shown in Figure 3.5-14.



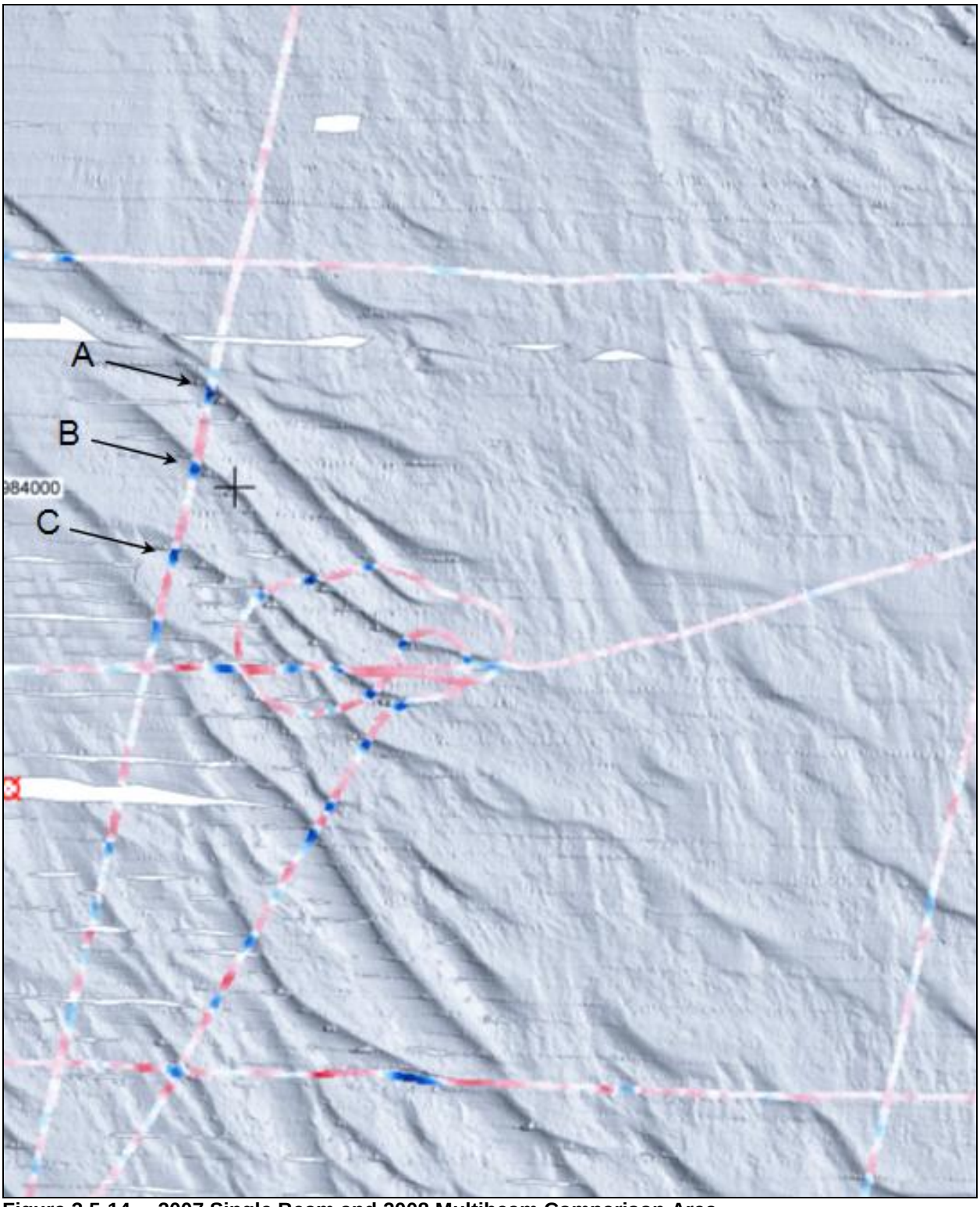


Figure 3.5-14 2007 Single Beam and 2008 Multibeam Comparison Area

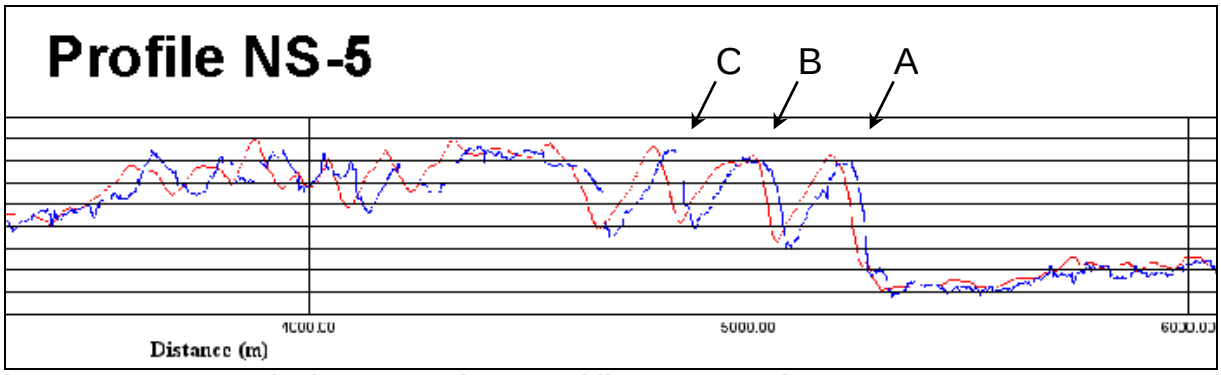


Figure 3.5-15 2007 Single Beam and 2008 Multibeam Comparison Area

Interpretation of Results

The comparison between the 2007 single beam echosounder bathymetry and the 2008 multibeam bathymetry indicates that:

- Large scale bedforms (2D dunes) present in 2008 were also present in 2007.
- There are differences in the location of the troughs and crest of the bedforms between the two years.
- The direction of transport is from the south-southwest toward the north-northeast and this trend is apparent throughout the site.
- These differences provide an indication of the scale of sediment transport and the vertical changes in seafloor elevation that can be expected between years.
- Areas of the seafloor where seabed forms were not present had very little change year-over-year (this includes the shallow water areas on the west side of the site and the deeper water areas on the east).
- The areas of changes are localized and relate to the presence of large scale seabed forms.
- The areas of greatest change in the seafloor are associated with the areas of steep slope. The following is a seafloor gradient map showing these areas.

Shallow Sub-Bottom Sediments

The 2007 and 2008 data indicated that the geological units present were deposited in a coastal setting influenced by rising sea-levels. Longshore sand and gravel bars, coastal lagoons, prograded sand and gravel spits, and finer silty sand and clay sediment sequences washed from the swash zone are typical of the depositional sequence observed on the seismic reflection data. These deposits reach thicknesses of up to 40 metres and may be stacked on top of each other in response to rising sea-levels.

The sediments at the borehole location, and throughout the northeastern region of the wind farm, were dominantly formed within a regressive - transgressive sea-level rise environment. Similar depositional environments have been studied in detail throughout the Hecate Strait and Queen Charlotte Sound,

where they display thicknesses of greater than 30 metres and occur in water depths of 150 metres to the present-day shoreline.

The seismic data in both 2007 and 2008 was correlated to one borehole and, as such, most of the interpretation of the data had to rely on the acoustic character.

The only borehole to tie to the seismic data was acquired at the MET station and showed:

- 0 (seafloor) to 6.3 metres: Dense grey fine sand with some shell fragments below 4 metres.
- 6.3 to 13.9 metres: Primarily dense dark grey fine sand with some silt and clay.
- 13.9 to 41.9 metres: Silty clay, fine sand, and silty sand
- 41.9 to 48.9 metres (end of borehole): Stiff grey silty clay to very stiff to hard clay.

R3 Seismic Reflector

The uppermost regional reflector, designated as R3, coincides consistently with the base of the upper sand. This marks the most regionally extensive seismic horizon. This seismic and stratigraphic unconformity is interpreted to reflect the erosional surface formed when rising sea-levels transgressed across Dogfish Banks approximately 9,500 years ago. The upper sands are similar to the sediments found at the modern beach face observed along the Naikoon Park coast.

Regional Variation in Shallow Sub-Bottom Sediments

Interpretation of the 2007 geophysical and borehole data and observations of the coastal sections exposed at the coastline adjacent to the trapezoid provided a good indication of what can be expected in the wind farm. From these observations a geological model having the following basic units was interpreted:

- Unit A: Uppermost sands.
- Unit B: Channel fill deposits (sands and gravels) and lagoonal silts and clays.
- Unit C: Prograding deposits comprising sands and gravels and clays.
- Unit D: Glacial outwash deposits and ice contact deposits comprising sands and gravel and bouldery muds respectively.

Unit A – Uppermost Sand

The 2007 study found that this unit is widespread and ranged in thickness from less than 0.5 metres to 8 metres, Based on the more dense data collected in 2008 the thickness of this uppermost unit was mapped throughout the site and showed that this unit actually ranges from zero to 14 metres in thickness, and is thickest in the east-central part of the site where the eastern ridge is present.

Unit A thins gradually to the west to the point where it is undetectable (i.e. less than 0.5 metres). In these areas it appears to directly overlay Unit D (overconsolidated boulder clay and silts)

The age of the unit was assessed using C14 dating of buried organics. The C14 age analysis of shell hash in the upper-most sand layer from the MET station borehole shows that:

- NWDH#1-S3 = 4,190 ± 40 BP (depth 4.8 metres)
- NWDH#1-S5 = 8,250 ± 50 BP (depth 6.5 metres)
- NWDH#1-S8 = 4,700 ± 40 BP (depth 8.7 metres)

The results of this analysis indicate that these sediments below 4.8 metres were deposited four to eight thousands of years before present. The significance of this finding is that the upper-most sand unit is not eroded to its base. These results are consistent with dates found nearby in Hecate Strait. That the sample at 8.7 metres is younger than the sample at 6.5 metres suggests some degree of reworking of material during deposition.

Vibrocore and Grab Samples

Vibrocores: A total of twenty-four (24) vibrocores locations were attempted in 2008, and the location of the vibrocores are shown in Figures 3.5-8 to 3.5-11. The vibrocores confirm that seafloor is covered by sand (primarily fine to medium) with gravel and shell fragments.

Grab Samples: The Pacific Geophysical Centre collected IKU grab samples in 2008

3.5.3.2 Mainland Cable Route

This section presents an overview of the proposed mainland cable route from the wind farm to Ridley Island through Edye Pass.

The survey work along the proposed cable route was completed between September 6th and 20th, 2008. The survey systems used included a Uniboom surface-towed sub-bottom profiling system, sidescan sonar, single beam echosounder, and multibeam bathymetry system. The survey was conducted to determine whether there were any major impediments to cable routing.

Although initially three routes were considered this section focuses on the mainland cable route corridor identified in the preliminary project design.

Summary of Conditions Along the Route

The generalized conditions along the route are presented in Table3.5-1 for the corridor route sections shown in Figure 3.5-16. The sections of the route shown in Figure 3.5-16 extend from KP 0 at the Ridley Island Landfall to KP 90.350 at the proposed converter station location in the wind farm. Note that the term “KP” stands for Kilometre Posting, and the value represents the distance from the eastern end of the route.

Table 3.5-1 Summary of Individual Leg Conditions along Route

Section	Start KP	End KP	Summary of Section / Features
S1	0.000	2.000	Gently sloping sediment with abundant sediment well-suited for cable placement. A submerged bedrock escarpment with near vertical slope occurs appears to cut across the as-planned route at approximately KP 0.5; may need to locally redirect the cable around this escarpment to reach the as-planned landfall point, or consider a northwest shift to landfall by approximately 500 metres. A landfall survey is required to extend the offshore survey to the beach and refine this approach.
S2	2.000	8.719	Uniform sloping seafloor with some localized depressions. No impediments to cable installation are observed, and sediment is present for trenching.
S3	8.719	16.721	Broad low relief plateau with isolated bedrock outcrops to be avoided through selection of the route. Sediment present is for trenching.
S4	16.721	21.005	Extensive bedrock outcropping, with localized area of seafloor fault offset and sediment failure features. Problem areas can be avoided with careful consideration of cable routing.
S5	21.005	27.864	Area of greatest concern due to highly variable topography and significant bedrock outcrop at the seafloor. A short section of the route (approximately 500 metres in length) occurs where the only seafloor passage is through a narrow (<100 metres wide) bedrock valley. Careful consideration is required in this area to plan routing. Possible talus debris is also observed along the sides of this valley. In addition, there is one area where a sediment depression will have to be transacted with side slopes of 20-30 degrees. Routing through this area is possible with careful planning and armouring of cable in areas where bedrock is exposed. An ROV inspection survey during the next level of route evaluation is recommended.
S6	27.864	37.975	Some relatively steep slopes and various bedrock outcropping. Cable routing through this area can avoid bedrock, and sediment is evident for trenching.
S7	37.975	49.238	Represents initial portion of southern route with thickening sediments and bedrock outcrop ridges with sediment drape between.
S8	49.238	90.350	Two discernable morphologies: large-scale bedforms east of the rise to Dogfish Banks, and uniform seafloor on Dogfish Banks. No bedrock is observed, and abundant sediment is present for trenching. Local steep slopes of between 10-20 degrees exist along the rise to Dogfish Banks. Water depths in this section range from 165 to 15 metres.

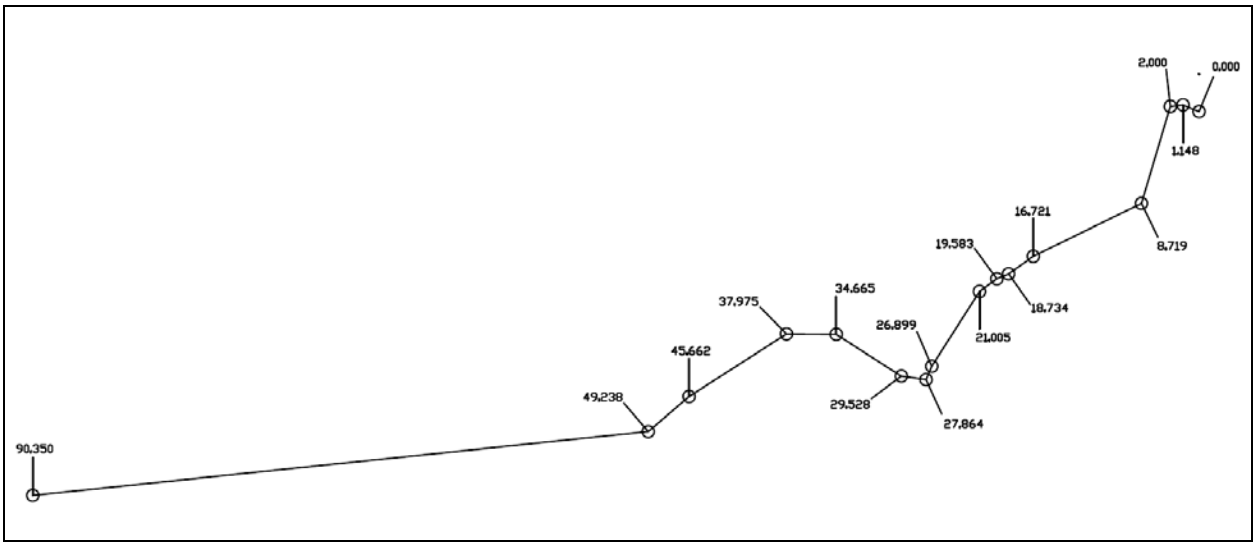


Figure 3.5-16. KP Junctions along Route

Figure 3.5-17 shows the profile of the seabed along the mainland cable route.

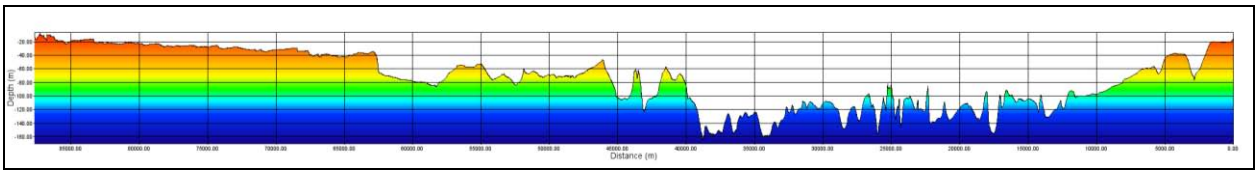


Figure 3.5-17. Profile along Centreline of Route

Detailed information is available for the entire route including the location of bedrock, water depths, unconsolidated sediment types and seabed gradients. In areas where bedrock occur route options are evident subject to more detailed investigations and consultations with local stakeholders and persons knowledgeable of local conditions and uses of the route.

3.5.3.3 Littoral and Coastal Areas near the Wind Farm – An Overview

The Geological Survey of Canada has classified the shoreline between Tlell to Rose Spit on Haida Gwaii in the top 3% of Canada's most sensitive coasts to accelerated sea-level–rise impacts (Shaw *et al*, 1998).

The moderate to high sensitivity of this coastline is due to a macrotidal range, erodible sediments, frequent windstorms and surges, and an energetic wave climate that produce a dynamic coast where some areas are eroding at 1-3 m/a to tens of metres in extreme seasons such as the 1997-1998 El Ninio event (Barrie and Conway, 1996, 2002).

Consequently, this coast is highly vulnerable to ongoing regional sea-level rise (1.6 mm/a), and to extreme water-level events related to climatic variability, which are rising at more than twice the rate of the regional sea-level rise (3.4 mm/a; Abeysirigunawardena and Walker (in press)).

Consideration has been given in this study to the potential of pilings to disrupt the wave, current and sediment transport patterns to such an extent that nearshore and onshore sediment transport will be altered and result in changes in shoreline position and sediment budgets that may enhance (or inhibit) ongoing erosion and deposition processes and, in particular, disrupt the maintenance of dune ecosystems and Rose Spit.

To assess the impact of the wind farm construction in this area on coastal processes the following considerations were made:

- the recent evolution of the coastline
- the nature of the sediments on the seafloor in the wind farm
- changes in seafloor morphology year over year and what does that tell us about sediment transport
- information from wind farm construction projects elsewhere in the world.
- the sediment regime of the nearshore zone dependent on the offshore mobile sediments.
- hydrodynamic modelling

The north-eastern tip of Graham Island is noted for its intensive and dynamic shore processes (Harper, 1980). This is evident in the high rates of coastal retreat along the eastern edge of Graham Island (>12 m/year) (Barrie *et al* 1991).

A 1995 paper by Amos (1995) examined:

- the processes and events that lead to sand transport on the Dogfish Banks and adjoining shoreline
- the transport pathways of the sand
- areas of net seabed accretion and erosion

The work of Amos (1995) characterized the Western Dogfish Banks as largely a shoreface inner shelf environment. Characterized by a well defined suite of shore connected ridges and shore parallel sand ridges based on regional bathymetry.

Amos (1995) reported that the literature indicate that the direction of closure of shoreface-connected ridges with the shoreline is thought to be diagnostic of the longshore and sediment transport direction which in the case of the Dogfish Banks is to the North. Amos *(1995)* also reports that the direction of low amplitude megaripples also indicates a transport in the northward direction.

It is worthwhile to note that the results of repetitive data collection and bedform symmetry in the wind farm found a northward transport direction.

To assess the impact of storms on the region Amos *(1995)* modelled the impact of a severe winter storm which was the most severe in the region. The storm selected for the modeling blew for 48hrs at speeds up to 50 knots. Although the storm magnitude was exceptional the spatial characteristics of the storm was typical of the region. Significant wave heights (Hs) over southern Dogfish Banks were 5.5m.

Wave propogation indicated the 1997-1998 storm tracked from south southeast to north northwest (heading at 330 degrees). Modelling indicated peak storm induced bottom currents on Dogfish Banks of 0.4m/s and combined currents (tidal and storm generated) of 0.5m/s. The model indicated that the shoreline was an area of strong northerly sand transport and that the magnitude of sediment transport was less of Southern Dogfish Banks and greater of Northern Hecate Strait.

Amos (1995) found that continuous coastal erosion of north eastern Graham Island is not surprising given the high rates of sediment removal by the northward directed longshore currents during the southeasterly winter storm.

Amos (1995) indicates that short parallel sand ridge on Eastern Dogfish Banks is predicted to accrete at its crest during storms. That study also indicated that the high transport rates over the ridge and the erosion of parts of the flank suggest that the ridge is active and migrating. It also predicted that the ridge is in dynamic equilibrium with the storm systems and that it is modified only slightly by each storm.

Rose Bar appears to be fed by sand transport from southern Dogfish Banks during storms. Little if any sand comes from the coastline of eastern Graham Island (this material being trapped and transported within the nearshore channel off Rose Spit). It concluded that Rose Bar is not an extension of Rose Spit as it is not feed by its adjacent shoreline.

In summary this modeling work indicated that storm sediment transport is a dominant process in the evolution of the coastal and surficial geology of the region. Sand transport is largely alongshore and to the north. The sand ridge on Dogfish Banks is modern, active and in dynamic equilibrium with modern storm conditions. The position of the ridge is apparently stable, being strongly aligned with the flows in the nearshore region.

3.6 MODEL STUDIES OF COASTAL IMPACTS OF AN OFFSHORE WIND FARM - A CASE STUDY OF CODLING BANK, IRISH SEA

The impact of many offshore wind farms in the UK and Irish waters on the coastal processes of the area has been investigated using advanced computational modelling studies. These studies have shown that apart from the area immediately around the turbine foundations, these developments have little or no impact on the coastal processes of the area or on the adjoining shoreline.

The Codling Bank case study has many similarities with the Dogfish Banks in Hecate Strait (RPS Energy 2009b). A review of the modelling carried out for the proposed Codling Bank wind farm in the Irish Sea provides a valuable case study from which to gauge the potential for littoral and shoreline effects of the wind farm on Dogfish Banks and the shoreline of Naikoon Provincial Park. The Codling Bank case study has many similarities with the Dogfish Bank in Hecate Strait (RPS Energy 2009b).

The Codling Bank is situated in the Irish Sea some 10 to 15 kilometres off the east coast of Ireland. The bank consists of sands and gravels with part of the seabed on the bank being armoured by gravel and boulders while other parts of the area have a mobile sand bed. The water depths across the proposed wind farm sites at Codling and Dogfish Banks are similar being between 10 to 20 metres. The storm

wave climate at Codling Bank is less severe than that of Dogfish Banks but the tidal currents are stronger on the Codling Bank.

The original Coding Bank development consisted of 220 turbines spaced at 400 metre centres along rows which are spaced at 600 metres apart. The studies outlined below relate to the larger wind farm proposal of 420 turbines for the Codling Bank.

3.6.1 *Hydraulic Computational Modelling*

3.6.1.1 Modelling Procedure

The modelling of the coastal processes around the Codling Bank was undertaken using the Mike21 suite of coastal process computational models. This software was developed by the Danish Hydraulics Institute and is recognised as one of the world's leading software packages for coastal process simulations.

The wave, tidal, sediment transport and water quality modelling was undertaken using a series of nested 135/45/15 metre rectangular grid models. The extent and bathymetry of models is shown in Figure 3.6-1 below. The conditions along the boundaries of the 135 metre model were taken from a regional model for Irish and western UK waters developed by RPS for use in storm surge analysis and storm forecasting. The models for the Codling Bank study were calibrated and verified against wave and tidal current measurements taken as part of the Coding Bank site investigation works.

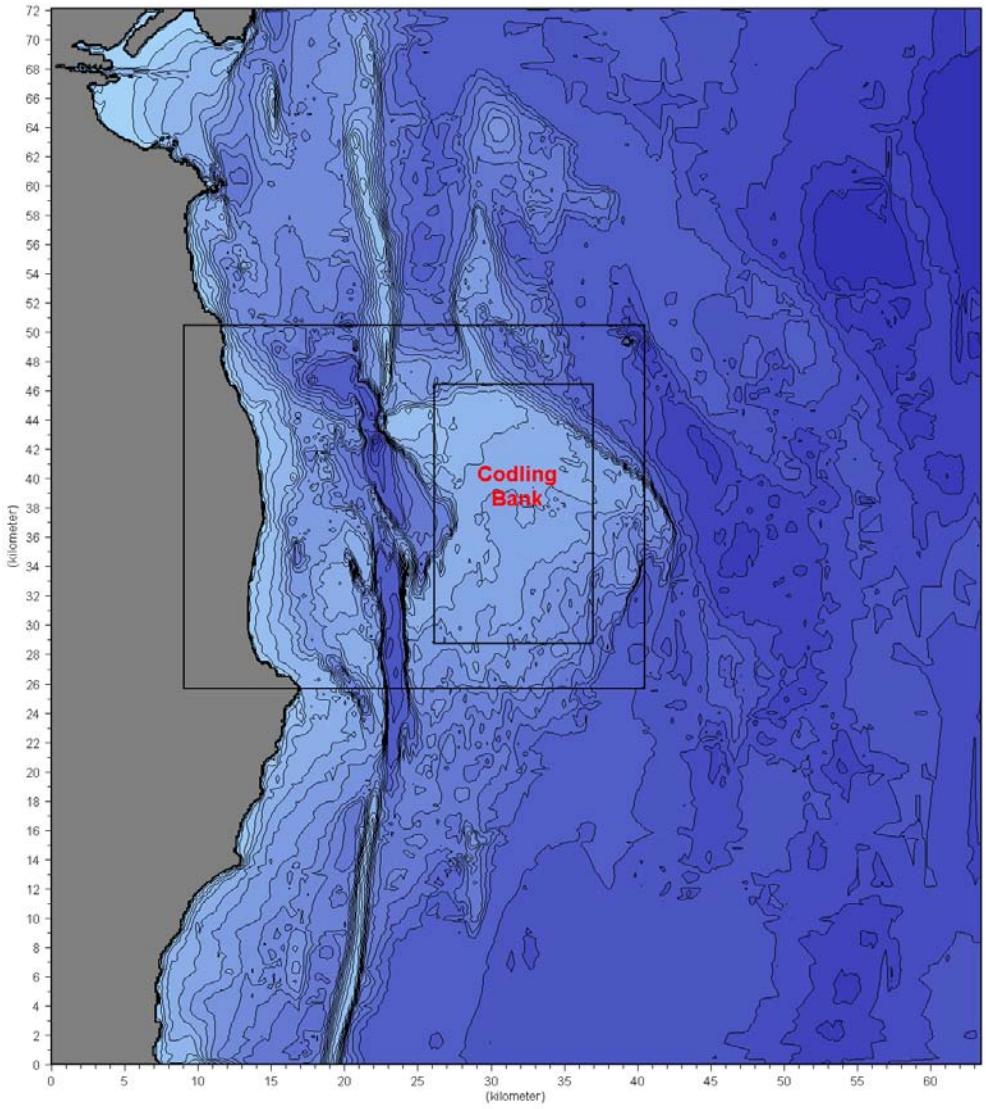


Figure 3.6-1 Extent and bathymetry of 135m – 45m – 15m nested models

The hydrodynamic model simulations were undertaken for the existing bathymetry and for the bathymetry with the wind turbine bases in place. A comparison was then made between the two results so that the effect of the proposed turbine foundations could be more easily be identified.

In the simulations for the proposed Codling Bank wind farm development, the turbine bases were assumed to have a size equivalent to 15 metres (i.e. one grid cell of the finest model bathymetry). This assumption was to allow for any form of base to be used, e.g. tripod, multi pile etc. in the development. In the case of a monopile foundation, the size of the monopile is likely to be not greater than about 6 metres so the results of the tidal, littoral current and sediment transport modelling will be conservative, i.e. the impact of the monopile foundations will be less than that indicated by the model results.

The location of the turbine array and the area covered by the site surveys is shown in Figure 3.6-2.

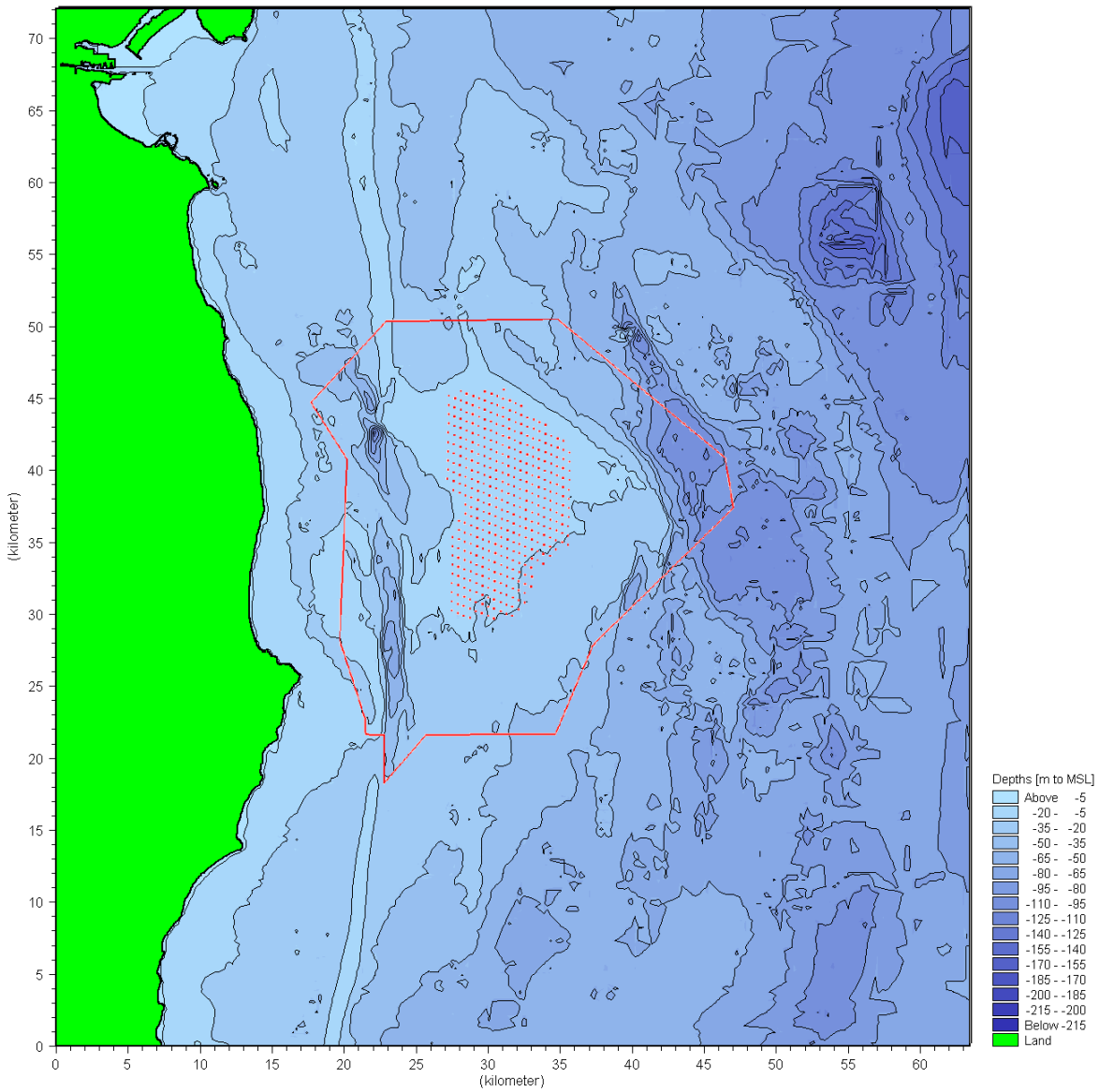
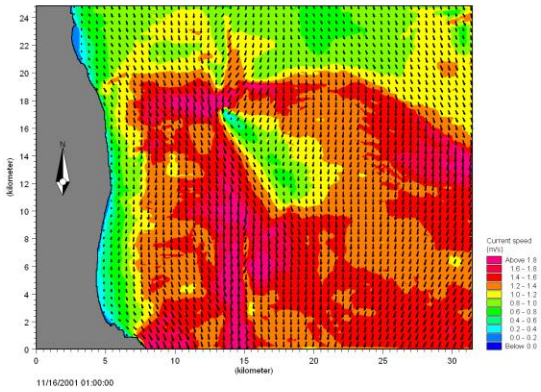


Figure 3.6-2 Location of proposed extended turbine array at Codling Bank

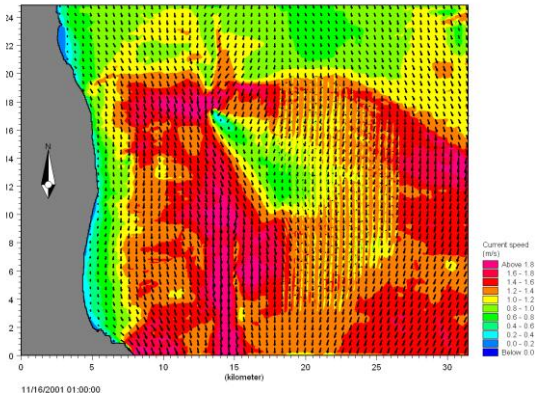
3.6.1.2 Impact on Tides

The impact of the wind farm on the tides was assessed by comparing the tidal currents distribution and tidal height on the site and surrounding area with and without the presence of the wind farm.

The flow pattern showing the tidal speeds during ebb and flood spring tides was simulated with and without the presence of the wind farm and are shown in Figures 3.6-3 and 3.6-4

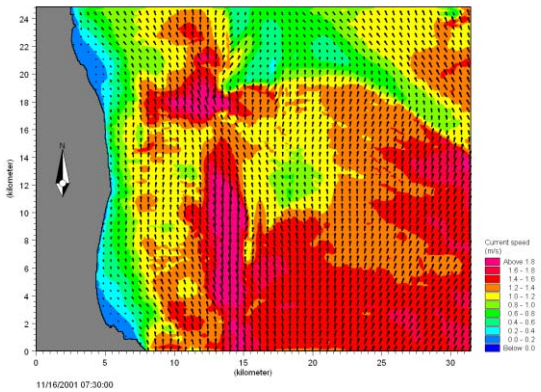


Ebb tidal velocities – without wind farm

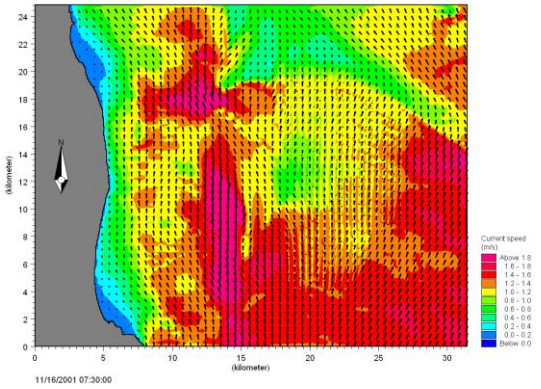


Ebb tidal velocities – with wind farm

Figure 3.6-3 Comparison of ebb tidal velocities with and without wind farm installed



Flood tidal velocities – without wind farm



Flood tidal velocities – with wind farm

Figure 3.6-4 Comparison of flood tidal velocities with and without wind farm installed

The presence of the turbines caused local disturbances that lead to small decelerations and accelerations of the tidal flow. However, on a larger scale, the wind farm has no significant impact on the general tidal flow characteristics.

3.6.1.3 Impact on Waves

The major storm events, which most significantly affect the coastal process on the Codling Bank and the surrounding coastline, are predominantly from the south, south-southeast and north-northeast. For storms from the south to south south-east direction the 1 in 50 year storm wave heights on the site have a significant height of up to 7.5 metres. For north north-easterly storms the 1 in 50 year significant wave height on the site will have a value of up to 5.7 metres

The 1 in 50 year return period events are extreme and not typical of events which will influence the day to day impact of the wind farm on the marine environment of the area. Therefore the wave climate was simulated for typical annual gales from the south to south-southeast and north-northeast directions with and without the presence of the wind farm. The waves generated during gales from the south south-east

direction propagate onto the site from the Irish Sea and the southwest approaches and are of a sufficiently long wave period, in the order of 11 seconds, that the turbine structures are almost transparent to the passing wave. The waves from the north north-east are generated in the Irish Sea itself and are of a smaller wave height and shorter period, approximately 7 seconds. However these waves are also too long to be significantly altered by the turbines.

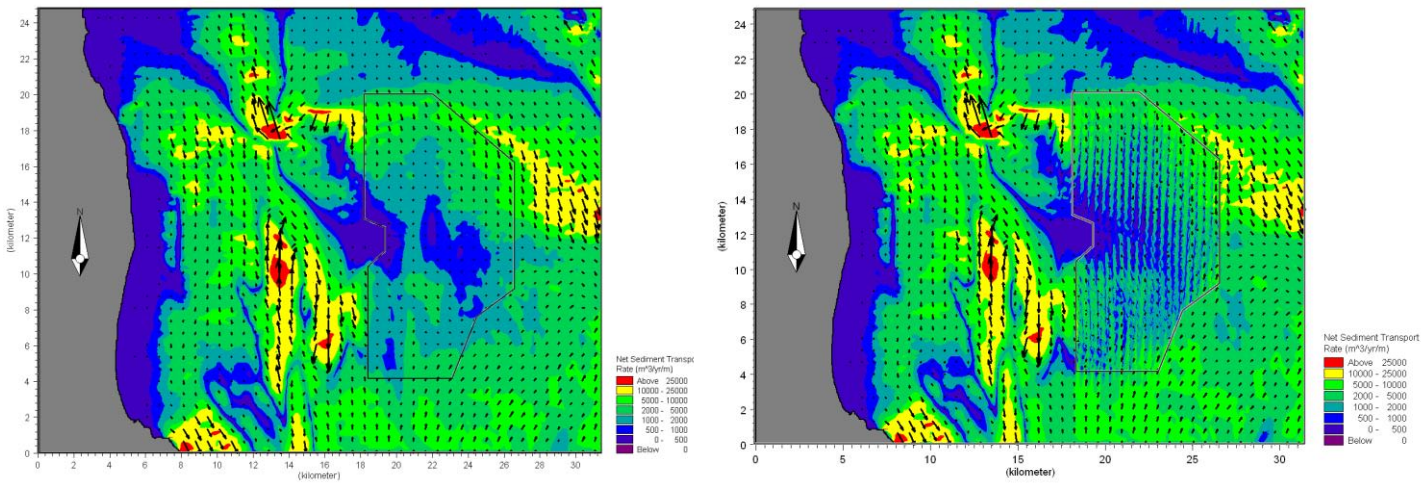
There is a small, local reduction in wind speed within the wind farm site, in the order of 10%, that slightly changes the wave climate around and immediately downwind of the turbines. The reduction in wave height at the leeward end of the farm does not exceed 25mm. This is not significant in the context of the wave heights on the site during these events, as it is only approximately a 0.5% reduction in wave height.

While there is a small impact within and immediately downwind of the wind farm itself, the overall reduction in the wave climate is confined to the area around the wind farm and does not affect the wave climate away from the immediate area of the site.

3.6.1.4 Impact on sediment movement and sediment transport

During calm weather the tidal currents are the main influence on the sediment transport process. Modelling of the sediment transport with and without the presence of the wind farm was undertaken to assess the impact of the wind farm during relatively calm conditions.

Figure 3.6-5 shows the net potential sediment transport rate (for sand) over a full tidal cycle during a spring tide with no waves, with and without the presence of the wind farm. The transport patterns are almost the same in the two different situations, although there is a local reduction in the sediment transport rates around the turbines at the eastern side of the site and a local increase around the turbines on the western edge.



without wind farm with wind farm

Figure 3.6-5 Net potential sediment transport rates for sand over full tidal cycle Spring tides – no waves

The residual tidal velocities represent the net movement of particles over the tidal cycle, and so reflect the sediment transport pathways due to tidal currents on the site and surrounding coastline. As noted previously, the difference in the tidal regime with and without the wind farm is negligible. Thus, apart from the area of the wind farm itself, the presence of the turbines would not have a significant effect on the sediment movement processes.

The combination of tidal currents and waves will result in an increase in the sediment transport rates during south south-easterly and north north-easterly gales around the Codling Bank.

Figure 3.5-6 shows the rate of potential sediment transport of sand sediments during a flood and ebb tide with a south south-easterly gale from 165°, with and without the turbines installation.

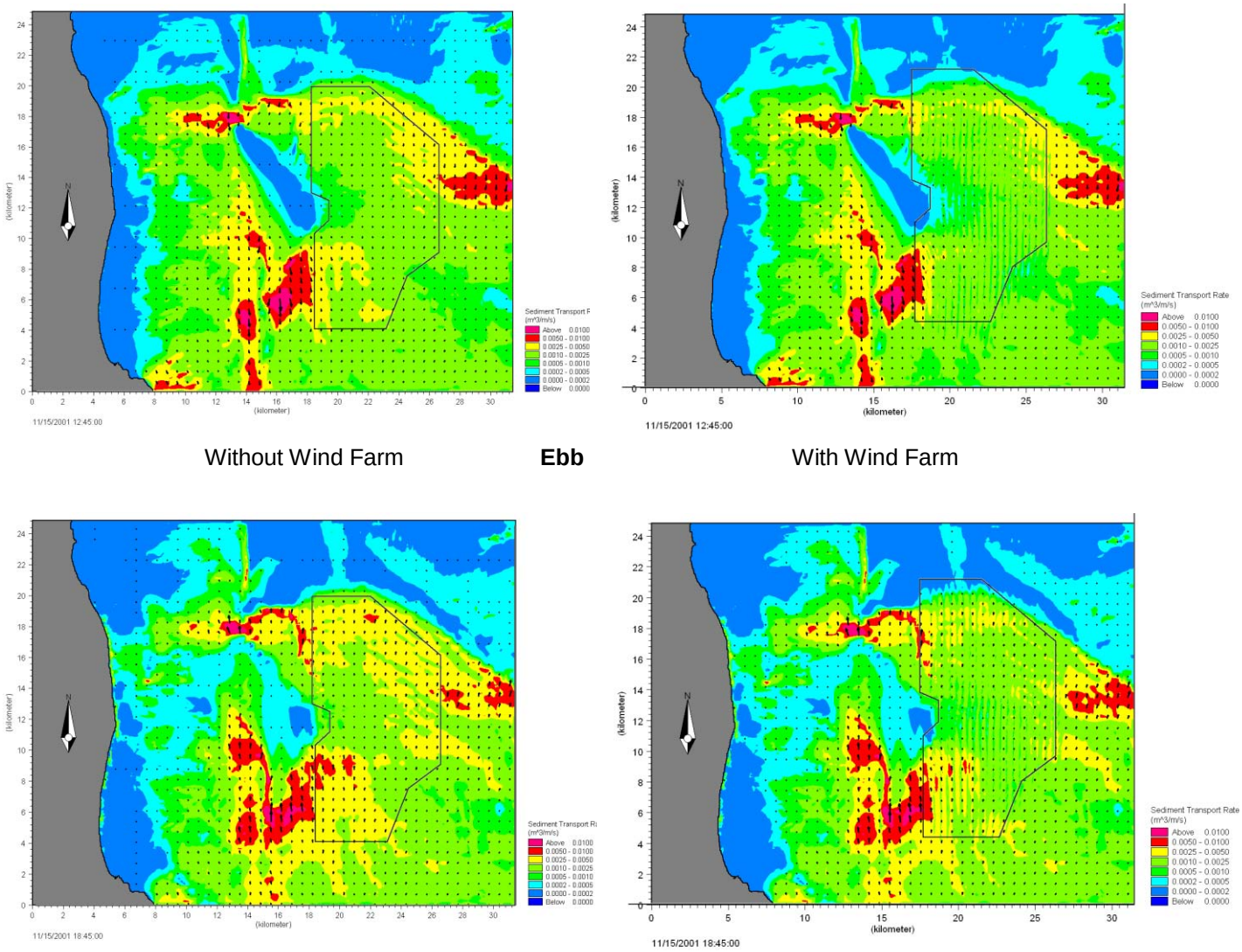


Figure 3.5-6 Rate of potential sediment transport of sand – Gale from 165°

It will be seen from the above that although there is a small change in the potential rate of sediment transport within the wind farm footprint, there are no changes in the rates outside the immediate farm area. This is not surprising since, as shown previously, there is no impact of the wind farm on the waves and tides remote from the wind farm area itself and since the turbines and structures occupy less than 3% of the cross sectional area of the site, the farm will have insignificant impact on the sediment transport processes in areas remote from the site.

3.6.2 *Cable Laying*

The inter-array cables connecting the turbines would be installed in trenches by ploughing or jetting within the seabed gravel layer or, where the gravel layer is thin, in the underlying clays. Only the smaller sand particles within the sediment would have the potential to be raised into suspension during this operation, the gravel and cobble components being too heavy to be suspended. The impact of the cable laying on the level of suspended sediments has been modelled by releasing the appropriate amount of sand particles in to the water column at 1 metre above the seabed.

It is estimated that potential volumes of sediments raised during inter-array cable installation would be in the order of 0.1 m^3/m. The 287kV cable running across the southern part of the wind farm is larger than the cables between the turbines and it is estimated that the volumes of sediments raised during the installation of this cable would be 0.15m^3/m. The installation of this cable has been simulated in the modelling as this will have a greater impact than the lighter cables between the turbines.

The installation of the 287 kV cable across the site has been modelled assuming continuous laying of a cable at a rate of 1 m/min which includes an allowance for delays/connections etc. The percentage time for sediment load exceeding a level of 50 mg/l in the bottom 2 metres of the water column under spring tidal conditions is illustrated in Figure 3.6-7. It can be seen that this level is only exceeded for a maximum of 7% of the installation time and this only in close proximity to the cable position (less than 250 m). The level of 50 mg/l is exceeded less than 1% of the time beyond a distance of 1000 m from the cable position.

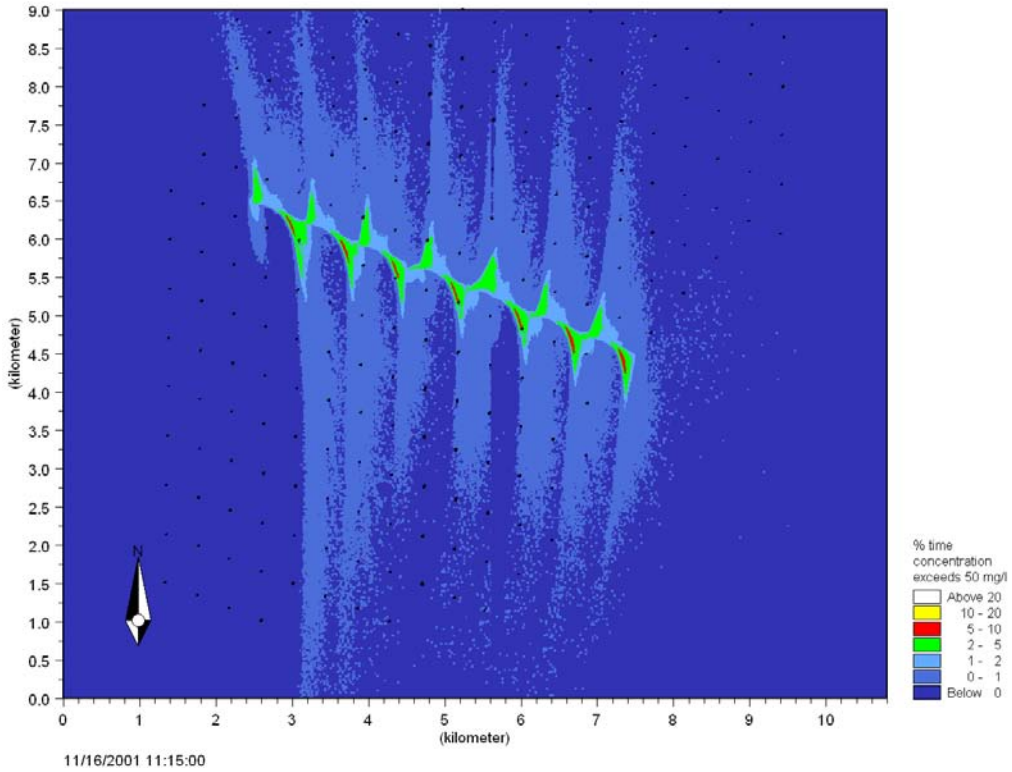


Figure 3.6-7 Percentage of time during cable installation when suspended sediment > 50 mg/l

Deposition rates on the seabed from this operation are generally less than 1 kg/m^2 (0.6 mm depth on the seabed). The nature of the seabed sediments along the cable route to land are more variable than on the main wind farm site; varying from fine sands to medium to coarse gravels. Once again, it is anticipated that ploughing or jetting would be employed to bury the cable within the bed sediments. The potential for the most material to be raised into suspension during this operation would occur on the sections of the proposed cable routes where the bed material comprises fine sands. The rate of installation in these sediments was considered to be 2 m/min in continuous operation and it is estimated that for the larger cables to land the amount of sediment raised in suspension would be in the order of 0.2 m^3/m.

The percentage time during cable installation where a level of 50 mg/l would be exceeded within a distance of 3000 m of the cable position would be for less than 1 % of the installation time. Closer to the cable route the maximum time in excess of 50 mg/l is 2% and this only within 450 m of the cable.

Deposition rates of material on the seabed, after a 19 hour period due to this operation generally do not exceed 1 kg/m^2 (0.6 mm depth) except for very small areas in the vicinity of the cable position where rates increase to 7 kg/m^2 (3 mm depth). Subsequent tidal cycles would rapidly disperse the deposited material to original background levels.

3.6.3 *Conclusions from Codling Bank Modelling*

Experience of offshore wind farm developments in the waters around Britain and Ireland indicates that these offshore wind farms only affect the coastal process locally around the immediate area of the turbine foundations and have no significant impact on the coastal processes of the region or on adjoining shorelines.

The modelling of the impact of a large proposed wind farm development of some 420 turbines on the Codling Bank in the Irish Sea, spaced more densely than the NaiKun wind project, has been examined to demonstrate the level of impact on a site that is broadly similar to the Dogfish Banks in Hecate Strait, BC.

The studies have shown that the Codling Bank development will neither have significant impact on the overall coastal processes of the area nor any significant impact on the adjoining shoreline. Small changes in the littoral flow conditions occur around the area of the turbine foundations. Similarly there are very small reductions in wave heights at the leeward side of the wind farm area due to the reduction in the wind wave generation within the wind farm area itself.

The Codling Bank development assessment was undertaken assuming 15m wide turbine foundations which were located at 400m centres along rows which were 600m apart. The proposed NaiKun wind project at Dogfish Banks in Hecate Strait has only 110 turbines compared with the 420 at Codling Bank and the turbines are more widely spaced at 800m by 1200m (versus 400m and 600m for Codling Bank). In addition, the proposed turbine foundations at the Dogfish Banks site are 5m monopiles thus the foundations at the proposed NaiKun development site are smaller, spaced further apart and only one quarter of the number that are proposed at Codling Bank. It is therefore concluded that the impact of the proposed development at Dogfish Banks on the coastal processes will be even smaller than that shown in the modelling for the Codling Bank development.

Based on the experience of offshore wind farms in UK and Irish waters, and as demonstrated by the Codling Bank development, it can be concluded that the proposed NaiKun wind farm development in North Hecate Strait will have no significant impact on waves, littoral currents and sediment transport away from the immediate area of the turbine foundations. The proposed development will have no impact on coastal erosion or deposition along the adjoining shorelines.

3.7 STUDIES OF IMPACT OF OFFSHORE WIND FARMS ON COASTAL PROCESSES - A CASE STUDY OF SCROBY SANDS

The effect of offshore wind farms on coastal processes has been reported in detail elsewhere including on Scroby Bank offshore from Great Yarmouth UK in the Southern North Sea. (Cefas, 2006) The Scroby Bank is comparable to the Dogfish Banks in that it is in very shallow water (7 m) and exposed to the dominant storms (in this case from the NE) and the seabed conditions at this site were expected to be very mobile. This work has indicated that the impacts of monopiles on coastal processes are probably limited to scour pits and scour wakes.

Scour pits are associated with monopiles and are typically up to 5 m deep, with a horizontal diameter of 60 m (30 m radius). The scour wakes are approximately 300 m long by 100 m wide with a depth of approximately 1m and are considered insignificant in comparison to the natural changes which occur at Scroby Bank. These features are a negative relief as a “wake” of sediment disturbance (i.e. bedforms) on the seabed.

An important finding is that the wind farm resulted in no change in overall elevation across the bank and the bank has appeared to maintain its overall morphology, with no creation of channels across the bank’s flanks or crest. Monopiles may act to initiate trains of sedimentary bedforms. However such bedform generation is unlikely to alter either the net sediment transport rates along sandbank flanks or the overall sediment budgets of such sandbanks.

As reported in the Scroby Sands monitoring report, these conclusions provide a degree of confidence to regulators and offshore wind farm developers that bathymetric impacts of monopile-based OWFs are probably limited to the order of 100 m around each monopile. Given the monopile spacings bathymetric impacts from on monopole will not affect neighbouring monopiles.

It is worth noting that the Scroby Bank was first identified as the worst-case scenario of the UK Round 1 developments, in terms of potential impacts on coastal processes. The results of monitoring post construction indicate that there is little impact likely on coastal processes in the area.

The sedimentary features associated with turbine foundations at Scroby Bank are likely to be typical of those likely to identified in other (but not all) offshore wind farms. Other features which were noted during monitoring included impacts of jetting the inter-array cable close to the monopiles as shown by a trench; traces of the ploughing of the inter-array cable across the offshore wind farm site and secondary scour pits associated with the scour protection deposited to stabilise the monopile.

Figures 3.7-1 and 3.7-2 illustrate the physical changes in the seafloor at the Scroby Bank sites. Note that the water depth is comparable to that for the NaiKun Project. Note also that the spacing of the WFA is 1200m x 800m for the NaiKun Project; much greater spacing than Scroby Bank and therefore much less opportunity for interaction and cumulative effects between turbines.

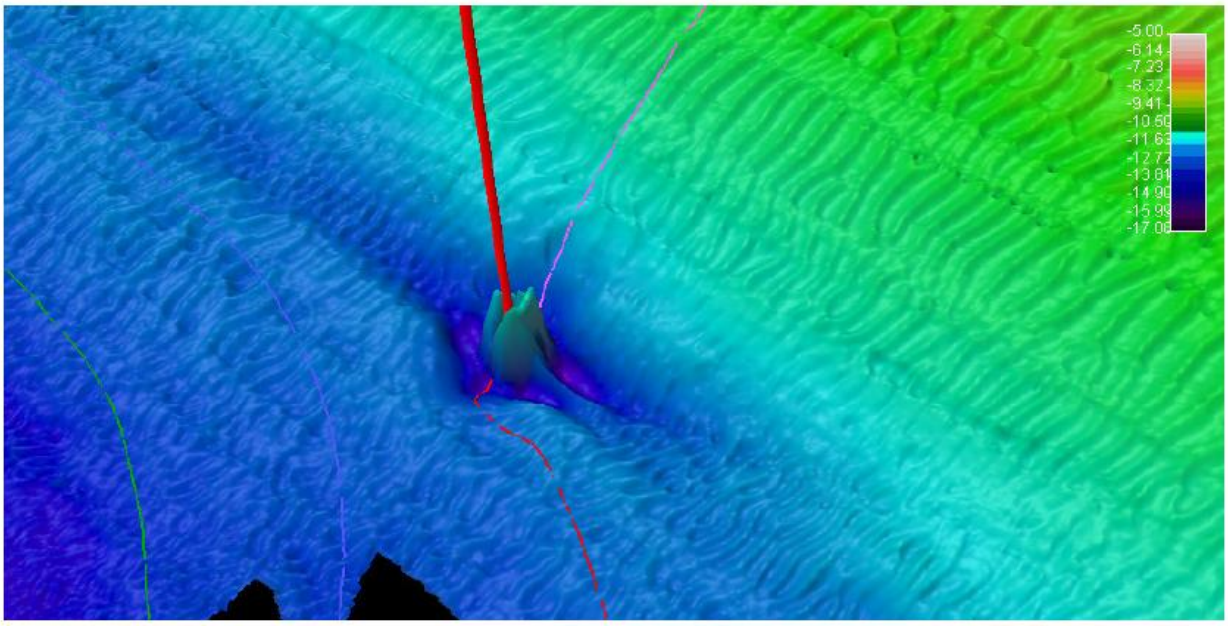


Figure 3.7-1 **Fledermaus image showing the scour protection around the base of a monopile (red cylinder ~4.2 m diameter, WTG01, Scroby Bank), along with the secondary scour pits and the "as laid" inter-array cable route (magenta line) and the export cables (red and green lines) (From Cefas, 2006).**

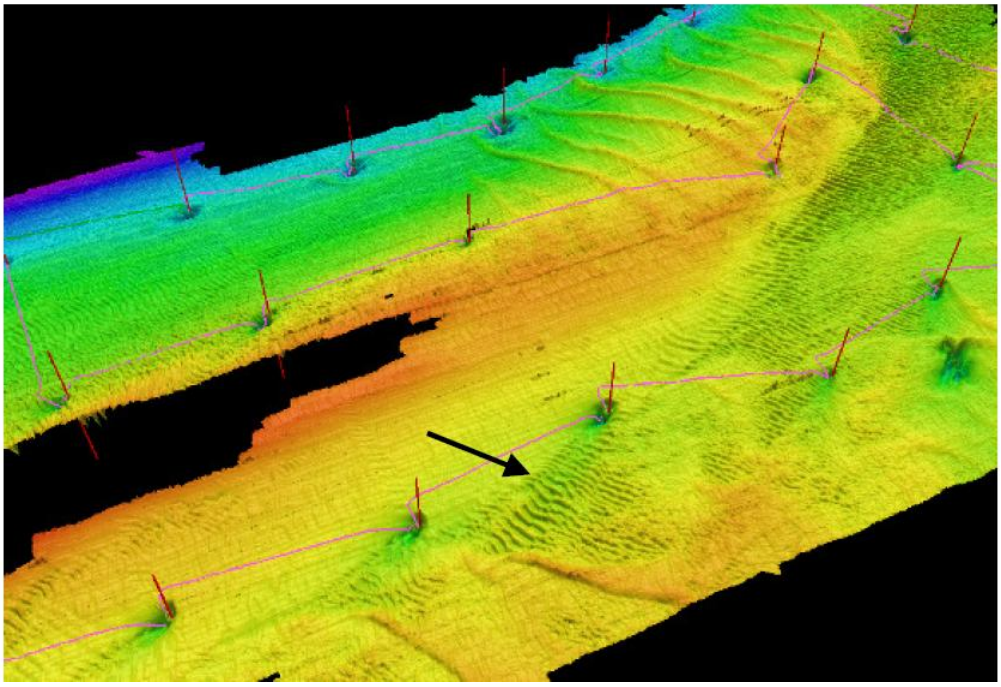


Figure 3.7-2 **Fledermaus image showing results from the swathe bathymetry survey of Scroby Sands OWF. The monopiles (vertical red cylinders) and intra-array cable route (magenta). The black arrow indicates a scour wake extending SE to the neighbouring monopile. Distance between these monopiles (WTG 19 to WTG23) is ~375 m (Cefas, 2006).**

It is important to note that at Scroby, as at the Dogfish Banks, sandwaves are an important aspect of the seafloor morphology. Based on monitoring work performed at Scroby there were no significant changes in sandwave geometry as a result of wind farm construction, including sandwave patterns, orientations, spacing and bifurcations of crests.

This implies that as well as there being no far field impacts on sediment patterns there is little impact in the near field (i.e. sediment transport patterns within the wind farm area are not modified beyond the immediate vicinity of the monopiles and those impacts are limited to scour pits and scour wakes).

3.8 HAIDALINK

The proposed HaidaLink is a submarine transmission cable from the wind farm (offshore converter station) to Graham Island with a proposed landfall near Tlell. A 1km wide corridor has been considered and the characterization of the seafloor geology along this section has been based on data collected from regional research surveys by the Pacific Geoscience Centre (PGC). This regional work is described in a data compilation and interpretation study performed by RPS Energy (referenced herein as RPS Energy 2006).

The two research surveys of relevance to this work are the PGC 1991 and 1994 surveys and the location of these survey lines relative to the Haida Link corridor is shown in Figure 3.8.1, presented at the end of this section. This regional dataset were obtained by the Pacific Geosciences Centre (PGC), Natural Resources Canada from two cruises - PGC 91006 and PGC 94007. The line separation on those cruises was ±10 kilometres and the regional grid included Huntec deep towed subsurface boomer with 120 kHz sidescan sonar, Seistec surface towed boomer, 5 cubic inch airgun reflection seismic, and sidescan sonar systems operated between 120 and 100 kHz. The data were groundtruthed by piston and vibracores and the location of those sample sites are shown in Mapsheet 2 of the RPS Energy 2006 report. The shallow water of the study area, combined with the reflective nature of the sandy and gravelly seafloor, made this a challenging area for subsurface definition. However, the combination of Huntec, airgun, and Seistec data and sidescan provided a sufficient range of frequencies that definition of sand ridge thickness and the location of isolated areas of softer sediment. It also allowed for broad characterization of the sediment distribution in the area. On the basis of regional information more detailed site work was performed in the wind farm area in 2007 and 2008 for site selection purposes and that is described elsewhere.

The regional seafloor geology was mapped from this research data as part of the reconnaissance study prepared in 2006 by RPS Energy for NaiKun. In summary that study found and reported widespread gravel lag deposits at the seabed in the southwest corner of the PGC survey grid (which is the area of the proposed HaidaLink). The study found sand ridges and sand lenses of variable thickness above this lag surface. These sands are very thin in the east part of the grid (in contrast to the western side of the wind farm). Sand is not an attribute common on the shallower water areas to the east where the HaidaLink is proposed to run. The area traversed by the Haida Link is mostly a slag surface, which is an unconformity marking 2,500 years of exposure, covered by a gravel and boulder armour with localized thin patches of sand.

In addition to the geophysical data collected along these survey lines the surface texture was mapped as a percent gravel, sand, silt, and clay (this is on Mapsheet 2 of the 2006 report). These analyses were provided by the Pacific Geosciences Centre and are based on analysis of a variety of bottom grab samplers including Van Veen, Shipeck, and large volume IKU samplers. Subsurface cores were obtained by gravity and vibracoring systems.

The grain size information obtained from the PGC archives was found to be helpful in understanding the geology relevant to the HaidaLink. The location of these samples is shown in Figure 3.8.2, presented at the end of this section.

Of particular relevance are a cluster of samples on the edge of the proposed corridor. These grab samples area labelled as PAR83A01, 02 and 03. Approximately 2.5km to the south is a sample called PAR84A008. All of these samples are comprised of gravel.

Figure 3.8.3, presented at the end of this section, is an extract from “Map 2 – PGC Grain Size and Cores” in the 2006 RPS Energy Report. Based on the regional survey grid and the associated mapping and the location of the proposed HaidaLink the seabed conditions along the corridor are expected to be very similar to those seen in the southeast portions of the PGC research survey grid.

Figure 3.8.4 is also taken from the regional report (RPS Energy 2006, Figure 12) and is combination of subbottom profiler data and sidescan sonar data. It shows that the seafloor in this area is comprised of gravel with boulders and occasional patches of sand in a thin veneer of sand. Based on this data and the regional bathymetry this is the most likely seafloor condition expected along the Haida Link from the wind farm to the near shore areas on Graham Island .

The upper panel in Figure 3.8.4 is the uninterpreted subbottom profiler data. The mid panel is the data with interpretation. The yellow shading indicates the areas of sand at the seafloor. The lower panel is the sidescan sonar. Low reflectivity (white because the energy in absorbed and not reflected) is sand. High reflectivity (grey/black) is gravel because the energy is reflected. The objects with shadows (which are black with white lines behind them are boulders) and some of these are labelled.

In Figure 3.8.5 (taken from RPS Energy 2006 where it is presented as Figure 14) the upper panel is the uninterpreted subbottom profiler data. The mid panel is the interpreted data, where the yellow shading indicates a layer of sand.

The lower panel is the sidescan sonar. Low reflectivity (white because the energy in absorbed and not reflected) is sand. High reflectivity (dark grey) is gravel because the energy is reflected.

The subbottom profile and sidescan example in Figure 3.8.5 crosses the proposed HaidaLink. This combined data example indicates areas of a very thin sand veneer and areas of abundant gravel. There is also an area which was originally interpreted as possible bedrock. However, more recent data collected in the wind farm shows similiar features and these are now thought to be areas of outcropping glacial till with boulders (rather than bedrock).

In summary, Figure 3.8.6 shows the regional bathymetry along with a profile from the landfall at Tlell along the corridor to the windfarm, across the windfarm site and along the cable corridor across Hecate Strait to the mainland. The HaidaLink runs parallel to the slope of the Dogfish Banks and as a result has little relief. The two exceptions are a) an area 10km south of the offshore converter station (TP2) which is a seabed depression with a small high in the middle and b) the shoreface at Tlell (west of TP1). There is the possibility of occasional small scale sand ridges along the HaidaLink.

This information provides a reasonable understanding of the seabed conditions for purpose of assessing the HaidaLink cordridor. Within this corridor it is anticipated that detailed survey work, comparable to that required for the mainland cable route will be performed to facilitate final cable alignment within the corridor prior to final design.

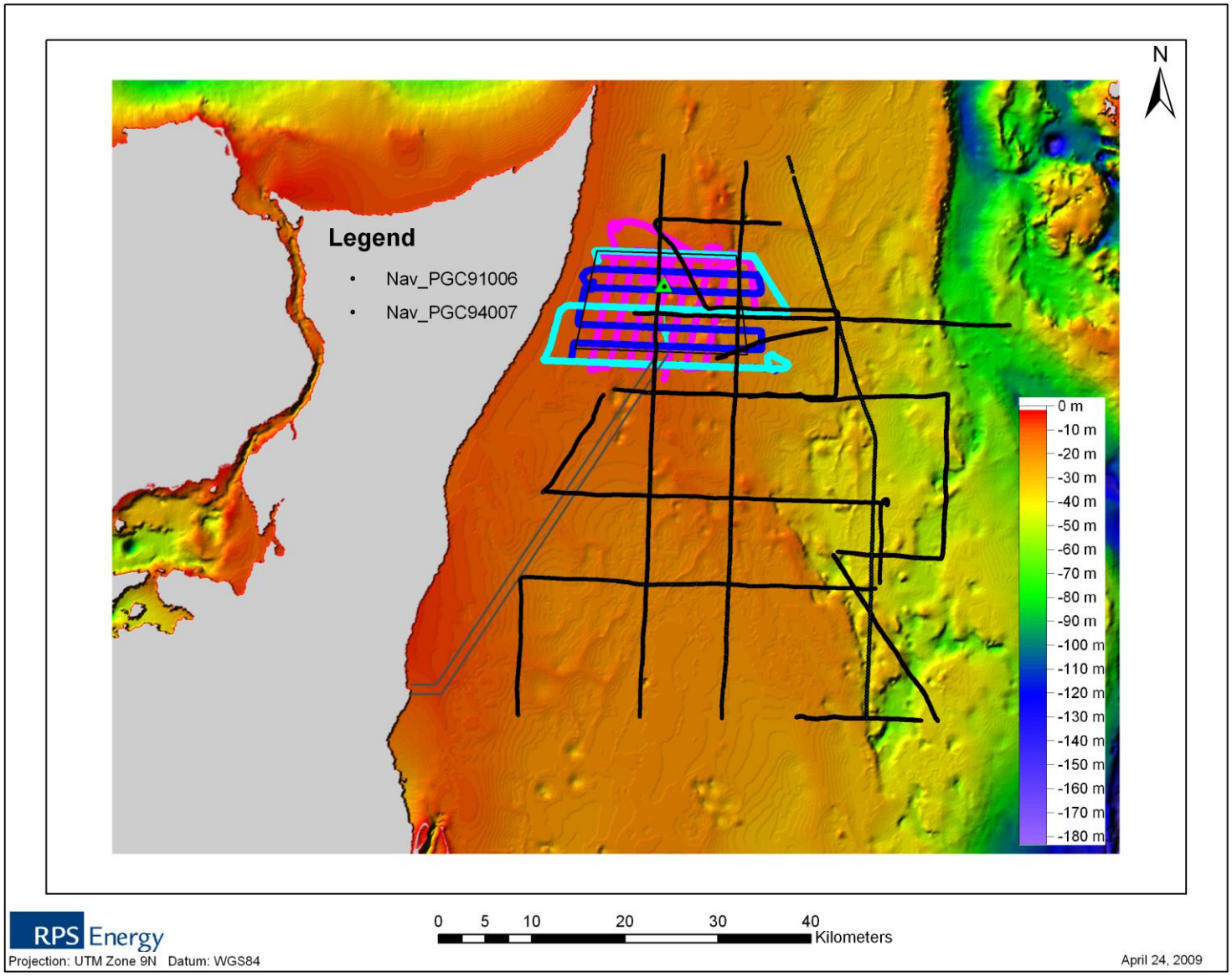


Figure 3.8.1 Regional Survey Lines relative to Haida Route Corridor along with regional bathymetry

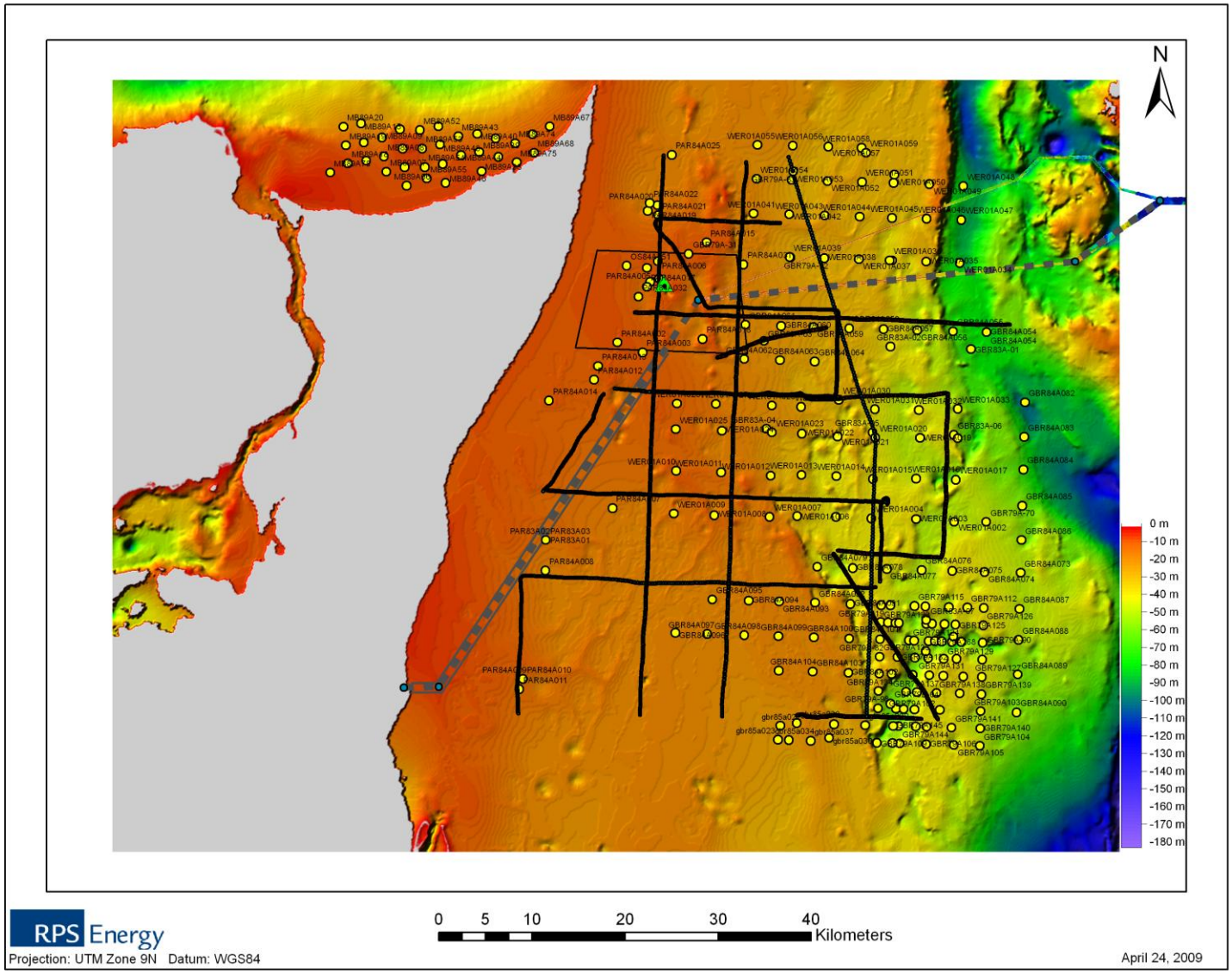


Figure 3.8.2 Location of Grab Samples relative to Regional Survey Lines and Haida Route Corridor

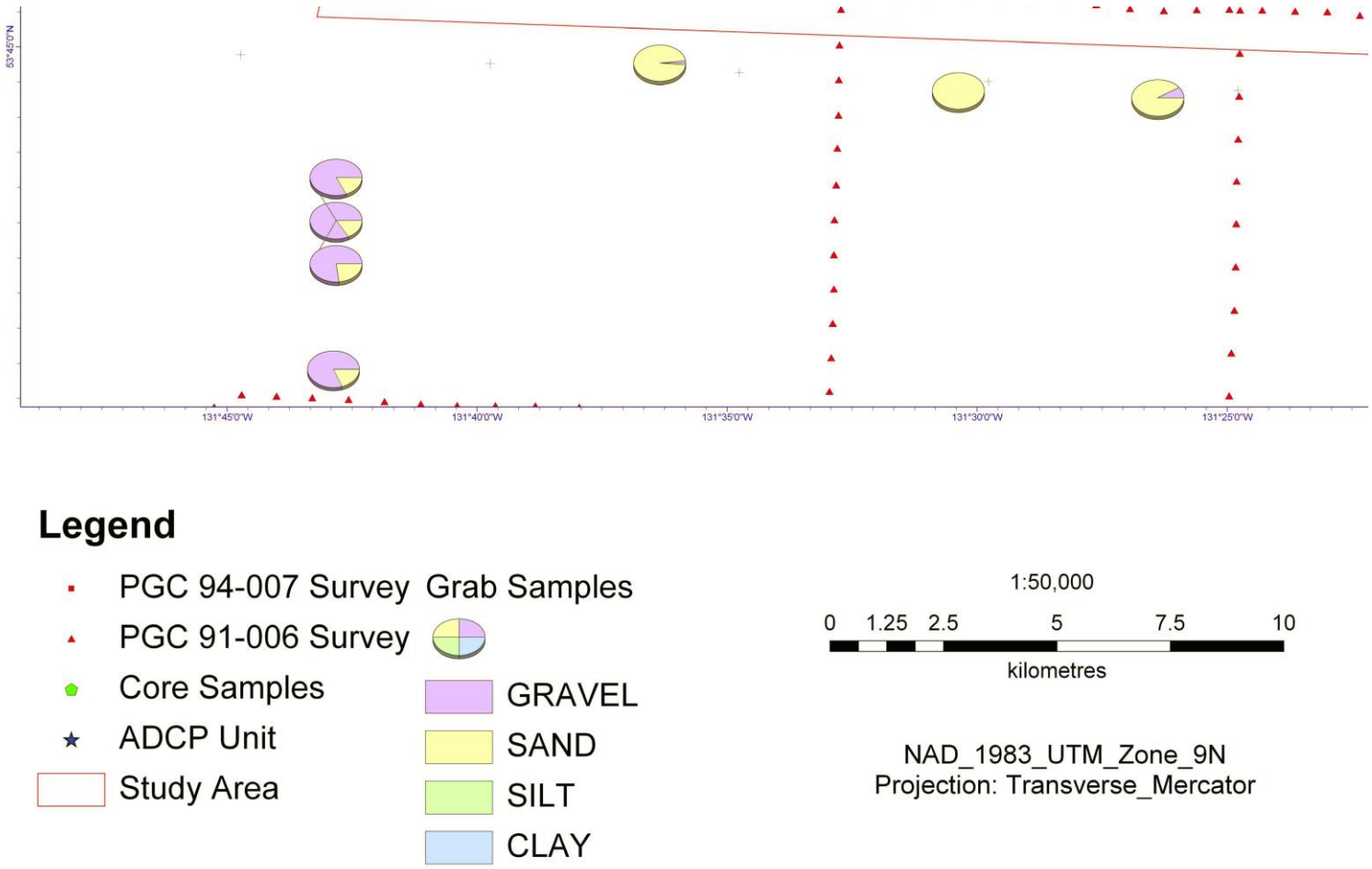


Figure 3.8.3 **Extract from Map 2 – PGC Grain Size and Cores of the 2006 RPS Energy Report. Note gravel samples on east (in areas of the Haida Link) in contrast to sand in samples to the west.**

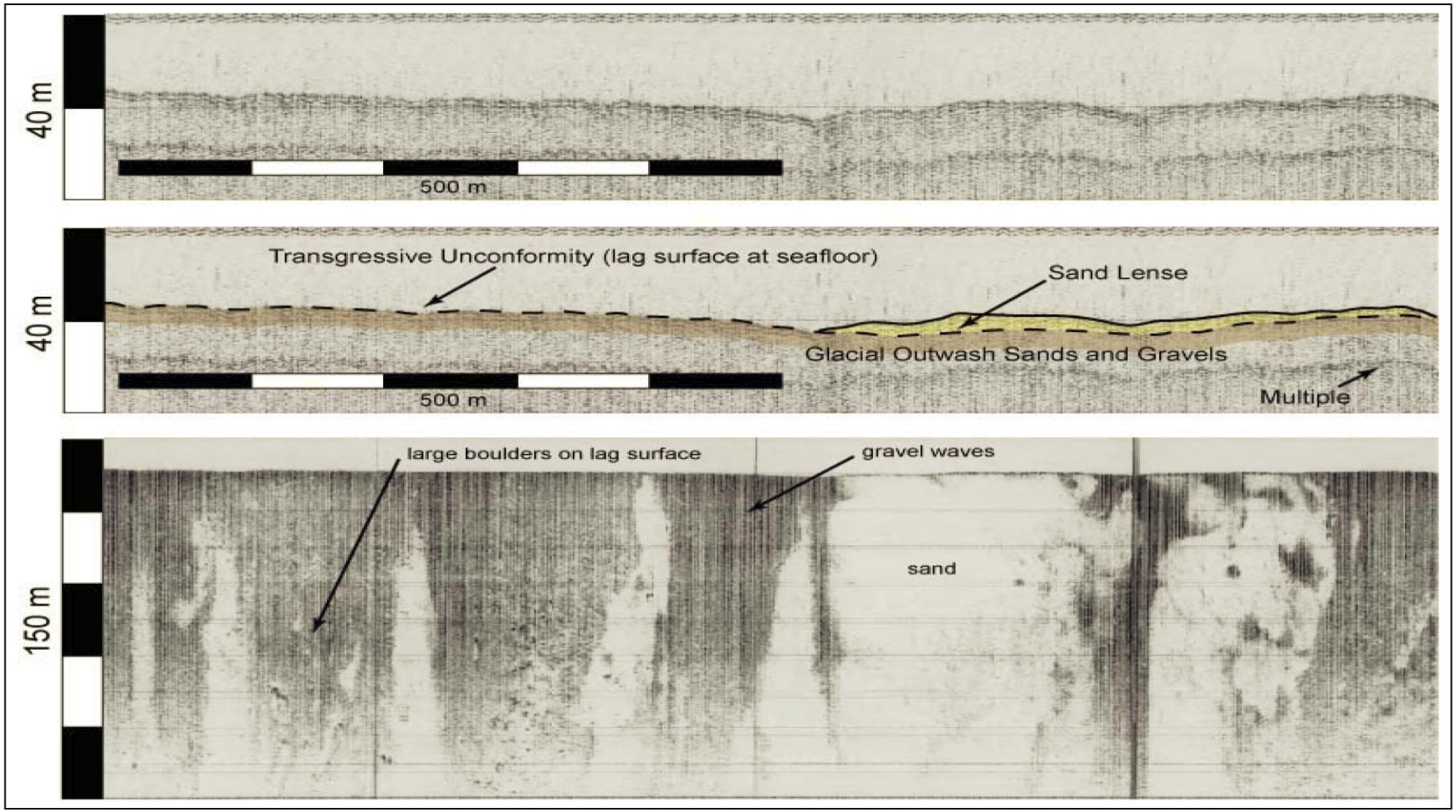


Figure 3.8.4 **Data example from the 2006 RPS Energy regional report where is was originally presented as Figure 12 showing areas areas comprised of gravel with boulders and occasional patches of sand in a thin veneer of sand.**

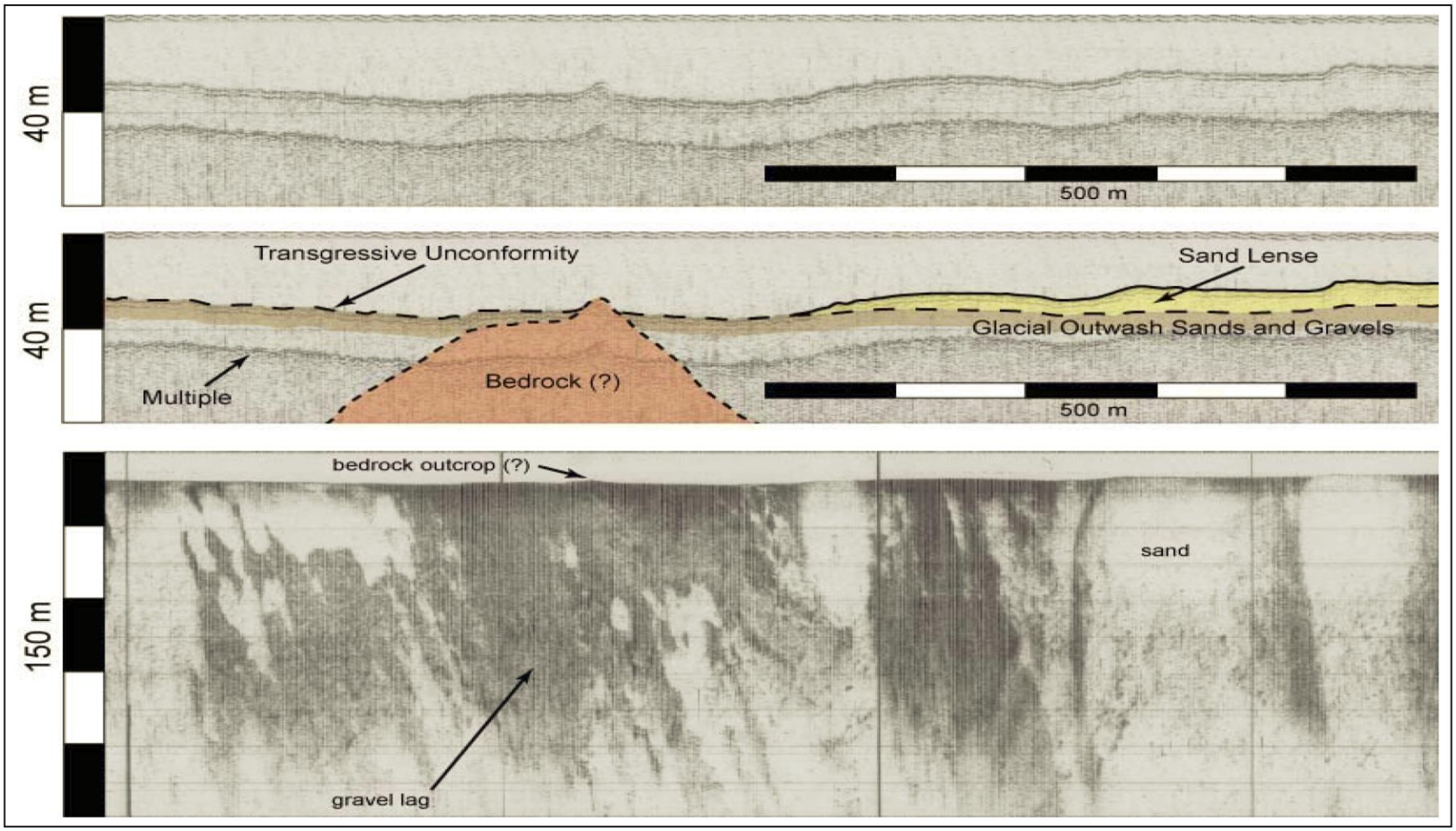


Figure 3.8.5 **Data example from the 2006 RPS Energy regional report where is was originally presented as Figure 14. The area labeled as bedrock is most likely bouldery glacial till based on more recent data collected in the WFA in 2007 and 2008.**

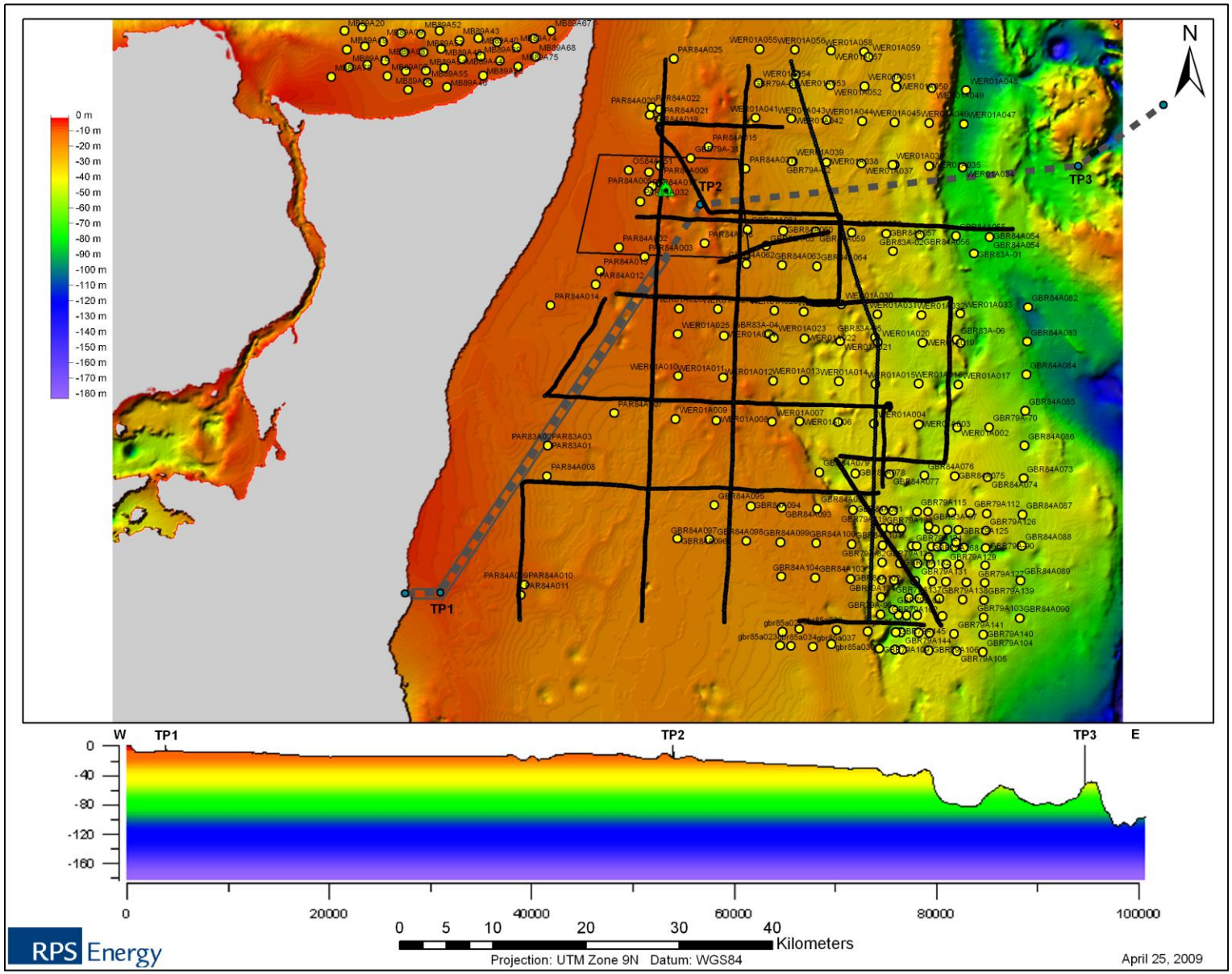


Figure 3.8.6 Summary Bathymetry Profile showing the low relief along the Haida Link corridor

3.9 REFERENCES AND SOURCES

Abeysirigunawardena DS and IJ Walker, 2008. Sea Level Responses to Climatic Variability and Change in Northern British Columbia. Canadian Meteorological and Oceanographic Society, Volume 46, Number 3, September 2008. pp 277-296.

Adams, J. and S Halchuk, 2003. *Fourth Generation Seismic Hazard Maps of Canada: values for over 650 Canadian Localities intended for the 2005 National Building Code of Canada*. Geological Survey of Canada open file No. 4459.

Amos CL, Barrie JV and JT Judge, 1995. *Storm-Enhanced Sand Transport in a Macrotidal Setting, Queen Charlotte Islands, British Columbia, Canada*. Spcl. Publs. Int. Ass. Sediment. V. 24, p 53-68.

ASL, 2007. *NaiKun Wind Development, Report on Wave & Current Measurement*. ASL Environmental Sciences Inc., July 2007.

Axys, 2007. *NaiKun – Hecate Strait, Test Platform Oceanographic Instrumentation Data Report*. September to November 2007. Axys Technologies Inc., February 2007.

Barrie, J.V. (1988), *Surficial Geology of Hecate Strait, British Columbia Continental Shelf*. Geological Survey of Canada, Open File 1682

Barrie, J.V. (1993). *Modern Evolution of a Nearshore and Coastal Macrotidal Sand Transport System, Queen Charlotte Islands*. Abstract Published in CANQUA 1993 abstracts.

Barrie, J.V., Conway, K.W., Mathewes, R.W., Josenhans, H.W. and Johns, M.J. (1993). *Submerged Late Quaternary Terrestrial deposits and Paleoenvironments of Northern Hecate Strait British Columbia Continental Shelf, Canada*. Quaternary International 20:123-129

Barrie, J.V., Luternauer, J.L. and Conway, K.W. (1990). *Surficial geology of the Queen Charlotte Basin: Moresby Island- Queen Charlotte Sound*. Geological Survey of Canada, open file 2196, 8maps (1:250,000).

Bornhold, B. D., (2004). *Interpretation of Seismic Profiling Data Northern Hecate Strait, British Columbia*. Report Prepared For NaiKun Wind Development Inc., April 2004.

Boston, N. 1963. *Tidal Calibration of the Hecate Model*. Jour. Fisheries Research Board Canada. Vol. 20, No. 50, pp. 1197 -1212.

CANADIAN HYDROGRAPHIC SERVICE. 1991. Sailing *Directions British Columbia Coast* (north portion), Vol. 2, 12th ed. 306 p.

CANADIAN TIDE AND CURRENT TABLES (annual). *Barkley Sound and Discovery Passage to Dixon Entrance,* Vol. 6. Fisheries and Oceans Canada.

CEFAS, 2006. *Scroby Sands Offshore Wind Farm – Coastal Processes Monitoring*. Final Report, 12th April 2006, Cefas Lowestoft Laboratory

Clague, J.J. (1983). *Glacio-Isostatic effects of the Cordilleran Ice Sheet ,British Columbia Canada in Shoreline and Isostacy*. Edited by D. Smith and A. Dawson ,pp 321-343, Academic Press London.

Clague, J.J., Mathewes, R.W. and Warner, B.G. (1982b). *Late Quaternary Geology of Eastern Graham Island, Queen Charlotte Islands, British Columbia*. Canadian Journal Of Earth Sciences,19:1786-1795.

Crawford, W.R., (2003). *Oceanography and Ocean Currents* at: ftp.pac.dfo.mpo.gc.ca/pub/crawford/Oceanography.

Crean, P.B. 1967. *Physical oceanography of Dixon Entrance British Columbia*. Bull. Fish. Res.Board Can. 156: 66p.

DHI, nd. *MIKE21 coastal modeling system*. DHI Water & Environment, Agren Alle 11, DK-2970 Horsholm, Denmark. Information available from DHIsoftware.com

Dietrich, J R. (1995). *Petroleum Resource Potential for the Queen Charlotte Basin and Environs, west coast Canada*. Bulletin of Canadian Petroleum Geology (43)1, page 20-34.

Ekman, V. W. 1905. *On the influence of the earth's rotation on ocean currents*. Ark. Mat. Astron. Fys. 2: 1 – 52.

Extract from E. A and Outreach, (2006)

Fedje, D.W. and Josenhans, H.W. (2000). *Drowned Forests and archaeology on the continental shelf of British Columbia, Canada*. Geology vol. 28, 99-102.

Haggart, J. W., Dietrich, J. R. and Lyatsky, H. V., 1999, *Petroleum geology framework, West Coast Offshore Region*.

James, R. W. 1969. *Abnormal changes in wave heights*. Mariners Weather Log. 13: 252 – 255.

Josenhans, H.W., Barrie, J.V., Conway, K.W., Patterson, R.W., Mathewes, R.W. and Woodsworth, G.J. (1993). *Surficial geology of the Queen Charlotte Basin: Evidence of submerged proglacial lakes at 170m on the continental shelf of western Canada*. Current Research Part A, Geological Survey of Canada paper 93A, p 119-127.

Josenhans, H.W., Fade, D.W., Conway, K.W. and Barrie, J.V. (1995). *Post glacial sea levels on the Western Canadian continental shelf: evidence for rapid change, extensive subaerial exposure and early human habitation*. Marine Geology vol.125 73-94.

Josenhans, H.W., Fedje, D.W., Pienitz, R. and Southon, J. (1997). *Early Humans and Rapidly Changing Holocene Sea Levels on the Queen Charlotte Islands-Hecate Strait, British Columbia, Canada*. Science vol. 277: 71-74

MARINE ENVIRONMENTAL DATA SERVICE, Department of Fisheries and Oceans. (unpublished manuscript) *Waves recorded off Prince Rupert, B.C., September 28, 1972 to June 13, 1973.* File 104-1.

Marine Weather Hazards Manual. 1992. Minister of Supply and Services, Canada. 2nd ed. 138 p.

PGC, 1991. Geophysical Data and Navigation Data from Cruise 91006. Accessed from PGC Archives by RPS Energy for regional geophysical and geological interpretation study for NaiKun Wind in 2006

PGC, 1994. Geophysical Data and Navigation Data from Cruise 94007. Accessed from PGC Archives by RPS Energy for regional geophysical and geological interpretation study for NaiKun Wind in 2006.

PGC, nd. Geophysical Data and Navigation Data from Cruise 91006. Obtained from PGC Archives by NaiKun for regional interpretation study in 2006

RPS Energy, 2006. Geological Conditions Related To The Naikun Wind Farm Development Project Haida Energy Field Hecate Strait, Offshore British Columbia For Naikun Wind Development Inc. Report number 06-276.1. November 27, 2006.

RPS Energy, 2007 Unpublished, *Regional Engineering Geological Assessment of Hecate Strait Offshore British Columbia,* for Proposed Naikun Windfarm Development, prepared For Naikun Wind Development Inc. March 28, 2007

RPS Energy (2008) Unpublished. *Hecate Strait Wind Energy, Metocean Study*. Prepared for Naikun Wind Development Inc. August 2008

RPS Energy, 2009a Unpublished. *Final Report, 2008 Geophysical Survey and Interpretation, Northern Naikun Trapezoid Survey and Data Analysis, Haida Energy Field, Hecate Strait, Offshore British Columbia*. Prepared for Naikun Wind Development Inc. January 9, 2009

RPS Energy, 2009b Unpublished. *Hecate Strait Wind Energy, Environmental Impact Assessment, Impact of the Wind Farm on the Coastal Processes*. Prepared for NaiKun Wind Development Inc. February 2009

Stride, A.H. (editor) (1982). *Offshore Tidal sands*. published by Chapman and Hall

Thomson, R.E., (1981). *Oceanography of the British Columbia Coast*. Canadian Special Publication of Fisheries and Aquatic Sciences 56: 258pp.

Thomson, Richard E. 1981. *Oceanography of the British Columbia Coast*. Department of Fisheries and Oceans. Ottawa, 1981